Vulnerability of Vegetation to Mining Dust at the Jack Hills, Western Australia

by

Gillian Frances Turner

THE UNIVERSITY OF WESTERN AUSTRALIA

Achieve International Excellence

This thesis is presented for the degree of

Master of Science

of The University of Western Australia

School of Plant Biology

November 2013

Vulnerability of Vegetation to Mining Dust at the Jack Hills, Western Australia

Abstract

This thesis examines if dust produced by an iron-ore mine in the Jack Hills, Western Australia, has a negative impact on health and physiological function of the surrounding native flora. To this end, I characterised dust generated by the mine in terms of grain-size distribution and mineralogy and measured its spatial and temporal 'footprint'. I then classified the dominant perennial species around the mine in terms of their structural and morphological 'traits' (e.g., plant height, leaf area, leaf surface characteristics) and quantified the dust trapped on the leaves of these species. I analysed the relationship between these plant 'traits' and dust on the leaves with Linear Mixed Effect Models (LMEM). Multivariate cluster analysis was used to group species based on similar traits to test if a group of species with similar traits increased dust loading. I then quantified the physiological performance of plants under different dust load conditions via stomatal conductance (g_s), chlorophyll fluorescence (Φ_{PSII}) and carbon isotope composition ($\delta^{13}C$). The correlation between the physiological measures, dust load and/or plant traits, was then examined with LMEM.

I found that the Jack Hills mine generated dust in excess of natural background levels at distances of up to 2000 m from the mining operations. It thus imposed elevated dust loads on the surrounding vegetation. Leaf morphological traits relating to surface roughness (e.g. the presence of hairs and unevenly textured surface) and leaf posture (revolute, involute, or flat) predicted dust load. Plant structural traits, including plant height and leaf orientation,

did not significantly contribute to dust accumulation of plants in this study. The plant trait group analysis was not forthcoming, mainly because of restrictions in the spatial distribution of species across the study area.

The physiological response of stomatal conductance was reduced in the species *Acacia aneura* and *Acacia rhodophloia* down to 50% of maximum levels under heavy mining-induced dust load (5 g/m^2). Other physiological performance measures did not indicate a significant reduction. Qualitative observations indicate that *Acacia* spp. at sites with the highest dust loads feature dead or heavily stressed specimens with high levels of leaf shedding. Understorey shrubs also exhibited plant death and stress. No significant effects were observed for the other species.

In addition, I found that plant traits, which correlated significantly to dust accumulation, also correlated to physiological function. Interestingly, this correlation is reciprocal: traits attracting the lowest dust load (‘flat’, ‘striate’ leaves) incurred the most physiological stress. This implies that the interaction between dust particles and leaf surface controls the impact on physiology, not the total dust weight. The main mechanism for a reduction of stomatal conductance is inferred to be blocking or occlusion of stomata. This is based on micro-morphological inspection of leaf surfaces, where dust is observed within the ‘striate’ grooves of the *Acacia* spp. However, a possible negative contribution of metal toxicity due to metal-rich dust incorporated into low-pH soils close to the mine cannot be entirely ruled out. This remains to be tested.

The main conclusions of my study are:

1. *A. aneura* and *A. rhodophloia* experienced reduced stomatal conductance (< 50%) at dust levels ≥ 5 g/m^2. This dust level may be seen as a critical dust threshold, in accordance with previous literature.

2. This physiological critical dust level is reached at distances of < 600 m to the mining operations. Therefore, this distance may be seen as critical impact distance of the Jack Hills mine.

3. *A. aneura* and *A. rhodophloia* are most sensitive to dust. As they are very common in semi-arid Australia, they may serve as important indicator species for anthropogenic dust and its impact on native vegetation.

4. Other plant species with the traits ‘flat, striate’ leaves may also be more susceptible to dust damage. This hypothesis could be examined to determine additional indicator species.

Acknowledgements

I would like to thank the following people and companies for their support and guidance through this Masters thesis:

- First and foremost to my supervisors Pauline Grierson and Gerald Page for providing thesis guidance, scientific discussions, technical material and lab and field support.

- Crosslands Resources Pty Ltd for generously funding the research and providing an ideal study area. Special thanks goes to former Environment Manager Lara Jefferson and Environment Advisor, Sandra Varone, for championing the research and always striving for environmental research and excellence in their operations.

- To all Crosslands site staff, most importantly Kate Eiloart and Rob Mills, for driving us around site, provided field support, answering our many questions about site geology, provided us with data and equipment and most importantly a few beers after a long hard day. A special thanks to Rob Mills for extended field help, discussions and collecting dust traps.

- Jennifer Firn from the Queensland University of Technology for providing invaluable statistical support for the final analysis and interpretation of my field data. Jennifer explained the use of LMEM for data analysis provided me with a crash course in the use of R-studio. She also provided technical material and scientific papers for the interpretation of the models. Thank you for your time and kindness.

- Kate Bowler and Kelly Paterson of the ERGO lab for both lab and field support. Thanks to Kate for instruction on laboratory techniques for soil analysis, and providing helpful ideas on other analysis techniques. Thanks to Kelly for fantastic field support and a happy smiley attitude even after 12-hour days in 30 degree plus heat.

- Bob Gilkes and Georgie Hoelbeche for dust analysis advice and analysis. Specifically to Georgie for the dust mineralogy analysis (X-Ray Diffraction) as well as some great and amusing lunch chats.

- Greg Foord and Grzegorz Skrzypek from the Australian Geochemistry centre for foliar and soil C^{13} and N^{15} Isotope analysis and providing technical literature on these methods.

- Greg Cawthray for providing advice and instruction on the use of chlorophyll fluorescence, including technical material. That plant physiological ecology field trip to Jurien certainly gave me good practice.

- My previous employer, Emerge Associates and Jason Hick, for allowing me time off work to run off to the Jack Hills every other weekend.

- To all my friends and family for providing emotional support.

- The last and most important acknowledgment goes to my awesome partner Christoph Schrank for all aspects of support. He provided guidance in the use of the scientific method, provided suggestions on how to analyse dust particle distribution, guidance in the use of ImageJ, Grapher and Corel Draw, provided scientific review and discussions and field support on my October 2011 trip. On top of this he has provided emotional support and attempted to keep me smiling the whole way. You are the best!!

CHAPTER 3. RELATIONSHIPS BETWEEN MINING DUST AND PLANT TRAITS IN VEGETATION AT THE JACK HILLS

CHAPTER 4. PHYSIOLOGICAL RESPONSE OF PLANTS TO DUST DEPOSITION AT THE JACK HILLS

CHAPTER 5. SUMMARY AND IMPLICATION

APPENDICES

LIST OF FIGURES

CHAPTER 2 FIGURES

CHAPTER 3 FIGURES

CHAPTER 4 FIGURES

LIST OF TABLES

CHAPTER 3 TABLES

CHAPTER 4 TABLES

Chapter 1. Vulnerability of Vegetation to Dust - A Review

1 Introduction

Mining activities, including quarrying, transport and the various processing operations regularly create dust problems (Farmer, 1993). Current regulatory and research initiatives relating to dust production are mainly driven by effects on human health, with much less emphasis on the potential effects of dust on the function of natural ecosystems (Grantz et al., 2003). The research presented in this thesis examines the potential impacts of dust produced by the Jack Hills iron ore mine in the Murchison region of Western Australia on the physiological functioning of the surrounding vegetation.

Dust is generated by both natural and anthropogenic processes and can impact on the functioning of vegetation either through chemical toxicity (Darley, 1966, Grantz et al., 2003) or physical interference with gas exchange and thermal regulation (Eller, 1977, Hirano et al., 1995, Sharifi et al., 1997). Natural dust (i.e., Aeolian dust that is generated and deposited by wind) is a common phenomenon in Australia and originates most frequently in arid and semi-arid regions, especially where average annual rainfall is low (< 400 mm), vegetation cover is sparse, and there are large expanses of loose, dry soil (Ekström et al., 2004, McTainsh and Strong, 2007). In these regions, large-scale desert storm events can entrain and transport millions of tons of soil over large distances (Knight et al., 1995, Greene et al., 2001). Anthropogenic disturbances, such as mining and agriculture, also create dust, which is generated from removal of vegetation, overgrazing and disturbance of the soil surface. Thus, while vegetation in the arid and semi-arid zone may be subject to a natural background of dust exposure, the influence of the anthropogenic dust generated from mining on plant health and function has not been quantified locally.

The mining industry in Western Australia has undergone rapid expansion over recent years primarily driven by demand for raw materials from China and others parts of Asia (Department of Industry and Resources, 2009, Minerals Council of Australia, 2010). Whilst the mining operations themselves occupy a relatively small physical footprint in the Australian landscape, dust generated by the various operations including digging and blasting of soil and rock, through to the transportation, handling and processing of ores (Farmer, 1993, Petavratzi et al., 2005), can create a 'dust footprint' over a much larger area (Ong et al., 2003). Moreover, a considerable network of rail lines, roads and other infrastructure is often associated with mining developments that also generate dust. While the air around these sites are often monitored for aspects related to human health, little is known of the size of the dust footprint of various mining operations and there is a paucity of information available to evaluate the impact of dust generation on the surrounding vegetation.

Dust emissions are regulated in Australia through national air-quality standards for atmospheric pollutants and particulate matter (PM 10 and PM 2.5) (DSEWPAC, 2012). These standards have been developed based on human health studies. At a state level, impacts on the Western Australian environment are considered as part of an Environmental Impact Assessment (EIA) process and enforced under the 'Environmental Protection Act 1989' (EP Act). If the activity under assessment is considered to result in dust pollution that may impact on the environment, the Environmental Protection Authority (EPA) will propose that conditions be placed on the project. These conditions are legally enforceable under the EP Act and usually require an Environmental Management Plan (EMP) that includes a Dust Management Plan (DMP). However, given the scarce knowledge of how dust affects native vegetation in Australia, it is very difficult to prepare a robust DMP.

Studies undertaken outside of Australia have demonstrated that dust can impact on plant species through both physical and chemical means (Darley, 1966, Ricks and Williams, 1974, Farmer, 1993, Hirano et al., 1995, Sharifi et al., 1997, Grantz et al., 2003). However, dust is very heterogeneous, varying in chemical composition and physical characteristics among sites, which in turn influences the nature of impacts on plant species (Farmer, 1993, Grantz et al., 2003). In addition, even closely related plant species can respond differently to dust based on their mechanisms or strategies to deal with dust exposure and/or the dusts chemical or physical properties (Kuki et al., 2008b). For example, two species of *Restringia* vegetation, *Schinus terebinthifolius* Raddi and *Sophora tomentosa* L., exhibited differing responses to acid mist and iron particulate matter treatments, with results suggesting that *S. terebinthifolius* avoided stress, while *S. tomentosa* used antioxidant enzyme systems to partially neutralize oxidative stress (Kuki et al., 2008b). Therefore, it is difficult to conclusively extrapolate results from these studies to the potential effects various dust types have on Australian plants, and thus the management of this dust as part of mining developments and DMP's.

Dust generated by hard-rock mining, including iron-ore, is often chemically inert (Farmer, 1993). Thus, in these environments, the physical interaction of dust with vegetation will be more important than chemical toxicity effects. However, there have been limited field studies on the physical impacts of dust on vegetation, especially in semi-arid and arid environments where high levels of natural atmospheric dust are present and plant species are adapted to such conditions (see, for example Sharifi et al., 1997, Gleason et al., 2007). Even less information is available about the effects of dust on Australian plant species (see, for example Paling et al., 2001, Chaston and Doley, 2006, Butler, 2009). This is of particular concern in regions where the flora is not well described, such as the banded

ironstone formation (BIF) ranges in the Murchison Region of Western Australia (Department of Industry and Resources, 2009, Gibson et al., 2007), which are currently being mined, or considered for future mining of iron ore. These BIF ranges possess a high percentage of endemic plant species and restricted vegetation types (Gibson et al., 2007, Department of Industry and Resources, 2009) that have unknown vulnerability to dust deposition that may arise from mining activities.

In this chapter, I present an overview of the nature of dust and its potential impacts on vegetation. First, I define what constitutes 'dust'. I then explore the varied effects dust can have on vegetation, emphasising physical impacts. I then briefly outline the traits that may influence the susceptibility of different plant species or groups of species to dust deposition. The discussion provides the background that has formed the basis for the subsequent research. The broad aims of my research project are presented at the end of the review.

2 Dust

Dust is defined as terrestrial sediment < 100 micron (μm) in size and therefore small enough to be lifted and transported in Aeolian suspension (McTainsh and Strong, 2007). The upper size limit of dust reported in the literature ranges from < 63 μm (Bullard and Livingstone, 2009) to < 100 μm (IUPAC, 1990, McTainsh and Strong, 2007). Once dust particles are suspended in the atmosphere, they can be carried by wind at various heights and over a range of distances (Bullard and Livingstone, 2009), from local transport of a few hundred metres, to regional and global transport of thousands of kilometres (McTainsh and Strong, 2007).

The distances that dust travels (i.e. the ability of particles to remain airborne) and its subsequent deposition on vegetation depend upon complex interactions between the physical properties of the dust particles, atmospheric conditions and land-surface topography (Grantz et al., 2003, Litschke and Kuttler, 2008). For example, the size distribution of dust particles in the atmosphere depends strongly on the time lapsed since emission (Pye, 1987). Larger and heavier particles drop out of suspension first through the action of gravity (Bullard and Livingstone, 2009), with long-range dust particles, generally measured to be < 20 μm in size, being carried long distances, such as across continents (Gillette, 1981, Prospero, 1999, Shao, 2008). Atmospheric conditions including wind speed, rainfall and atmospheric pressure also influence the velocity of dust and the distance travelled (Shao, 2008, Litschke and Kuttler, 2008, Bullard and Livingstone, 2009). For example, increased air humidity causes the hygroscopic dust particles to attached to water, thus chaging the dust properties (e.g. size) and thus their deposition pattern (Winkler, 1988). Topographic relief and surface features including vegetation cover can influence dust movement and deposition rates, by creating macro- and micro-surface roughness, allowing dust particles to impact with vegetation, perturbation of airflow and reduction in wind speed, causing dust particles to drop from suspension (Armbrust et al., 1964, Hosker and Lindberg, 1982). Vegetation also has the ability to capture (or filter) dust particles from the air based on the structural features of the vegetation including height, width and leaf canopy density (Chepil and Woodruff, 1954, Freer-Smith et al., 1997, Raupach and Leys, 1999, Beckett et al., 2000, Litschke and Kuttler, 2008). For example, a species of pine (*Pinus nigra* Aiton) and cypress (x *Cupressocyparis leylandii* (A.B.Jacks. & Dallim.) Dallim.) increased dust particle capture due to their finer, more complex structure of the foliage (Beckett et al., 2000).

2.1 Mining dust: Transport and deposition

In Australia, the deposition of mining dust on surrounding vegetation has been well observed, with visible dust coating leaves adjacent to disturbance areas (Paling et al., 2001, Ong et al., 2003, Butler, 2009). The highest concentrations of dust on vegetation has been recorded directly adjacent to the emission source, with dust concentrations declining with distance from disturbance (Ong et al., 2003, Butler, 2009). Dust from mining operations has been identified on vegetation up to 1-3 km from the point of origin, with diffuse dust still being recorded up to 15 km from the point source (Vardaka et al., 1995, Ong et al., 2003, Kuki et al., 2008a). For example, iron ore dust was deposited onto the leaves of mangrove trees (*Avicennia marina* (Forssk.) Vierh.) up to 2 km from a port handling facility in Port Headland, Western Australia, although the heaviest deposition was recorded immediately adjacent to the port (Ong et al., 2003). Likewise, a study of iron ore dust deposition onto the leaves of *Restringia* ecosystems in coastal areas of Brazil identified the highest loadings within 1 km from the iron ore facility, with diffuse dust still being recorded 15 km away (Kuki et al., 2008a). A limestone dust generated by a quarry near Thessaloniki, Greece, was detected on leaves of scarlet oak (*Quercus coccifera* L.) up to 3 km from the quarry, with leaves within 300 m of the mine collecting 15 times the amount of dust as the 3 km site (Vardaka et al., 1995).

Studies of dust transport and deposition onto vegetation adjacent to linear infrastructure, e.g. road and rail lines, have reported a non-linear decline in dust load away from the road/rail source (Everett, 1980, Gleason et al., 2007, Butler, 2009). For example, dust generated from an unsealed road in Alaska, recorded highest deposition rates immediately adjacent to the road and declined logarithmically over a distance of 1000 m from the roadside (Everett, 1980). Similarly, a study from Hawaii measured dust load that followed a

two-parameter exponential decay model with distance from an unsealed road up to a distance of 40 m (Gleason et al., 2007). A non-linear decline was also recorded between 0-100 m of an unsealed haul road in the Pilbara region of Western Australia, with particles > 30 μm dropping out of suspension between 5-35 m from the road (Butler, 2009).

3 Dust impacts on vegetation

Dust associated with hard rock mining, such as iron ore, is considered to be relatively chemically inert (Farmer, 1993, Chaston and Doley, 2006, Petavratzi et al., 2005). Therefore, in this review I will focus on the physical effects of dust on plant health and function. Dust can physically affect plant health and function in a number of ways: i) leaf tissue damage through abrasion, ii) blocking the plants stomata, iii) dust accumulation leading to absorbance of incident radiation and/or shading of the leaf surface.

3.1 Leaf tissue damage through abrasion

Accumulation of dust on the leaf surface can damage leaf tissues or cuticular waxes through abrasion or adsorption/absorption of a component of the wax (Eveling and Bataillé, 1984, Eveling, 1986, Gleason et al., 2007). For example, leaves and petals of glasshouse and field-grown plants (e.g. *Phaseolus coccineus* L., *Coleus blumei* Benth., *Urtica dioica* L., and *Pelargonium* sp.) treated with small particles (< 10 μm) of quartz and clay significantly increased water loss (Eveling and Bataillé, 1984, Eveling, 1986). These small particles caused epidermal cell and cuticle damage through mechanical abrasion and/or adsorbing or absorbing a component such as wax from the cuticle when deposited in aqueous solution (Eveling and Bataillé, 1984). Larger particles (> 10 μm in diameter) of silicon carbonate and larger polystyrene particles did not result in mechanical abrasion and increased water loss. This implies that dust particles below 10 μm in size increase leaf

tissue damage by abrasion when deposited with water (Eveling and Bataillé, 1984, Eveling, 1986). Dust applied with water is also known as 'wet deposition' (Grantz et al., 2003). The exception to this finding was encountered in the plant species *Tradescantia pendula* (Schnizl.) D.R. Hunt (syn. *Zebrina pendula* (Schnizl)) and *Pinus sylvestris* L., which were also tested in the treatment (Eveling and Bataillé, 1984). Both species have tougher leaf cuticles and therefore were not affected by mechanical abrasion. This indicates that mechanical abrasion from dust particles of small size (<10 μm) depends on leaf cuticle characteristics, with tougher leaf cuticles not affected. As the plants growing in semi-arid and arid regions of Western Australian are adapted to the hot, dry climate, many species possess sclerophyllous leaves (small, hard, thick and waxy cuticles), or have other adaptations such as thick layers of hairs or resins (Seddon, 1974, Chaves et al., 2002). Consequently, semi-arid and arid species may be less likely to be impacted through physical abrasion.

3.2 Blocked stomata

Dust can block or partially occlude stomata (Ricks and Williams, 1974, Borka, 1990, Hirano et al., 1995, Vardaka et al., 1995). Cement dust applied to the leaves of sunflowers (*Helianthus annuus* L.) partially closed the stomata by creating cement plugs (Borka, 1990). As cement dust typically has very small particle sizes, with 80-90% of particles being less than 30 μm in diameter (Darley, 1966), the dust is more likely to become lodged in stomatal openings, as stomata of plants have an upper aperture size of 38 x 8 μm (Eckerson, 1908). Consequently, the application of cement dust reduced transpiration and respiration rate in the sunflower leaves (Borka, 1990). The low rate of evapotranspiration caused internal leaf temperature to increase by 8-10 °C (Borka, 1990). A later study, which applied dust of Kanto Loam (KL) and Carbon Black (CB) to the leaves of cucumber

(*Cucumis sativus* L.) and kidney bean (*Phaseolus vulgaris* L.), resulted in a reduction in the plants stomatal conductance under lights, and an increase in stomatal conductance in the dark (Hirano et al., 1995). The effect became greater with a reduction in particle size of the dust. This change in stomatal conductance was thought to be caused by dust clogging stomata open in the light, and preventing them from closing in the dark. The effect was only observed if the stomata were open at the time of dust application (Hirano et al., 1995).

Reduced stomatal conductance due to stomatal blockage may have a particularly strong effect on the survival of plants in semi-arid and arid environments, which are already subject to harsh conditions including high temperatures and water scarcity. As mentioned, blocked stomata can reduce the ability of a plant to transpire, thus increasing internal leaf temperature (Borka, 1990), which can result in a down regulation in photosynthesis (Chaves et al., 2002). At the same time, blocked stomata could also lead to a reduction in carbon uptake by the leaves, leading to a down regulation of photochemistry, and eventually photosynthetic capacity and growth (Chaves et al., 2002). Alternatively, and likely more detrimental in semi-arid and arid environments, dust may prevents stomata from closing (Hirano et al., 1995). Stomatal closure is an early response to prevent extensive water loss in semi-arid and arid climates (Chaves et al., 2002). Excessive water loss can lead to cell dehydration, xylem cavitation and plant death (Chaves et al., 2003). Regulation of stomatal function is paramount to Water Use Efficiency (WUE) of plants in semi-arid and arid environments (Ullmann, 1989, El-Gendy et al., 2012), therefore disruption of this function may severely affect their ability to persist in these climates.

Not all plant species, however, are equally susceptible to dust-induced stomatal blockage. Leaf morphology and surface properties influence the accumulation and interaction of dust with the leaf (Paling et al., 2001, Naidoo and Naidoo, 2005). For example, grey mangrove

(*A. marina*) adjacent to an iron ore loading facility in Western Australia (Paling et al., 2001) and a coal loading terminal in Richards Bay, South Africa (Naidoo and Naidoo, 2005), did not show any evidence of stomatal blockage because a dense mat of trichomes (hairs) prevented the ingress of dust particles into stomata. Other leaf characteristics such as the density and arrangement of stomata on the leaf surface (e.g. higher density of stomata on the abaxial surface of the leaf, sunken stomata or anatomical orientation of stomata) also influence the ability of dust particles to obstruct stomata (Hirano et al., 1995, Doley, 2006). In addition, the size and shape of the stomata and the size and shape of the dust particles will determine the ability of those particles to be lodged and the packing density of those particles in stomata.

3.3 Dust accumulation on the leaf surface

Dust deposited onto leaf surfaces can increase the absorptivity of light, thus leading to an increase in leaf temperature by up to 5 °C (Eller, 1977, Chaston and Doley, 2006). The capacity of dust to influence leaf temperature through heat absorption depends on the absorptivity of the particular dust, or its light extinction coefficient (fraction of light absorbed per unit weight of material per square metre) (Chaston and Doley, 2006). The light extinction coefficient thus expresses how much light can pass through the dust layer to the photosynthetic apparatus below. Therefore, dust mineralogy, colour, particle size distribution and thickness of coverage influence the extent of heating and therefore leaf temperature change (Chaston and Doley, 2006). Considering that photosynthesis may vary considerably within the change of a few degrees, an increase in temperature associated with dust deposition may have a large influence on net photosynthesis (Lambers et al., 2008).

How increased light absorption affects photosynthetic activity and leaf temperature has been investigated in a number of experiments conducted under laboratory conditions

(Hirano et al., 1995, Chaston and Doley, 2006) and in situ in a semi-arid climate (Sharifi et al., 1997). In the laboratory, Hirano et al. (1995) confirmed that the absorption of incident radiation by dust increased leaf temperature with an increase of either dust loading or light intensity. Dark-coloured CB dust increased leaf temperature much more than light-coloured KL dust, with a difference of 2-3 °C at 1.3 g/m^2 dust loading. This in turn affected the photosynthetic rate of plants in accordance with its response curve to leaf temperature (Hirano et al., 1995).

Another effect of dust loading on photosynthesis is the shading effect. If the dust shades the leaf below its light saturation point, photosynthesis is inhibited. The shading effect depends on the light saturation point of the particular plant species and the shading coefficient of the particular dust. The shading coefficient becomes larger when finer dust is applied, leading to larger packing density, and when deposition rates increase (Hirano et al., 1990, Chaston and Doley, 2006, Sharifi et al., 1997).

4 Plant traits and dust deposition

Plant 'traits', particularly plant structural and leaf morphological traits, influence the amount of dust deposited on or captured by a species (Chamberlain, 1975, Little, 1977, Yunus et al., 1985, Raupach and Leys, 1999, Beckett et al., 2000, Butler, 2009). Plant structural characteristics that influence dust-capture include plant height, canopy width and density, leaf size and shape as well as branch and leaf orientation (Raupach and Leys, 1999, Beckett et al., 2000). In a modelled investigation into different types of vegetation buffers on dust movement, taller plants with a higher Leaf Area Index (LAI) captured significantly more dust, compared to shorter vegetation with a lower LAI (Raupach and Leys, 1999). LAI is the total area of leaf surface per unit ground surface area (Maarel, 2005). A high

LAI can represent smaller, finer and more highly packed leaves which provide a large surface area for dust deposition and thus better 'filtering ability' (Raupach and Leys, 1999). This hypothesis was supported by a wind tunnel experiment where five tree species were tested for their particle capture ability (Beckett et al., 2000) The study concluded that the species of pine (*Pinus nigra*) and cypress (x *Cupressocyparis leylandii*) increased particle capture due to their finer, more complex structure of the foliage (Beckett et al., 2000).

Leaf morphological features that influence dust deposition include epidermal characteristics, the presence of resins or exudates and hair (trichome) type and cover (Little, 1977, Brabec et al., 1981, Yunus et al., 1985, Paling et al., 2001, Naidoo and Naidoo, 2005, Butler, 2009). For example, plants with rough and hairy leaves collected dust particles in the 5.0 μm size fraction seven times more effectively than smooth leaves (Little, 1977). Two mangrove species with a thick mat of hairs, grey mangrove (*A. marina*) and hibiscus (*Hibiscus tiliaceus* L.*)*, increased coal dust loading on the abaxial surface of the leaf compared to two mangrove species with glabrous leaves (*Bruguiera gymnorhiza* (L.) Savigny and *Rhizophora mucronata* Lam.) (Naidoo and Naidoo, 2005). Furthermore, the sticky brine secreted by the salt glands of all three mangrove species increased coal dust accumulation (Naidoo and Naidoo, 2005). A study along an unsealed road in the Pilbara region of Western Australia found that dust accumulation was up to 40 times higher on leaves with a rough surface or with dense hairs (e.g. *Eremophila forrestii* F.Muell.) compared to plants with glabrous leaves (Butler, 2009).

As plant traits are co-occurring within a species, often a combination of traits are described as influencing dust accumulation. For example, taller plants with a higher LAI (Raupach and Leys, 1999), mangrove species with both a hairy leaf and one that secretes a sticky brine (Naidoo and Naidoo, 2005). Therefore as part of this study, plants have been assessed

not only on the individual traits that they possess, but also grouped based on their co-occurring structural and morphological traits.

5 Plant Functional Types

A grouping of plant species sharing morphological and functional traits has been termed a 'Plant Functional Type' (PFT) (Maarel, 2005). The main purpose of a PFT is to explain the functioning of a group of plants in an ecosystem at the vegetation scale (local, regional or global), rather than on an individual taxonomic level (i.e. simplification of floristic complexity) (Box, 1981, Box, 1996, Pillar, 1999, Grime, 2001, Lavorel et al., 2007). In disturbance ecology, the PFT concept is used to predict the vulnerability of plant groups to disturbance factors, such as natural or land use related events including fire or grazing, on the basis of shared characteristics (Lavorel and Cramer, 1999, Lavorel et al., 1997).

Structural and morphological traits can be used to establish PFTs because plant morphology reflects the adaptive strategy of a plant in response to factors such as, for example, climate and disturbance (Raunkiaer, 1935, Knight and Loucks, 1969, Box, 1981, Box, 1996, Lavorel and Cramer, 1999, Mueller-Dombois and Ellenberg, 1974). Therefore, it is conceivable that plants with similar structural and morphological traits in my research area also developed similar response mechanisms to dust loading. This hypothesis was tested in a previous study in the Pilbara (Butler, 2009). In this study plants were grouped based on similar traits, and it was shown that these groups had differing propensities for dust accumulation (Butler, 2009). For example, shrubs, < 2 m tall with a thick dense covering of hairs, represented by the species *Eremophila forrestii*, collected up to 40 times the amount of dust than the other plant groups. However, there was no correlational relationship between plant groupings based on their traits and physiological response to

dust loading. This finding highlights the intrinsic difficulty of predicting function from morphology alone, a fundamental challenge of the PFT approach (Lavorel et al., 2007). The data collected in this study will permit an independent test of Butler's (2009) hypothesis, and this is one of the aims of my study. It is therefore hypothesised that plant species that possess particular structural and leaf morphological traits, which increase dust loading, would also determine the plants physiological response to dust loading, based on those traits, thus providing PFTs for future prediction of impacts from dust.

6 Aims of this thesis

The main aim of my thesis is to test if mining-derived dust deposited onto plants surrounding the Jack Hills iron ore mine has a negative impact on physiological function and therefore plant health. I hypothesis that species that possess plant structural and leaf morphological 'traits', or a combination of 'traits', which influence dust accumulation will be equally susceptible to physiological stress imposed by the dust. Plants, which possess these 'traits' or combination of 'traits', could then be used as indicators for future environmental monitoring of dust impacts on plants. To achieve these goals, I have:

1. Measured the spatial and temporal dust deposition 'footprint' of the mine and characterised the dust in terms of its grain size distribution and mineralogy.

2. Identified plant species around the mine and classified them according to structural and leaf morphological 'traits' chosen *a priori* that may influence dust deposition.

3. Quantified dust on the leaves of plants surrounding the mine.

4. Analysed statistically if and how plant traits relate to dust loading using Linear Mixed-Effect Modelling (LMEM).

5. Grouped the plants species according to plant ‘traits’ using hierarchical cluster analysis and determined if the plant trait groups relate to dust loading using LMEM.

6. Measured relevant environmental factors at established site, namely electrical conductivity of soil (soil EC), soil pH, soil moisture, soil nitrate and ammonium concentration and topography.

7. Measured the in-situ physiological response (stomatal conductance, chlorophyll fluorescence and carbon isotope ratios) of plants to dust loading.

8. Applied LMEM to examine the correlation between physiological responses of plants and dust load, with reference to plant traits.

Chapter 2 describes the study area and ecological setting of the Jack Hills, including an overview of landform and geology, climate and flora. The experimental sections are in Chapters 3 and 4. Chapter 3 characterises the vegetation surrounding the Jack Hills mine based on structural and leaf morphological ‘traits’ chosen *a priori* and provides a classification of individual species in to groups based on plant ‘traits’. Chapter 3 also quantifies the physical and mineralogical characteristics of the dust, the dust ‘footprint’ and quantifies the dust loading on plants across the site. Chapter 4 assesses the physiological response of plants to dust loading and determines if physiological response is related to plant ‘traits’ or groups of plants based on ‘traits’ (i.e. functional types). Chapter 5 provides a final discussion of the overall findings of the research.

7 References

ARMBRUST, D. V., CHEPIL, W. S. & SIDDOWAY, F. H. 1964. Effects of Ridges on Erosion of Soil by Wind. *Soil Science Society of America Proceedings,* 28**,** 557-560.

BECKETT, K. P., FREER-SMITH, P. H. & TAYLOR, G. 2000. Particulate pollution capture by urban trees: Effects of species and windspeed. *Global Change Biology,* 6**,** 995-1103.

BORKA, G. 1990. The effect of cement dust pollution on growth and metabolism of Helianthus annuus. *Environmental Pollution Series A, Ecological and Biological,* 22**,** 75-79.

BOX, E. O. 1981. *Macraclimate and Plant Forms: an Introduction to Predictive Modeling in Phytogeography,* Junk, The Hague.

BOX, E. O. 1996. Plant Functional Types and Climate at the Global Scale. *Journal of Vegetation Science,* 7**,** 309-320.

BRABEC, E., KOVÁR, P. & DRÁBKOVÁ, A. 1981. Particle deposition in three vegetation stands: A seasonal change. *Atmospheric Environment (1967),* 15**,** 583-587.

BULLARD, J. E. & LIVINGSTONE, I. 2009. *Geomorphology of Desert Environments*, Springer Science.

BUTLER, R. 2009. *Vulnerability of plant functional types to dust deposition in the Pilbara, NW Australia.* Bachelor of Science (Environmental Science) (Honours), The University of Western Australia.

CHAMBERLAIN, A. C. 1975. *The movement of particles in plant communities* New York, Academic Press.

CHASTON, K. & DOLEY, D. 2006. Mineral particulates and vegetation: Effects of coal dust, overburden and flyash on light interception and temperature *Clean air and environmental quality,* 40**,** 40-44.

CHAVES, M. M., MAROCO, J. P. & PEREIRA, J. S. 2003. Understanding plant responses to drought - from genes to the whole plant. *Functional Plant Biology,* 30**,** 239-264.

CHAVES, M. M., PEREIRA, J. S., MAROCO, J., RODRIGUES, M. L., RICARDO, P. P., OSORIO, M. L., CARVALHO, I., FARIA, T. & PINHEIRO, C. 2002. How plants cope with water stress in the field. Photosynthesis and Growth. *Annals of Botany,* 89**,** 907-916.

CHEPIL, W. S. & WOODRUFF, N. P. 1954. Estimations of wind erodibility of field surfaces. *Journal of Soil and Water Conservation,* 9**,** 257-265.

DARLEY, E. F. 1966. Studies on the effect of cement-kiln dust on vegetation. *Journal of Air Pollution Control Association,* 16**,** 145-50.

DEPARTMENT OF INDUSTRY AND RESOURCES 2009. Strategic review of the banded iron formation ranges of the midwest and goldfields. *In:* DEPARTMENT OF INDUSTRY AND RESOURCES (ed.).

DOLEY, D. 2006. Airbourne particulates and vegetation: Review of physical interactions. *Clean Air and Environmental Quality,* 40**,** 36-42.

DSEWPAC. 2012. *Air quality standards* [Online]. Available: http://www.environment.gov.au/atmosphere/airquality/standards.html 2011].

ECKERSON, S. H. 1908. The number and size of the stomata. *Botanical Gazette,* 46**,** 221-224.

EKSTRÖM, M., MCTAINSH, G. H. & CHAPPELL, A. 2004. Australian Dust Storms: Temporal Trends and Relationships with Synoptic Pressure Distributions (1960-99). *International Journal of Climatology,* 24**,** 1581-1599.

EL-GENDY, S. A., ABD ELMONIEM, E. M., AL-ABUDALLA, M. M. & EISA, S. S. 2012. Morphological and Physiological Responses of *Acacia saligna* (Labill.) to Water Stress *Australian Journal of Basic and Applied Sciences,* 6**,** 90-97.

ELLER, B. M. 1977. Road dust induced increase of leaf temperature. *Environmental Pollution (1970),* 13**,** 99-107.

EVELING, D. W. 1986. Scanning Electron Microscopy of Damage by Dust Deposits to Leaves and Petals. *Botanical Gazette,* 147**,** 159-165.

EVELING, D. W. & BATAILLÉ, A. 1984. The effect of deposits of small particles on the resistance of leaves and petals to water loss. *Environmental Pollution Series A, Ecological and Biological,* 36**,** 229-238.

EVERETT, K. R. 1980. Distribution and properties of road dust along the northern portion of the haul road. *In:* BROWN, J. & BERG, R. (eds.) *Environmental Engineering and Ecological Baseline Investigations along the Yukon River - Purdhoe Bay Haul Road.* CRREL: US Army Cold Regions Research and Engineering Laboratory.

FARMER, A. M. 1993. The effects of dust on vegetation--a review. *Environmental Pollution,* 79**,** 63-75.

FREER-SMITH, P. H., HOLLOWAY, S. & GOODMAN, A. 1997. The uptake of particulates by an urban woodland: Site description and particulate composition. *Environmental Pollution,* 95**,** 27-35.

GIBSON, N., COATES, D. J. & THIELE, K. R. 2007. Taxonomic research and the conservation status of flora in the Yilgarn Banded Iron Formation ranges. *Nuytsia,* 17**,** 1-12.

GILLETTE, D. A. 1981. Production of dust that mat be carried great distances. *Geological Society of America,* 186**,** 11-26.

GLEASON, S., FAUCETTE, D., TOYOFUKU, M., TORRES, C. & BAGLEY, C. 2007. Assessing and Mitigating the Effects of Windblown Soil on Rare and Common Vegetation. *Environmental Management,* 40**,** 1016-1024.

GRANTZ, D. A., GARNER, J. H. B. & JOHNSON, D. W. 2003. Ecological effects of particulate matter. *Environment International,* 29**,** 213-239.

GREENE, R., GATEHOUSE, R., SCOTT, K. & CHEN, X. Y. 2001. Aeolian dust - implications for Australian mineral exploration and environmental management. *Australian Journal of Soil Research,* 39.

GRIME, J. P. 2001. *Plant Strategies, Vegetation Processes, and Ecosystem Properties,* Chichester, England, John Wiley & Sons, Ltd.

HIRANO, T., KIYOTA, M. & AIGA, I. 1990. The physical effects of dust on photosynthetic rate of plant leaves. . *Agricultural and Forest Meteorology,* 46**,** 1-7 (in Japanese with English summary).

HIRANO, T., KIYOTA, M. & AIGA, I. 1995. Physical effects of dust on leaf physiology of cucumber and kidney bean plants. *Environmental Pollution,* 89**,** 255-261.

HOSKER, R. P. & LINDBERG, S. E. 1982. Review: atmospheric deposition and plant assimilation of gases and particles. *Atmospheric Environment,* 16**,** 889-910.

IUPAC 1990. Glossary of atmospheric chemistry terms. *Pure and Applied Chemistry,* 66**,** 2167-2219.

KNIGHT, A. W., MCTAINSH, G. H. & SIMPSON, R. W. 1995. Sediment loads in an Australian dust storm: implications for present and past dust processes. *Catena,* 24**,** 195-213.

KNIGHT, D. H. & LOUCKS, O. L. 1969. A Quantitative Analysis of Wisconsin Forest Vegetation on the Basis of Plant Function and Gross Morphology. *Ecology,* 50**,** 219-234.

KUKI, K., OLIVA, M. & PEREIRA, E. 2008a. Iron Ore Industry Emissions as a Potential Ecological Risk Factor for Tropical Coastal Vegetation. *Environmental Management,* 42**,** 111-121.

KUKI, K. N., OLIVA, M. A., PEREIRA, E. G., COSTA, A. C. & CAMBRAIA, J. 2008b. Effects of simulated deposition of acid mist and iron ore particulate matter on photosynthesis and the generation of oxidative stress in Schinus terebinthifolius Radii and Sophora tomentosa L. *Science of The Total Environment,* 403**,** 207-214.

LAMBERS, H., CHAPIN, F. S. & PONS, T. L. 2008. *Plant Physiological Ecology*, New York, NY, USA, Springer New York.

LAVOREL, S. & CRAMER, W. 1999. Plant Functional Types and Disturbance Dynamics. *Journal of Vegetation Science,* 10**,** 603-730.

LAVOREL, S., DIAZ, S., HANS, J., CORNELISSEN, C., GARNIER, E., HARRISON, S. P., MCINTYRE, S., ROUMET, C. & URCELAY, C. 2007. Plant Functional Types: Are we getting any closer to the Holy Grail? *In:* CANADELL, J. G., PATAKI, D. & PITELKA, L. (eds.) *Terrestrial Ecosystems in a Changing World.* Berlin Heidelberg: Sprimger-Verlag.

LAVOREL, S., MCINTYRE, S., LANDSBERG, J. & FORBES, T. D. A. 1997. Plant functional classifications: from general groups to specific groups based on response to disturbance. *Trends in Ecology & Evolution,* 12**,** 474-478.

LITSCHKE, T. & KUTTLER, W. 2008. On the reduction of urban particle concentration by vegetation - a review. *Meteorologische Zeitschrift,* 17**,** 229-240.

LITTLE, P. 1977. Deposition of 2.75, 5.0 and 8.5 μm particles to plant and soil surfaces. *Environmental Pollution,* 12**,** 293-305.

MAAREL, E. V. 2005. Vegetation Ecology - an overview. *In:* MAAREL, E. V. (ed.) *Vegetation Ecology.* Oxford, UK: Blackwell Science Ltd.

MCTAINSH, G. & STRONG, C. 2007. The role of aeolian dust in ecosystems. *Geomorphology,* 89**,** 39-54.

MINERALS COUNCIL OF AUSTRALIA 2010. The Australian Minerals Industry and the Australian Economy. *In:* AUSTRALIA, M. C. O. (ed.).

MUELLER-DOMBOIS, D. & ELLENBERG, H. 1974. *Aims and Methods of Vegetation Ecology,* New Jersey, U.S.A., The Blackburn Press.

NAIDOO, G. & NAIDOO, Y. 2005. Coal Dust Pollution Effects on Wetland Tree Species in Richards Bay, South Africa. *Wetlands Ecology and Management,* 13**,** 509-515.

ONG, C. C. H., CUDAHY, T. J., CACCETTA, M. S. & PIGGOTT, M. S. 2003. Deriving quantitative dust measurements related to iron ore handling from airborne hyperspectral data. *Mining Technology,* 112**,** 158-163.

PALING, E. I., HUMPHRIES, G., MCCARDLE, I. & THOMSON, G. 2001. The effects of iron ore dust on mangroves in Western Australia: Lack of evidence for stomatal damage *Wetlands Ecology and Management,* 9**,** 363-370.

PETAVRATZI, E., KINGMAN, S. & LOWNDES, I. 2005. Particulates from mining operations: A review of sources, effects and regulations. *Minerals Engineering,* 18.

PILLAR, V. D. 1999. On the identification of optimal plant functional types. *Journal of Vegetation Science,* 10**,** 631-640.

PROSPERO, J. M. 1999. Long-range transport of mineral dust in the global atmosphere: Impact of African dust on the environment of the southeastern United States. *Proceedings of the National Academy of Sciences of the United States of America,* 96**,** 3396-3403.

PYE, K. 1987. *Aeolian Dust and Dust Deposition,* London, Academic Press.

RAUNKIAER, C. 1935. *The life forms of plants and statistical plant geography,* Oxford, Oxford University Press.

RAUPACH, M. R. & LEYS, J. F. 1999. The efficacy of vegetation in limiting spry drift and dust movement. Canberra: CSIRO.

RICKS, G. R. & WILLIAMS, R. J. H. 1974. Effects of atmospheric pollution on deciduous woodland part 2: Effects of particulate matter upon stomatal diffusion resistance in leaves of *Quercus petraea* (Mattuschka) leibl. *Environmental Pollution (1970),* 6**,** 87-109.

SEDDON, G. 1974. Xerophytes, xeromorphs and sclerophylls: the history of some concepts in ecology. *Biological Journal of the Linnean Society,* 6**,** 65-87.

SHAO, Y. 2008. *Physics and Modelling of Wind Erosion*, Springer Science.

SHARIFI, M. R., GIBSON, A. C. & RUNDEL, P. W. 1997. Surface Dust Impacts on Gas Exchange in Mojave Desert Shrubs. *Journal of Applied Ecology,* 34**,** 837-846.

ULLMANN, I. 1989. Stomatal conductance and transpiration of *Acacia* under field conditions: similarities and differences between leaves and phyllodes. *Structure and Function of Trees,* 3**,** 45-56.

VARDAKA, E., COOK, C. M., LANARAS, T., SGARDELIS, S. P. & PANTIS, J. D. 1995. Effects of dust from a limestone quarry on the photosynthesis of Quercus coccifera, an evergreen

schlerophyllous shrub. *Bulletin of Environmental Contamination and Toxicology,* 54**,** 414-419.

WINKLER, P. 1988. The Growth of Atmospheric Aerosol particles with Relative Humidity. *Physica Scripta,* 37**,** 223-230.

YUNUS, M., DWIVEDI, A. K., KULSHRESHTHA, K. & AHMAD, K. J. 1985. Dust loadings on some common plants near Lucknow City. *Environmental Pollution Series B, Chemical and Physical,* 9**,** 71-80.

Chapter 2. The Jack Hills Study Area

1 Introduction to the Jack Hills

The Jack Hills is one of a series of ancient banded ironstone formation (BIF) ranges within the Murchison region of Western Australia, located 350 km inland from the Western Australian coastline (Figure 1). It forms a ~ 70 km long, northeast trending greenstone and meta-sedimentary belt (Spaggiari, 2007), which is best known for hosting the Earth's oldest detrital zircons, which are > 4.2 billion years old (Compston and Pidgeon, 1986, Wilde et al., 2000).

This study has been undertaken at the northeastern end of Jack Hills, on the northwestern side of the range. Sampling sites are located in a roughly rectangular region covering ~1200 ha, the long sides of which are parallel to the Jack Hills range (Figure 1). A line connecting the peaks Mount Matthew, Mount Hale, and further northeast, in line with the mining camp, defines the southeastern long side of the study area, which is ~ 5 km in length. From there, it extends ~ 2.4 km down the range to the northwest onto the surrounding Murchison plain, including the Crosslands Resources mining operations at the foot of the range (Figure 1). A photo of the northeastern end of the study area, looking northwest down onto the mining camp and surrounding floodplain is provided as Figure 2. Crosslands Resources currently undertakes iron ore extraction within this part of the range utilising open cut mining techniques to target the Magnetite and Hematite within the BIF.

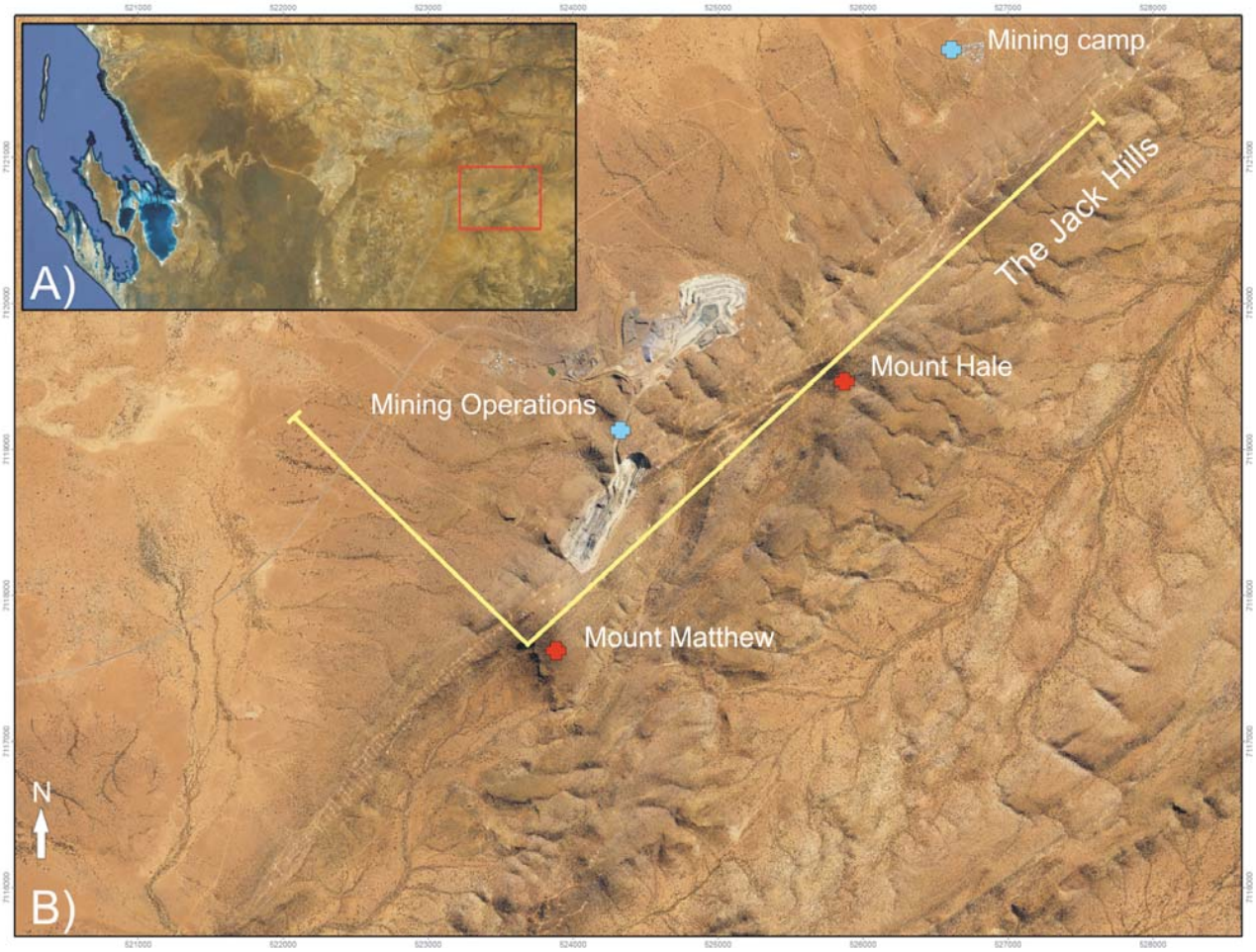

Figure 1: The Jack Hills study area located at approximately, 52400 m E and 7119000 m N (GDA ’94, UTM, Z 50J). The red box in insert A) shows the location of the Jack Hills in relation to the Western Australia Coastline, B) shows the study area, with sampling for this study occurring within a rectangular area, denoted by the yellow lines.

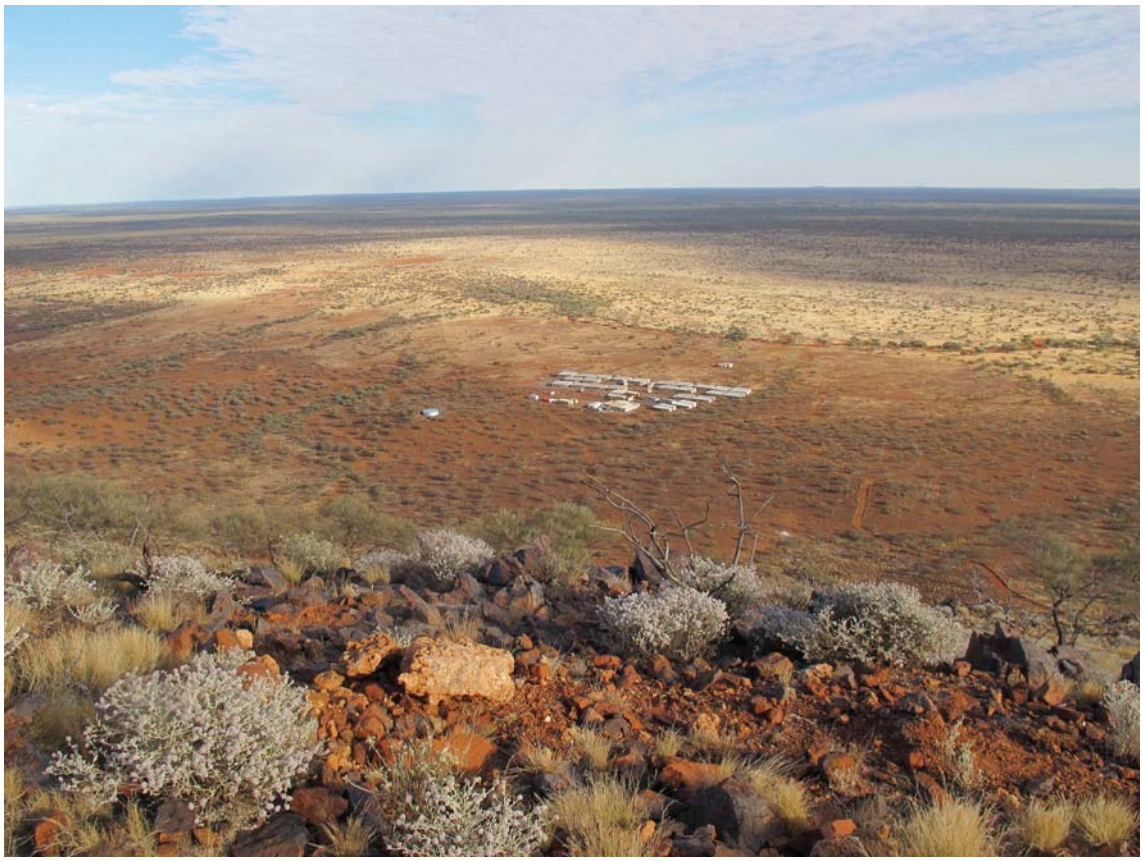

Figure 2: Photo taken from the ridgeline of the Jack Hills, north of Mount Hale, looking down onto the Jack Hills mining camp. The stunted purple flowering shrub in the foreground is the common species *Ptilotus obovatus* (Gaudich.) F.Muell., growing in association with the grass species *Aristida contorta* F.Muell.

1.1 Climate

The climate of the Jack Hills area is arid, as the long-term (1944-2012) average annual rainfall for the Jack Hills area is 238 mm (Bureau of Meteorology, 2012). Rainfall is episodic and highly variable both within and among years, with an average of 46 days rain days per year. Annual rainfall distribution is loosely bimodal with most precipitation associated with either northern summer tropical monsoonal systems that move inland from the northwest coast between January-March or from southern cold-fronts in May-July. September is usually the driest month, averaging only 4.8 mm of rain (Meekatharra airport, 653326 mE, 7055836 mN, UTM Z 50J) (Bureau of Meteorology, 2012) (Figure 3A).

The study region is generally warm-hot, with average daytime summer temperatures from 30 - 40 °C and daytime winter temperatures of around 20 °C (Figure 3B). The prevailing winds in summer are usually easterly in the morning and south easterly in the afternoon. In winter the winds are east north easterly in the morning and west north westerly in the afternoon (Bureau of Meteorology, 2012).

Field sampling for this project occurred between October 2010 and October 2011. For at least two years prior to October 2010, annual average rainfall was extremely low; only 119 mm in 2009 and only 70 mm in 2010 prior to December of that year (Figure 3A). However, heavy rainfall occurred in the study area in December 2010 (112 mm) and again in February 2011 (170 mm), resulting in inundation of the entire floodplain from the Murchison River up to the Jack Hills, a distance of ~ 5 km.

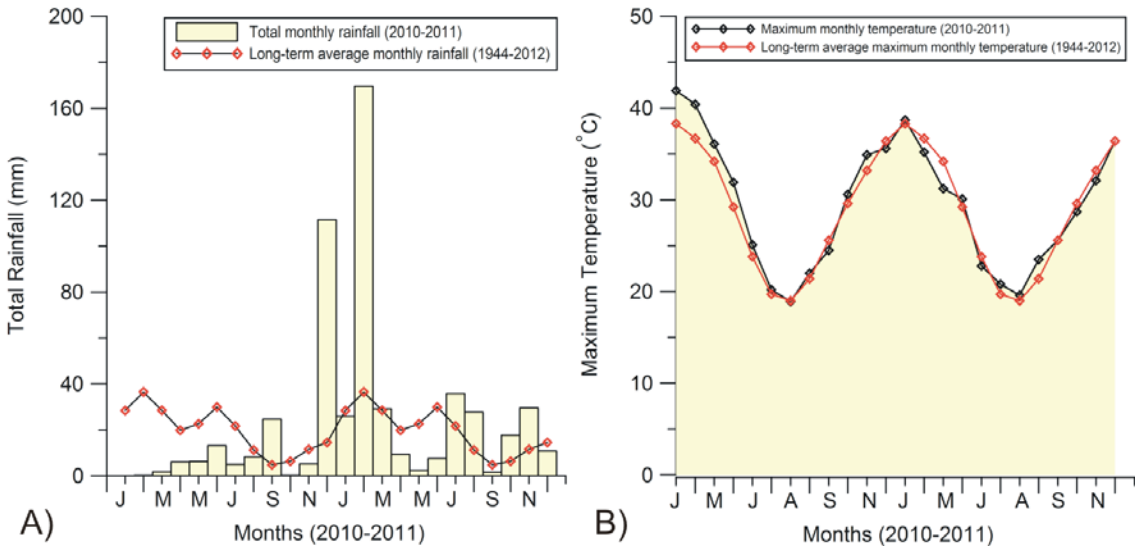

Figure 3: A) Total rainfall, and B) Maximum temperatures recorded at the Meekatharra airport weather station (007045) between 2010 and 2011, the period when field studies occurred.

1.2 Geology, landform and soils

The Jack Hills range is a greenstone belt in between Archeean granitoids and metagranitoids of the northwest Yilgarn Craton (Spaggiari, 2007). The dominant rock types of the Jack Hills are divided into three rock associations (Spaggiari, 2007): banded ironstone formations (BIF), chert, quartzite, mafic and ultramafic rocks; pelitic and semi-pelitic rocks including quartz-mica schist and andalusite schist; and a mature clastic succession comprising pebble metaconglomerate, quartzite, metasandstone, and quartz-mica schist.

Mining activities target the ironstone hills (which are predominantly BIF) (Figure 4), between Mount Matthew and Mount Hale. The BIF is generally composed of 25% to 35% iron (Fe), specifically hematite (Fe_2O_3) and magnetite (Fe_3O_4), with the remainder being mainly silicates (stilpnomelane, greenalite, riebeckite) and carbonates (ankerite, siderite) (Trendall 2005).

Figure 4: Banded Ironstone Formation (BIF) exposed on the upper slopes and ridges of the Jack Hills.

The study area falls within the Weld and Yarrameedie land systems (Curry et al., 1994). A land system is defined as an “area with a recurring pattern of topography, soil and vegetation” (Christian and Stewart, 1953). The Weld land system captures the ranges associated with the Jack Hills and is described as rugged ranges and ridges of mainly Archeean metamorphosed sedimentary rock supporting acacia shrubland. The Yarrameedie land system encapsulates the plains surrounding the Jack Hills range and is described as undulating stony interfluves, drainage floors and pediment (foothill) plains below major ranges of crystalline rocks (mainly Weld land system) (Curry et al., 1994). More detailed soil descriptions for each of the land systems in the study area were made by Landloch Pty Ltd (2010). The landform and soils of the ranges of the Jack Hills and the lower slopes and foot slopes are described as follows:

1. Crests, upper and mid slopes of the Jack Hills ranges: The gradients of the crests range from 1-5% and 10-40% for the upper and mid slopes. Soils are well-drained, gravelly red sandy loams to depth of 0.5 m underlain by hard rock or ironstone. Soils have coarse fragments of ironstone becoming more abundant at depth. The pH of the soil varies from 5.5 to 7.0.

2. Lower slopes or foot slopes of the ranges and undulating low hills and rises: The gradients range from 3-10%. Soils are well-drained, red sandy loams to depth of 0.5m. However, soil depths are generally greater than for the crests and mid slopes. Soils have coarse fragments of ironstone and cobbles, with surface fragments common. The pH of the soil is 5.5.

1.3 Vegetation of the Jack Hills

Vegetation of the Murchison Region is dominated by low *Acacia* spp. woodlands on lower slopes and plains, reduced to mixed shrubland or low very open *Acacia* sp. woodland on the hills and ranges (Beard, 1990). While the botanical uniqueness of the banded ironstone ranges has been historically recognised (Beard, 1981), recent botanical surveys have identified unique species composition, endemism and species rarity (DEC and Gibson). Detailed plant community mapping and descriptions of the vegetation at the Jack Hills has been undertaken by Mattiske Consulting Pty Ltd (2005), which has been used in this study to define three broad plant communities. The figure of the spatial distribution of these plant communities is provided in Chapter 3, and they are described as follows:

1. Low open woodland of *Acacia aneura* Benth., *Acacia rhodophloia* Maslin, *Acacia citrinoviridis* Tindale & Maslin and *Grevillea berryana* Ewart & Jean White over *Dodonaea petiolaris* F.Muell., *Eremophila* spp. and *Ptilotus obovatus* (Gaudich.) F.Muell. on foot slopes and plains surrounding the Jack Hills (Figure 5A).

2. Low open woodland of *Acacia aneura, Acacia ramulosa* W.Fitzg., *Acacia xiphophylla* E.Pritz., *Acacia pruinocarpa* Tindale and *Grevillea berryana* over *Eremophila margarethae* S.Moore and *Thryptomene decussata* (W.Fitzg.) J.W.Green over *Solanum lasiophyllum* Poir., *Ptilotus obovatus* and *Aristida contorta* F.Muell. on shallow gravelly mid slopes of the Jack Hills range (Figure 5B).

3. Hummock grasslands of *Triodia melvillei* (C.E.Hubb.) Lazarides with emergent *Acacia aneura*, *Acacia* sp. Jack Hills (R.Meissner & Y. Caruso 4), *Acacia xiphophylla*, *Grevillea berryana* over *Eremophila* spp. on upper slopes and main ranges (Figure 5C).

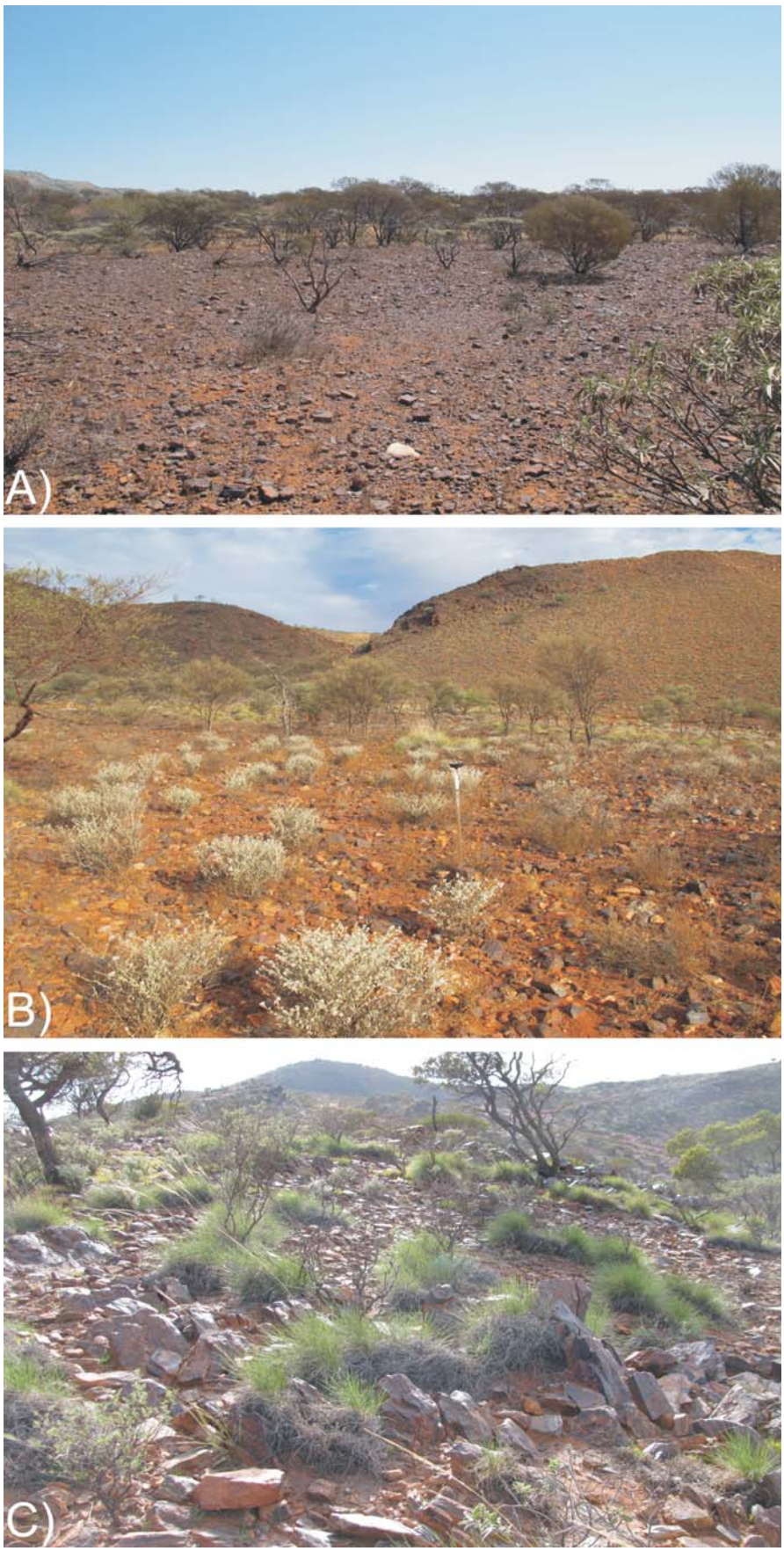

Figure 5: Broad plant communities at the Jack Hills, A) Low open woodland of *Acacia* spp. on footslopes and plains B) Low open woodland of *Acacia* spp. over *P. obovatus* on low to mid slopes C) Hummock grassland of *T. melvillei* on upper slopes and crests.

Fourteen plant species of conservation significance have been recorded at the Jack Hills (Ecologia Environment, 2009, Mattiske Consulting Pty Ltd, 2005), with one in particular, *A.* sp. Jack Hills (Figure 6A), being restricted in distribution to the Jack Hills and nearby Weld Range. The hummock grassland community of *Triodia melvillei* that is confined to the ridges and breakaways of the Jack Hills (Mattiske Consulting Pty Ltd, 2005) (Figure 6B), has been recognised as restricted by the Department of Environment and Conservation (DEC) and have thus been listed as a "Priority 1" Ecological Community: 'Jack Hills vegetation complexes (banded ironstone formation)' (Department of Environment and Conservation, 2012). These species and communities highlight the botanical importance of the Jack Hills.

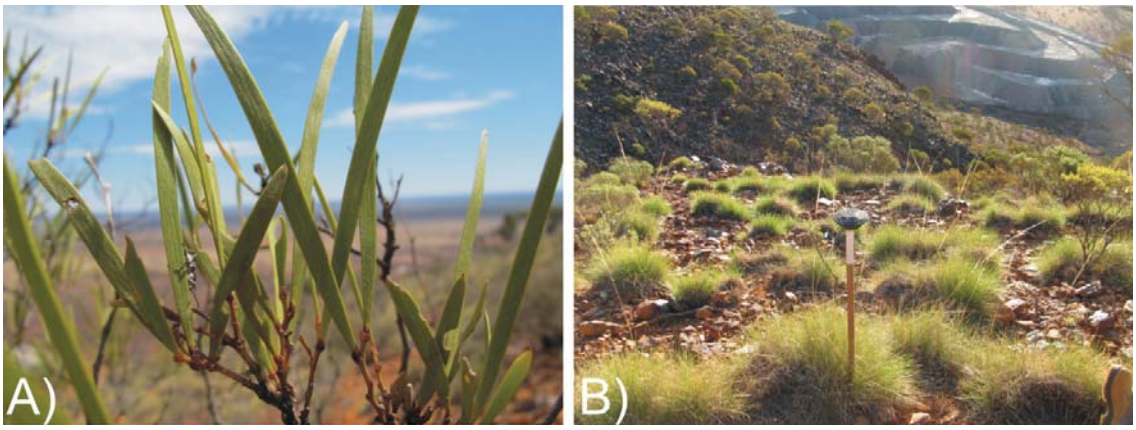

Figure 6: A) *Acacia* sp. Jack Hills and B) *Triodia melvillei* upland community.

1.4 Dust generation at the Jack Hills

Local mining dust is produced by the mining operations and is easily visible on dry, hot, windy days and in association with machinery and road traffic (Figure 7A). Dust is also visible on the leaf surfaces of surrounding vegetation (Figure 7B). A detailed characterisation of the nature and extent of dust generated by the Jack Hills mine is presented in Chapter 3.

Figure 7: A) Machinery working in the main pit and haul road (top) and dust produced from the crushing facility (middle), B) Dust visible on surrounding plant species *A. aneura* (left), *A. rhodophloia* (middle) and *Eremophila fraseri* F.Muell (right).

2 References

BEARD, J. S. 1981. *Vegetation of the Swan area,* Nedlands, WA, University of Western Australia.

BEARD, J. S. 1990. *Plant Life of Western Australia,* Perth, Western Australia, Kangaroo Press.

BUREAU OF METEOROLOGY. 2012. *Climate Data Online* [Online]. Australian Government, . Available: http://www.bom.gov.au/jsp/ncc/climate_averages/ 2012].

CHRISTIAN, C. S. & STEWART, G. A. 1953. General Report on Survey of Katherine-Darwin Region, 1946. *Land Research Series No. 1.* Melbourne: Commonwealth Scientific and Industrial Research Organisation, Australia.

COMPSTON, W. & PIDGEON, R. T. 1986. Jack Hills, evidence of more very old detrital zircons in Western Australia. *Nature,* 321**,** 766-769.

CURRY, P. J., PAYNE, A. L., HENNIG, P. & BLOOD, D. A. 1994. An inventory and condition survey of the Murchison River catchment, Western Australia. *Technical Bulletin No. 84.* South Perth, Western Australia: Department of Agriculture.

DEPARTMENT OF ENVIRONMENT AND CONSERVATION 2012. Priority Ecological Communities for Western Australia. *In:* SPECIES AND COMMUNITIES BRANCH (ed.). Department of Environment and Conservation.

ECOLOGIA ENVIRONMENT 2009. Jack Hills Stage 2: Flora and Vegetation Assessment. Draft ed.: Ecologia Environment.

LANDLOCH PTY LTD 2010. Soil Quality Assessment of the Jack Hills Project. *Draft Final Report.* Crosslands Resources Limited.

MATTISKE CONSULTING PTY LTD 2005. Flora and Vegetation on the Jack Hills project area. Mattiske Consulting Pty Ltd.

SPAGGIARI, C. V. 2007. The Jack Hills greenstone belt, Western Australia Part 1: Structural and tectonic evolution over > 1.5 Ga. *Precambrian Research,* 155**,** 204-228.

WILDE, S. A., VALLEY, J. W., PECK, W. H. & GRAHAM, C. M. 2000. Evidence from detrital zircons for the existence of continental crust and oceans on the Earth 4.4 Gyr ago. *Nature,* 409**,** 175-178.

Chapter 3. Relationships between Mining Dust and Plant Traits in Vegetation at the Jack Hills

1 Introduction

Dust characteristics including particle size and composition, as well as total dust weight are important variables that influence the effect dust has on plant health and function (Hirano et al., 1995, Farmer, 1993, Grantz et al., 2003, Eveling and Bataillé, 1984). The structural and morphological features or 'traits' of plants also influence the amount of dust deposited on, or captured by a species (Chamberlain, 1975, Beckett et al., 2000, Raupach and Leys, 1999, Little, 1977, Butler, 2009) and how the dust interacts with the leaf surface (Paling et al., 2001, Naidoo and Naidoo, 2005). For example, a plants height and width, branch and leaf density and orientation can affect the amount of dust intercepted by a plant by increasing or decreasing the contactable surface area (Raupach and Leys, 1999, Petroff et al., 2008). Plant structure also influences airflow through plants (Beckett et al., 2000), i.e., their dust filtration ability. Leaf morphological traits, such as the presence of hairs, pits, uneven surfaces or resins can increase surface roughness and/or stickiness, thus increasing dust deposition potential (Grantz et al., 2003, Naidoo and Naidoo, 2005, Butler, 2009, Paling et al., 2001). Plants traits are complex, however, and it is often a combination of traits which are described as influencing dust accumulation (Raupach and Leys, 1999, Butler, 2009).

This chapter has three main objectives. First, I sought to characterise the dust at the Jack Hills, specifically to quantify the amount, distribution and type of dust generated. I expected that dust surrounding the mine would be above natural background levels, with the highest dust loading occurring close to main dust emission sources (e.g. mining pit, waste rock stockpile, crushing facility and haul roads). I also predicted that dust levels are

greatest in summer owing to drier conditions, reduced vegetation cover and higher wind speeds. Moreover, I expected that the prevailing wind direction and landform will influence dust deposition patterns. Second, I aimed to characterise plant species across the Jack Hills based on structural and morphological traits chosen *a priori*, and determine if these traits influence dust loading. I hypothesised that plants within and across communities could be grouped by similar traits and that these traits would influence dust loading. For example, I expected that plants that were taller and/or had leaves that increased surface roughness such as hairy, resinous or unevenly texture leaves would have the greatest dust deposition. Thirdly, I aimed to group plant species based on a similar combination of traits they possess (i.e., plant trait groups), to examine the interaction between individual and multiple traits, and to establish morphological groups which could be analysed for potential functional response in Chapter 4, thus representing Plant Functional Types.

2 Materials and methods

2.1 Sampling design

Twenty-eight dust collector stations were established around the Jack Hills mining area in October 2010 (Figure 1). Dust collectors were set for dust collection in April 2011 for 47 days and in October 2011 for 36 days to capture different seasonal periods (Table 1). Dust collectors were initially set in October 2010. However, they could not be retrieved in a timely manner. In December 2010, the Jack Hills received flooding rains (see Chapter 2), therefore the traps were washed out.

Table 1: Total number of sampling days and climatic conditions recorded at the closest [1]weather station for each seasonal sampling period.

Sampling period	No. of sampling days	[2]Rainfall total (mm)	Mean max. monthly temp. (°C)	Mean min. monthly temp. (°C)
April 2011	47	10.6	20.8 to 30.1	9.2 to 17.6
October 2011	36	39	28.7 to 32.1	16 to 18

[1]Bureau of Meteorology, Meekatharra airport station 007045. [2] The highest total rainfall to fall in a single day was 20 mm in October (50% of the total rainfall for this sampling period). All other values for any one day were < 5 mm and more commonly < 1 mm.

Dust collectors were set up along three main axes radiating from the main dust emission sources, taking into consideration prevailing wind direction and the surrounding landforms (Figure 1). The main dust emission sources are a) mining pit, b) waste rock stockpile c) crushing facility and d) haul roads (Figure 1). Axis 1 was oriented north-west and perpendicular to the mining pit. Axis 1 crossed the mining pit on the crests and upper slopes of the ranges and headed northwest down the Jack Hills range and out onto the foot slopes and floodplain. Axis 2 ran north from the mining pit and intersected disturbance areas around the waste dump, haul roads and crushing facility on the foot slopes of the

range and finished out on the floodplain. Axis 3 was oriented northeast from the mining pit parallel to the main ridgeline of the Jack Hills. At each dust collector station, a dust collection number, GPS co-ordinates, topographic position, representative photos, and soil observations were recorded.

It was expected that dust levels would decrease with increasing distance from the mining pit. Consequently, more dust collectors were placed closer to the emission source areas in order to sample comprehensively within the area where the largest variations in dust deposition are likely to occur (Everett, 1980, Farmer, 1993, Butler, 2009). Dust collectors were also established further away (> 1000 m) in order to capture the large-scale spatial distribution of the deposition pattern. Dust collectors at the greatest radial distance from the disturbance areas, Site 1 (2723 m), Site 9 (1069 m), Site 27 (1863 m) and Site 28 (1838 m) were considered ‘control’ sites that provided information on natural background levels of dust because dust from local anthropogenic sources is most abundant directly adjacent to the disturbance with significant amounts of dust still recorded up to 1000 m away (Kuki et al., 2008, Ong et al., 2003).

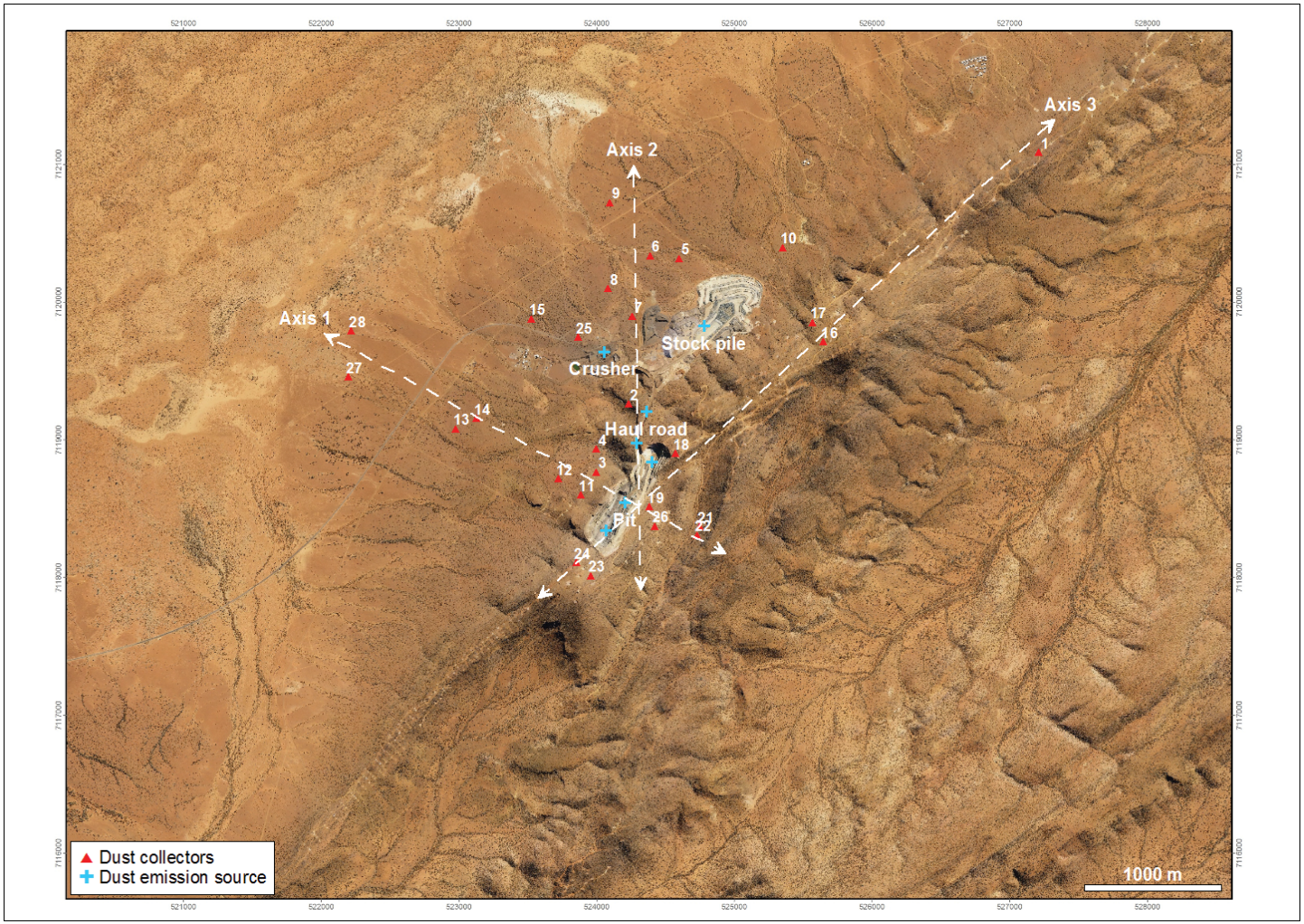

Figure 1: Sampling design for dust collector stations, arranged along three main axes surrounding the Jack Hills mining pit. Sites 1, 9, 27 and 28 are control sites because they are furthest from the dust emission sources. Geographic co-ordinates are in GDA ’94, Zone 50.

Three broad plant communities occur across the study area (refer to Chapter 2 for community description), within which the dust collectors were established (Figure 2). The presence and distribution of the three communities across the study area presents variability in species composition across the three axis and at varying distances from the dust emission sources. This presented a limitation for the analysis of plant trait groups, because not all species with a similar combination of traits occurred across the three community types. Notwithstanding, at least a portion of the species are common across the sampling area (e.g. *Acacia aneura, Ptilotus obovatus*). Hence, comparability of the leaf dust data (Section 3.5) and physiological response (Chapter 4) to dust according to species and individual traits was possible even if assessment of plant trait groups presented a challenge.

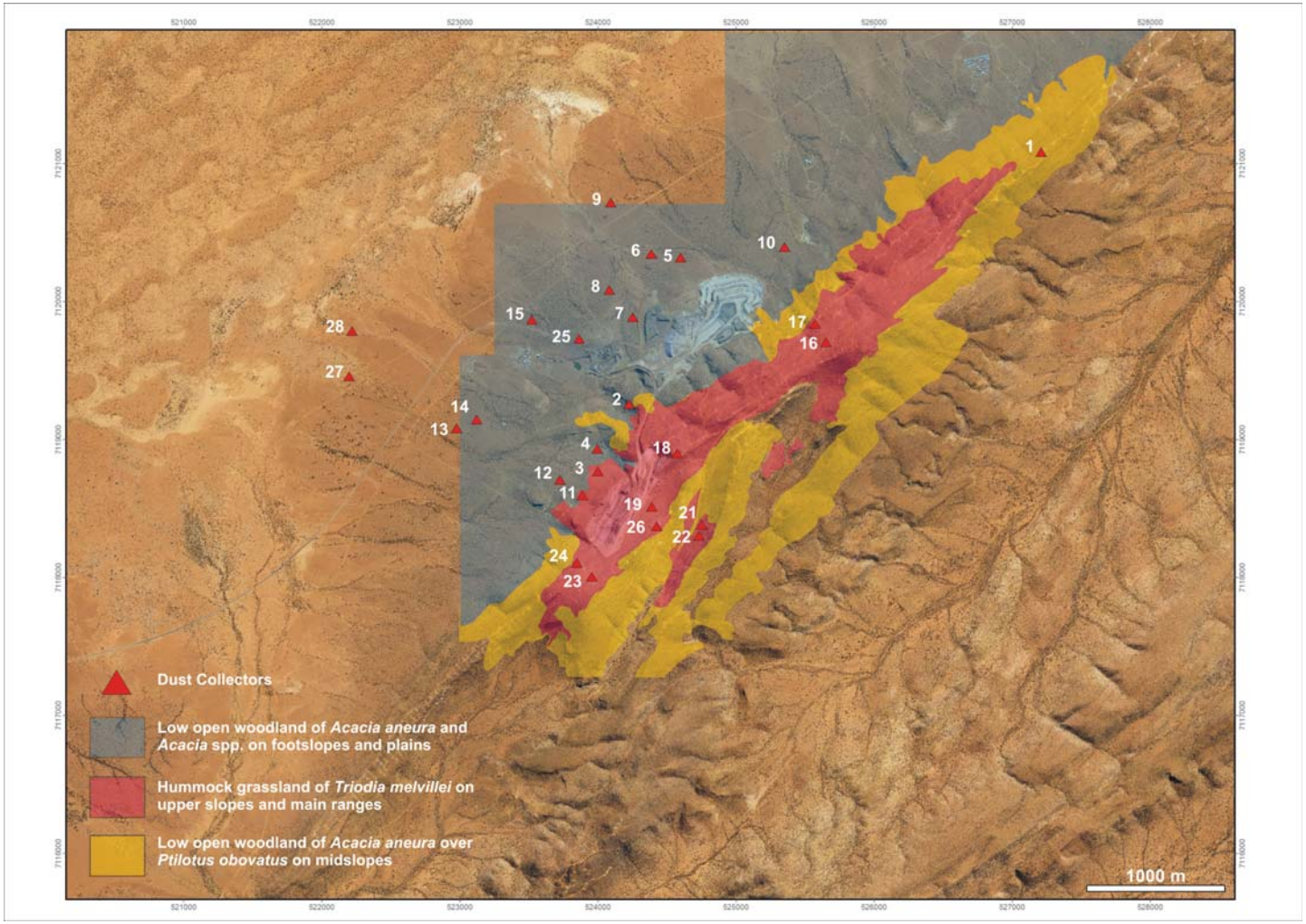

Figure 2: Broad plant communities across the study area, modified from plant community mapping undertaken by Mattiske Consulting Pty Ltd (2005).

The dust collector design follows that used previously in the Pilbara by Butler (2009), who derived her design from Reheis and Kiln (1995). Wooden stakes of 1.5 m length were driven into the ground to a depth of approximately 50 cm with the trap at 1 m above the ground surface. A Teflon-coated aluminium cake-tin with a diameter of 10 cm (total surface area of 79 cm^2) was nailed onto the wooden stake. A second cake-tin of the same diameter was placed inside the first cake-tin and secured with blue-tack. Aluminium wire mesh was fitted into the second cake-tin and filled with approximately 30 glass marbles, each 10 mm in diameter. Another layer of wire mesh was placed on top to secure the marbles (Figure 3). The dust traps were collected by removing the inner cake-tin including the marbles and mesh, and double-bagging the contents in sealable plastic bags. The dust was collected from the traps and analysed in the laboratory.

Figure 3: Dust collectors established at the Jack Hills. Left: topside view of dust trap; right: dust trap on stake adjacent to the mine pit, looking in a northeasterly direction.

2.2 Dust deposition and characterisation

Dust weight collected in each trap was measured the following way. First, the traps and the interior of the plastic zip-lock bags were washed with 200 mL of ethanol. The liquid was then filtered through a pre-weighed 0.8-micron (μm) nitrocellulose filter using vacuum filtration. Ethanol was used instead of de-ionised water to retain the soluble mineral components (e.g., salts) of the dust. The filter papers were then left to air-dry for one week before they were weighed. Dust weight was obtained by subtracting the initial weight of the filter paper. As the surface area of dust trap is known (79 cm^2), the dust weight was normalised to dust trap surface area and then converted to g/m^2. Total dust loads were corrected against the number of days collected.

The grain-size frequency distribution for each dust sample was determined from photographs obtained with a transmitted-light microscope, using an automated image analysis routine. The filtered and air-dried dust was carefully sprinkled onto a microscope slide with a fine-tipped brush. For each slide, between 80 and 200 photographs were taken using the x-y-table under fixed magnification, with a resolution of 0.44 μm per pixel (Tiff image size: 2592 x 1944 pixel). The number of images was chosen according to the density of the dust on the slide so that a minimum of 6700 grains were recorded for each sample. An image analysis routine was then used to determine grain-size frequency distribution with the software Matlab (MathWorks Inc., 2000). For a description of the image analysis routine, see Appendix 3.A.

Dust mineralogy was determined using powder X-Ray Diffraction (XRD). The air-dried dust samples were first ground manually using an agate mortar and pestle. The powder samples were analysed with a Phillips PW 1830 Diffractometer with CuK-α radiation and diffracted beam monochromator. XRD patterns were determined for the range 3 - 70° (2θ)

with a step size of 0.02°. The XRD patterns were then smoothed. The area under the peak was used as a semi-quantitative proxy for the proportion of each mineral. The software Traces 5.0.5 (Diffraction Technology 1999) and XPAS version 3.0 (Singh and Gilkes, 1992) were used for pattern generation and data manipulation, and Brindley and Brown (1980) was used for mineral identification.

2.3 Plant traits

The dominant perennial plant species located within a 15 m radius of each dust collector station were characterised according to traits chosen *a priori* (Table 2). Plant traits recorded in the field were: 'plant height', 'leaf orientation', 'petiole length', '2D leaf shape' and '3D leaf shape'. Herbarium samples were collected for all species, which were then used for taxonomic identification, measurement of mean leaf area (Section 2.3.1), and assessment of leaf micro-morphological characteristics (Section 2.3.2). Plant traits measured in the laboratory were: 'leaf area', 'trichome type and cover', presence or absence of 'resin' and 'leaf surface configuration'. The plant traits '2D leaf shape', '3D leaf shape/posture', 'trichome cover and type' and 'leaf surface configuration' were modified from the taxonomic plant descriptions in Simpson (2006).

For the purpose of the plant group analysis, the plant trait dataset collected at the dust stations was expanded to include other perennial plant species within the Jack Hills to increase the rigour of the plant trait hierarchical cluster analysis (Section 2.5.2 Multivariate analysis of plant trait groups). This increased the number of considered species from 18 to 53. Plant traits of the additional species were recorded as above. The additional species were not examined for leaf dust (Section 2.4) or physiological response (Chapter 4).

Table 2: Plant structural and morphological traits chosen for measurement.

Plant traits	Description
plant height (m)	numeric value
leaf area (mm^2)	numeric value
2D leaf shape (aspect ratio)	linear (12:1-6:1) narrowly oblong/elliptic, oblong/elliptic (6:1-3:1, 2:1-3:2) widely elliptic, circular (6:5, 1:1)
3D leaf shape/posture (Figure 4)	flat (A) terete (B) clavate-turbinate (C) conduplicate-involute (D) cup-revolute (E) undulate (F)
petiole length (mm)	numeric value
leaf orientation (degrees)	appressed (0-15) inclined-ascending (15-75) horizontal (85-105) reclined-descending (105-165) depressed (165-180)
trichome cover and type (Figure 5)	glabrous (without trichomes) (A) ciliate/ciliolate (marginal trichomes) (B) tomentose (dense trichomes) (C) strigose (Coarse, bent, flat trichomes) (D) sericeous (long, appressed trichomes) (E)
resin	resin (Yes) resin (No)
leaf surface configuration (Figure 6)	smooth (A) striate (fine longitudinal lines) (B) unevenly textured (bumps, reticulate leaf venation, pits, irregular fine lines) (C)

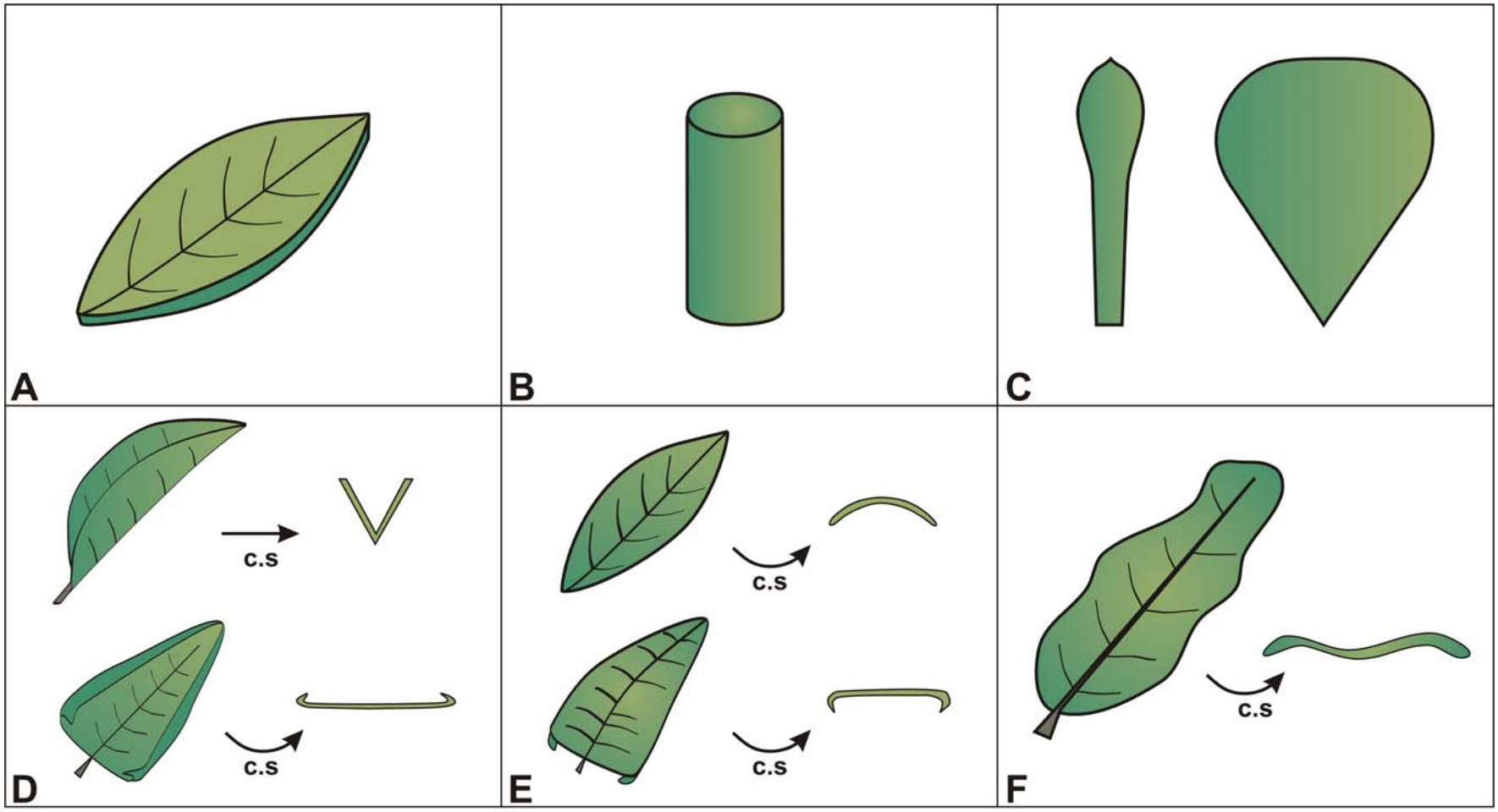

Figure 4: Plant trait ‘3D leaf shape/posture’, modified from the descriptions of Simpson (2006). The plant trait illustrations show A) flat, B) terete, C) clavate/turbinate, D) conduplicate/Involute, E) cup/revolute and F) undulate type.

Figure 5: Plant trait ‘trichome type and cover’: A) glabrous (*Calytrix desolata* S. Moore), B) ciliate (*Homalocalyx echinulatus* Craven), C) tomentose (*Ptilotus obovatus* Gaudich.), D) strigose (*Grevillea berryana* Ewart & Jean White) and E) sericeous (*Halgania gustafsenii* F.Muell.).

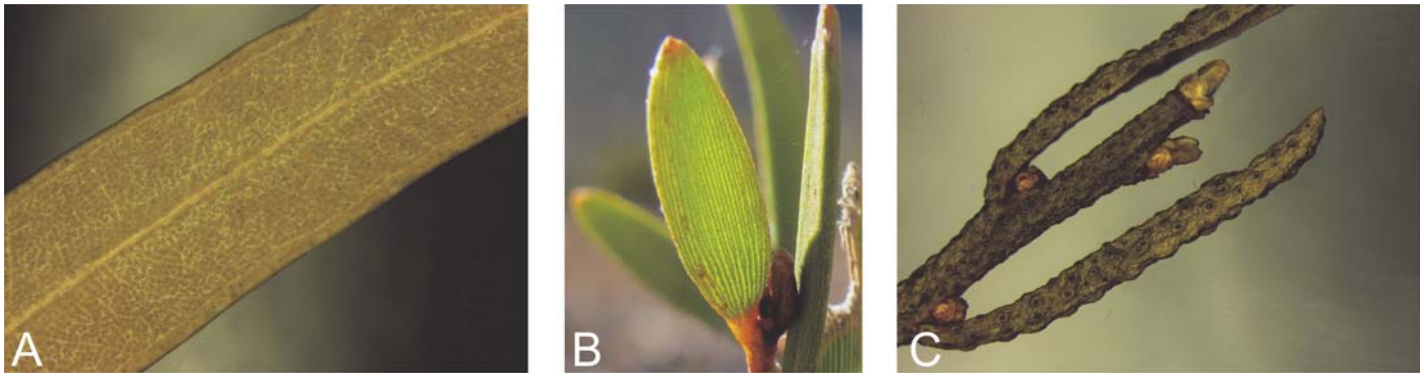

Figure 6: Plant trait ‘leaf surface configuration’: A) smooth (*Corymbia ?lenziana*), B) striate (*Acacia rhodophloia* Maslin.) and C) unevenly textured (*Philotheca brucei* (F.Muell.) Paul G. Wilson).

2.3.1 Leaf area analysis

Average leaf area was determined for each plant species from digital photos using the image analysis software ImageJ (Rasband, 1997-2012). Digital photos were taken of dried and pressed leaf specimens on a white-card background with a ruler as scale. Between three and eight replicates of leaves for each species were used, depending on the leaf size. A greater number of leaves were used if leaf area was small (< 100 pixel).

Images were processed as follows. First, the image scale was set (in menu bar: "Analyse", > Set-scale"). Then, shadows and unwanted spots were removed manually by drawing polygons around the shaded areas and filling them in with the white background colour. The image was then converted into a black-and-white binary image with the threshold tool of ImageJ and the leaf area estimated (mm^2). An example of an original and thresholded image is provided as Figure 7.

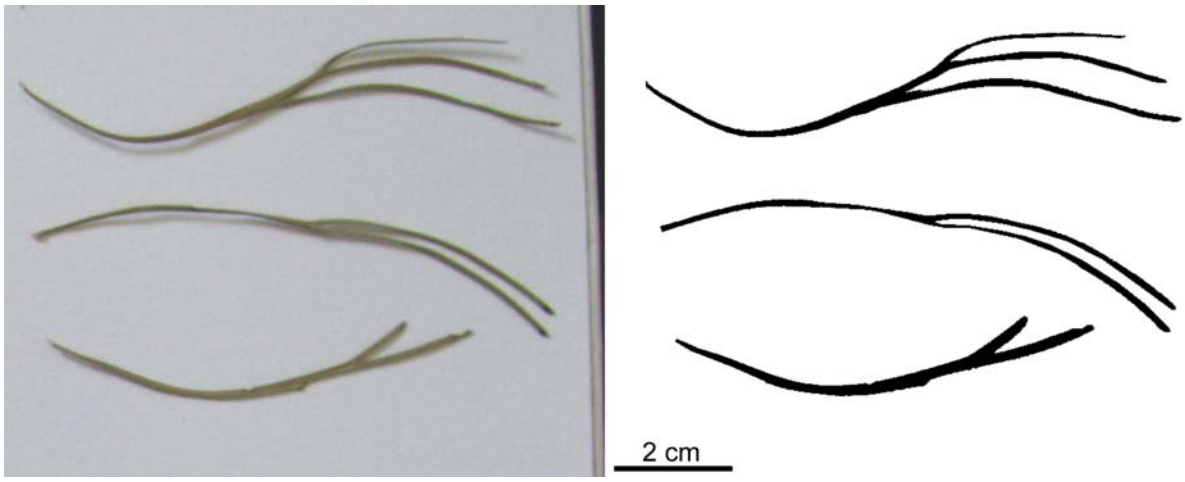

Figure 7: Digital image of *Grevillea berryana* leaves (on left) and thresholded image of the same species (on right).

2.3.2 Leaf micro-morphological characteristics

All pressed and dried plant samples were examined under a light microscope to determine the leaf micro-morphological characters, namely 'leaf surface configuration', 'trichome cover and type' and the presence/absence of resins. Fresh leaf samples were also collected in April 2011 for environmental Scanning Electron Microscopy (eSEM). Leaf samples were bagged in zip-lock bags, transported back to the laboratory and kept refrigerated (< 4°C) until examination. Fresh leaf samples were arranged on a metal viewing plate, fixed with adhesive tape and digital images taken using eSEM at the CSIRO Australian Research Resource Centre.

2.4 Quantification of leaf dust

Dust deposition on leaves was measured in October 2011. Between 10 and 20 fresh mature leaves of each plant species were collected at a sub-set of the dust stations at increasing distance from the disturbance areas. The leaves were bagged in zip lock bags, labelled, kept cool (< 10°C), and transported back to the laboratory for analysis.

In the laboratory, the fresh leaves were washed with 100 mL of ethanol (including the inside of the zip-locked bags) and shaken for approximately 1 minute to dislodge all dust particles. The ethanol was then filtered through a pre-weighed filter of 0.8 μm mesh size using vacuum filtration. Filter papers were left to air-dry for one week and then re-weighed. Dust weight was calculated by subtracting the original filter paper weight from the weight of the filter with dust and recorded in grams (g). The dust weight was then normalised by leaf area. The total leaf area of each sample (in cm^2) was measured with a leaf-area meter (LI-3100, LI-COR inc., Lincoln, NE) at a resolution of 0.1 mm^2.

2.5 Data analysis

2.5.1 Univariate analysis of leaf dust and plant traits using Linear Mixed Effect Model

To analyse whether the dust loading on leaves is related to plant traits, a Linear Mixed Effect Model (LMEM) was developed using R Studio (R. 0.95.265) and the nlme package (R Development Core Team, 2012). The dust weight on the leaves of each species (response variable) was modelled as a function of each of the measured plant traits and the distance from the dust source (predictor variables). I included a random-effect structure of sample location and used maximum likelihood to investigate the contribution of fixed effects. The model assumptions (data are normally distributed and independence of errors) were confirmed using diagnostic plots, including quantile – quantile (Q-Q) and residual plots, in R. The equation that represents the LMEM is:

Equation 1:

$$LDW_{ij} = \beta_0 + \beta_1 H_{ij} + \beta_2 LSC_{ij} + \beta_3 TT_{ij} + \beta_4 3DLS_{ij} + \beta_5 2DLS_{ij} + \beta_6 R_{ij} + \beta_7 LA_{ij} + \beta_8 PL_{ij} + \beta_9 LO_{ij} + \beta_{10} DS_{ij}\ (\mathbf{fixed}) + u_j + e_{ij}\ (\mathbf{random}),$$

where LDW = 'Leaf dust weight', the indices i and j represent the value of the response variable at plot i nested within site j; β_n represent the fixed intercept (n = 0) and the fixed effects of variables (n = 1, 2,…, 6); H = 'plant height', LSC = 'leaf surface configuration', TT = 'trichome type and cover', 3DLS = '3D leaf shape', 2DLS = '2D leaf shape', R = 'resin', LA = 'leaf area', PL = 'petiole length', LO = 'leaf orientation' and DS = 'distance to dust source'; u_j is the random effect associated with the intercept for site j, and e_{ij} represents the residual associated with the observation on an individual plot i at site j.

I used Likelihood Ratio (LR) tests to simplify the fixed effects. Akaike's Information Criterion was employed for small samples (AICc) (Burnham and Anderson, 2002), and I found similar

results to the LR tests. Finally, I used F-tests (ANOVA) to determine the significance of the fixed effects within the simplified models (Pinheiro and Bates, 2000).

The use of LMEM requires replication in variables, therefore, species with plant traits that only occurred once in the dataset were excluded from the analysis. The final dataset included fifteen of the eighteen plant species recorded at the dust stations. The three species removed from the dataset were *Eremophila fraseri* F.Muell, *Homalocalyx echinulatus* Craven. and *Solanum lasiophyllum* Poir., because they possessed an unique plant trait, which could not be analysed meaningfully in the LMEM. For example, *H. echinulatus* was the only species with 'ciliate' trichomes.

2.5.2 Multivariate analysis of plant trait groups using hierarchical cluster analysis

A multivariate hierarchical cluster analysis was undertaken to group plants based on similar traits using PRIMER-E V.6 (Clarke and Gorley, 2006). The final plant trait dataset consisted of 53 species with the plant trait attributes converted into a binary dataset and imported in PRIMER-E V.6. The 'Sorenson' resemblance measure was used to calculate the similarity of species based on plant traits. A subsequent 'hierarchical cluster' analysis using the 'group average' method was performed on the resulting resemblance matrix. The Sorenson measure is identical to the Bray-Curtis measure when the data is binary (Clarke and Warwick, 2001). A similarity profile permutation test (SIMPROF) identified significant groupings in the dendrogram at 99% similarity. Analysis of similarity (ANOSIM) was used to test the null hypothesis that groups determined using SIMPROF were not significantly different. The average contribution of plant traits to the average similarity between groups was calculated using a similarity percentage test (SIMPER) (Clarke and Warwick, 2001).

To analyse if the resulting plant groups influenced dust weight, the identified groups were then added to the LMEM and analysed against dust weight (see Section 2.5.1 on univariate analysis). The resulting 'plant groups' replace the plant traits as fixed effects in the model (Equation 1).

3 Results

3.1 Spatial and temporal dust 'footprint' of the Jack Hills mine

Dust levels recorded in April 2011 ranged from 0.53 g/m^2 to 11.9 g/m^2 and were about half of those recorded in the October 2011 sampling period (1.24 g/m^2 to 21.5 g/m^2) (Figure 3). Dust levels were higher closer to the dust emission sources in both seasons (see Figure 8 and Figure 9). In April, dust levels directly adjacent to dust emission sources (e.g. Site 19) were more than 20 times greater than control sites (11.9 g/m^2 compared to 0.53 g/m^2) and in October around 17 times greater (21.5 g/m^2 compared to 1.24 g/m^2) (Figure 8). The highest level of dust recorded in October was at Site 25 (21.5 g/m^2), which is only 210 m from the crushing facility (Figure 9). In contrast to the general trend of higher October dust levels, six sites, all on Axis 1, had higher dust levels in April compared to October (Table 3: Dust weight collected in each trap for the April and October sampling periods 2011), likely reflecting an influence of the prevailing wind direction and topography, as well as unquantified factors related to the timing and location of specific mining activities at this time of year, e.g., more movement along haul roads or blasting in the mining pit.

Table 3: Dust weight collected in each trap for the April and October sampling periods 2011.

Dust collector No.	April dust levels (g/m^2)	October dust levels (g/m^2)
1	0.53	1.43
2	9.09	[1]Na
3	7.13	3.59
4	8.35	5.88
5	0.67	2.76
6	1.44	4.48
7	7.56	16.5
8	1.12	3.86
9	0.81	2.50
10	1.73	2.69
11	6.15	5.00
12	4.00	5.39
13	4.19	3.49
14	4.52	3.60
15	2.62	7.72
16	1.86	2.19
17	1.06	1.24
18	5.17	10.8
19	11.9	10.7
21	2.04	[1]Na
22	2.51	3.85
23	4.16	4.89
24	4.27	5.86
25	9.29	21.5
26	2.83	3.85
27	1.08	3.85
28	1.08	2.88

[1] Dust stations had fallen over in the October sampling period, therefore dust levels could not be analysed for these sites.

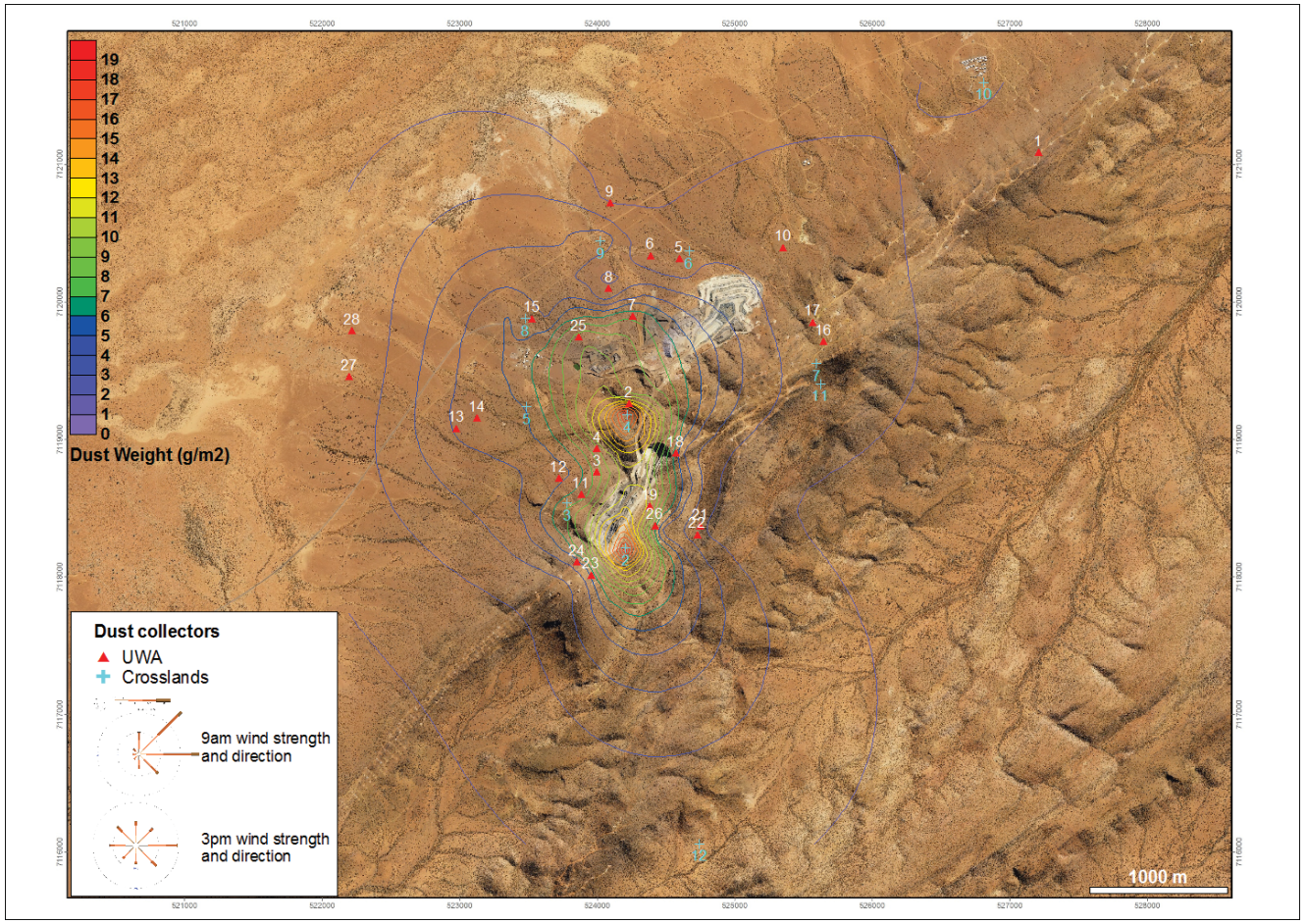

Figure 8: Dust deposition pattern at the Jack Hills during April 2011. Dust density contour lines were interpolated with the geostatistical method of Kriging from 38 sampling points that included 10 dust stations maintained by Crosslands Resources. The predominant wind direction during April is east-northeast in the morning (recorded at 9 am) and east-southeast in the afternoon (recorded at 3 pm). Note that the main pattern of dust deposition does not follow the prevailing wind direction.

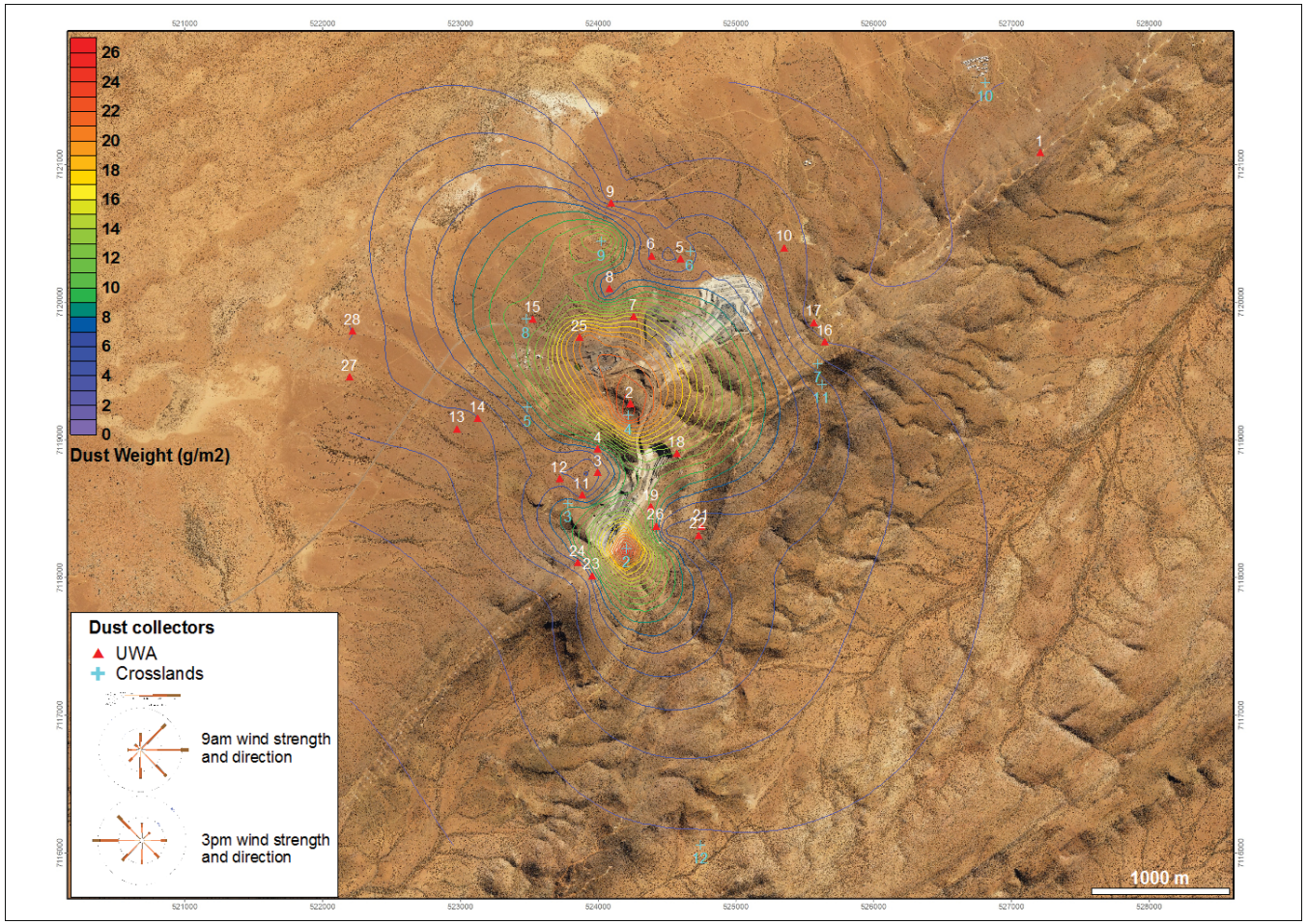

Figure 9: Dust deposition pattern at the Jack Hills during October 2011. Dust density contour lines were interpolated with the geostatistical method of Kriging from 38 sampling points that included 10 dust stations maintained by Crosslands Resources. The predominant wind direction in October is east in the morning and west-southwest in the afternoon. Note that the main pattern of dust deposition does not follow the prevailing wind direction.

Dust levels declined in a strongly non-linear fashion away from the mining disturbance areas (Figure 10A). Overall, dust was negligible above background levels at distances of ca. 2000 m from the mining areas (Figure 10A). Dust levels were significantly increased (> 5 g/m^2) within ca. 350 m of the mine in April and within ca. 600 m of the mine in October (Figure 10A). Within these zones, average dust levels increased 5 fold. Background dust levels in April were < 1 g /m^2 while in October, control site 1 recorded 1.5 g/m^2 and control sites 27 and 28, recorded 2.5 – 3.8 g/m^2.

Site 26, 21 and 22 provide exceptions to the observation that dust levels increase with proximity to the dust source. Site 26 is located 280 m from the open cut mining pit, yet dust deposition was low (3.85 g/m^2 in October), comparable to sites greater than 1000 m from disturbance. Sites 21 and 22 occur within 600 m of the mining pit but recorded dust deposition below 4.00 g/m^2 in both April and October. All three sites were protected from excessive dust exposure due to the Jack Hills ridgeline acting as a topographic barrier.

3.2 Dust grain size distribution

Dust grains ranged in size from ca. 2 – 1000 μm, with the mean grain size of each dust collector ranging between 12 – 32 μm. Mean grain size increased with distance from the mining operation (Figure 10B). The most frequent grain size, i.e., the mode of the grain size distribution, encountered at all sites was 2.55 μm. The percentage of dust particles < 30 μm decreased with increasing distance from the mining operations (Figure 10C). Grain size frequency distributions are shown for two sites: Site 19, which is adjacent to the mining pit, and Site 1, which is a reference site located 2737 m from the pit (Figure 10D). Site 19 has a higher frequency of smaller grain sizes than Site 1.

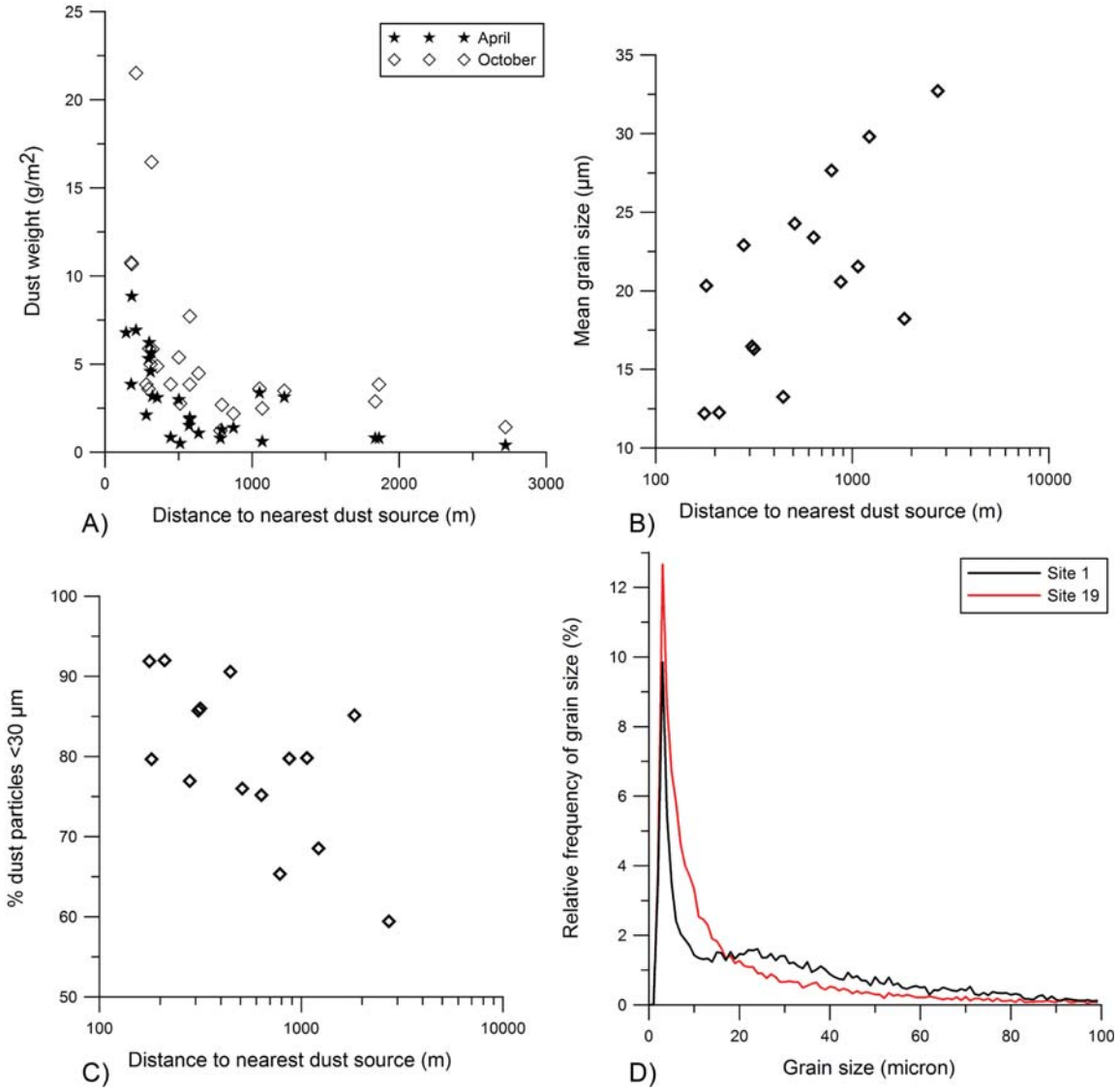

Figure 10: A) Dust deposition levels at dust collector stations during the April and October sampling periods at increasing distance from nearest dust sources, B) mean grain size, and (C) proportion of dust particles below 30 µm in dust traps as a function of distance from dust source in October 2011, and D) relative frequency (%) of grain sizes for dust collector site 1 (reference site) and dust collector site 19 (adjacent to mining pit). Bin size is 1 µm.

3.3 Dust mineralogy

The main mineral components of the dust were quartz, talc, chlorite, magnetite and hematite, ranging from trace amounts (< 5%) to greater than 50% of the sample. The mineral composition of dust particles was also variable among sites. Dust stations in close proximity to the ore crushing facility and overburden waste dump (sites 5,6,7,8 and 25) contained the highest concentrations of magnetite (20 to > 50% of the total sample). Dust stations close to the mining pit (sites 18, 19 and 26) contained 20 to 50% quartz and talc, 5 to 20% chlorite and < 5 to 20% magnetite. Similarly, dust at the reference sites (Sites 1, 9 and 28) contained mostly quartz (> 50%), with 5 to 20% talc and chlorite, but only traces of magnetite (< 5%). Dust mineralogy results for all sites and a selection of XRD patterns is provided as Appendix 3.B.

3.4 Dominant species and characteristic plant traits at the Jack Hills

Eighteen perennial plant species were identified at the 28 dust collector stations. The most ubiquitous species collected were *Acacia aneura, Acacia rhodophloia*, *Grevillea berryana, Ptilotus obovatus*, *Halgania gustafsenii*, *Dodonaea petiolaris* and *Triodia melvillei*. A sub-set of species recorded and their associated plant traits is provided in Table 4. A complete species list with associated trait data is provided as Appendix 3.C.

Table 4: A sub-set of the dominant perennial plant species and their traits recorded at the Jack Hills.

Plant species	Max. Height (m)	[1]Leaf Area (mm^2)	2D Leaf Shape	3D Leaf Shape	Leaf orientation	Trichome type and cover	Resinous	Surface configuration
Acacia aneura	5	52.02 (± 1.89)	Linear	Flat	Appressed	Strigose	No	Striate
Acacia sp. Jack Hills (Figure 11A)	2.5	191.28 (± 25.57)	Linear	Flat	Appressed	Strigose	Yes	Striate
Calytrix desolata	1	5.46 (± 0.99)	Narrowly oblong	Clavate	Appressed	Glabrous	No	Unevenly textured
Dodonaea petiolaris (Figure 11B)	1.5	167.27 (± 1.32)	Narrowly oblong	Involute	Inclined	Glabrous	Yes	Unevenly textured
Grevillea berryana	7	187.18 (± 32.60)	Linear	Revolute	Appressed	Strigose	No	Smooth
Halgania gustafsenii	0.7	571.56 (± 46.47)	Linear	Involute	Inclined	Tomentose	No	Unevenly textured
Ptilotus obovatus (Figure 11C)	1	66.56 (± 22.66)	Oblong	Involute	Inclined	Tomentose	No	Smooth
Triodia melvillei (Figure 11D)	0.5	36.04 (± 04)	Linear	Involute	Appressed	Glabrous	Yes	Striate

[1]Leaf area is mean values ± Standard Error (SE).

Plant height ranged from 0.4 m (*Homalocalyx echinulatus*) to 7 m (*G. berryana*). Mean leaf area ranged from 3.96 mm^2 ± 0.33 (*Aluta aspera* (E.Pritz.) Rye & Trudgen) to 608 mm^2 ±142 (*Corymbia ?lenziana*). Petiole length range from 0 mm (*Calytrix desolata* S.Moore and *T. melvillei*) to 5.80 mm (*C. ?lenziana*) and leaf orientation was either 'appressed' (0-15°), or 'inclined' (15-75°).

All *Acacia* species recorded 'flat' leaves that were either 'linear' (length:width; 12:1-6:1) or 'narrowly oblong/oblong' (6:1-3:1, 2:1-3:2) with leaves that were either 'strigose' (coarse, bent flat) trichomes or 'glabrous' (no hairs) (only *A. rhodophloia*). Most *Acacia* species, with the exception of *A. cuthbertsonii*, recorded a 'striate' (fine longitudinal lines) leaf surface configuration, seen both macroscopically and under magnification (Figure 11A). Of the *Acacia* spp. Only *A.* sp. Jack Hills was resinous (Figure 11A). *G. berryana* was the only species with 'revolute' (curled downward) leaves.

Two shrub species, *Dodonaea petiolaris* (Figure 11B) and *Eremophila fraseri* were 'resinous'. Under magnification (on right), the 'resinous' surface is dried and thus cracked, revealing the stomata underneath. Four species of shrubs had 'tomentose' (thick dense hairs) trichomes; *Eremophila maitlandii* Benth., *P. obovatus* (Figure 11C), *Solanum lasiophyllum* and *H. gustafsenii*. Under magnification, the thick 'tomentose' hairs of *P. obovatus* are revealed as heavily branched, dendritic hairs. *H. echinulatus* was the only species with 'ciliate' trichomes (Figure 5B). *T. melvillei* was the only grass species recorded, and has long 'linear' leaf blades that are 'involute', 'glabrous', have longitudinal 'striate' lines and had sand grains stuck into its 'resinous' surface (Figure 11D).

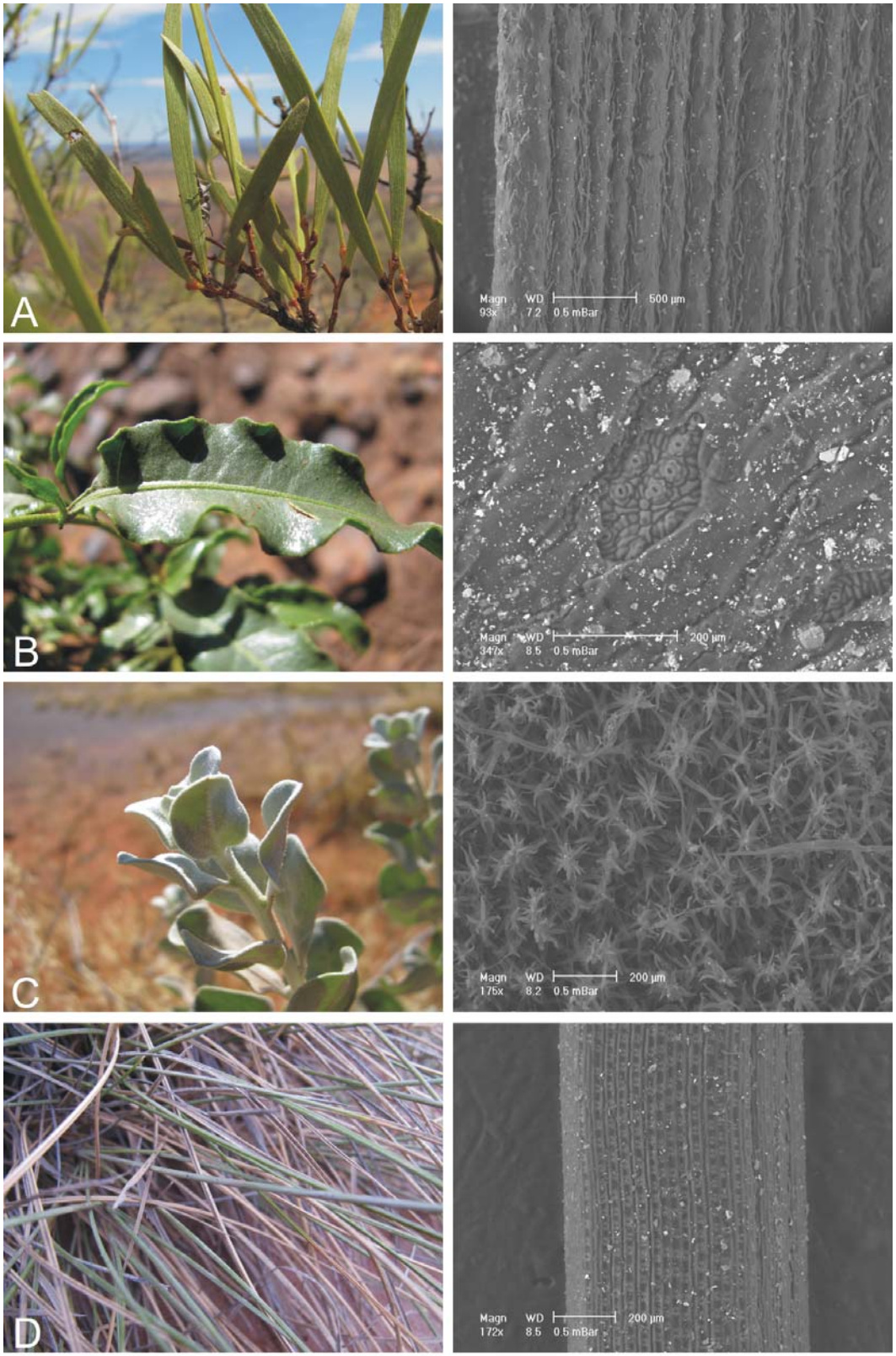

Figure 11: Selected plant species for trait analysis showing field photograph (left) and leaf eSEM image (right) for A) *A.* sp. Jack Hills, B) *D. petiolaris* C) *P. obovatus* and D) *T. melvillei*.

3.5 Leaf dust

The dust weight on the leaves of the eighteen plant species ranged from 0 g/m^2 up to 53 g/m^2 (Figure 12). *H. gustafsenii* recorded the highest dust weight (53.5 g/m^2) and the highest average dust weight across sites (23.4 g/m^2 ± Standard Error (SE) 8.54). While *G. berryana, A. cuthbertsonii, A. rhodophloia* and *A. aneura* accumulated the lowest dust weights (0 – 2 g/m^2) and the lowest average dust weights (1.09 g/m^2 ± SE 0.45, 1.76 g/m^2 ± SE 0.95, 3.08 g/m^2 ± SE 0.88 and 6.51 g/m^2 ± SE 1.12, respectively). *D. petiolaris* and *T. melvillei* collected average dust weights of 8.66 g/m^2 (± SE 2.11) and 10.0 g/m^2 (± SE 2.00). Species with only one or two values, or which did not provide adequate replication across the site, cannot be interpreted meaningfully. These species are *A. citrinoviridis, A.* sp. Jack Hills, *Al. aspera, C. desolata, E. fraseri, E. maitlandii, H. echinulatus, S. lasiophyllum* and *Senna* sp. (Figure 12).

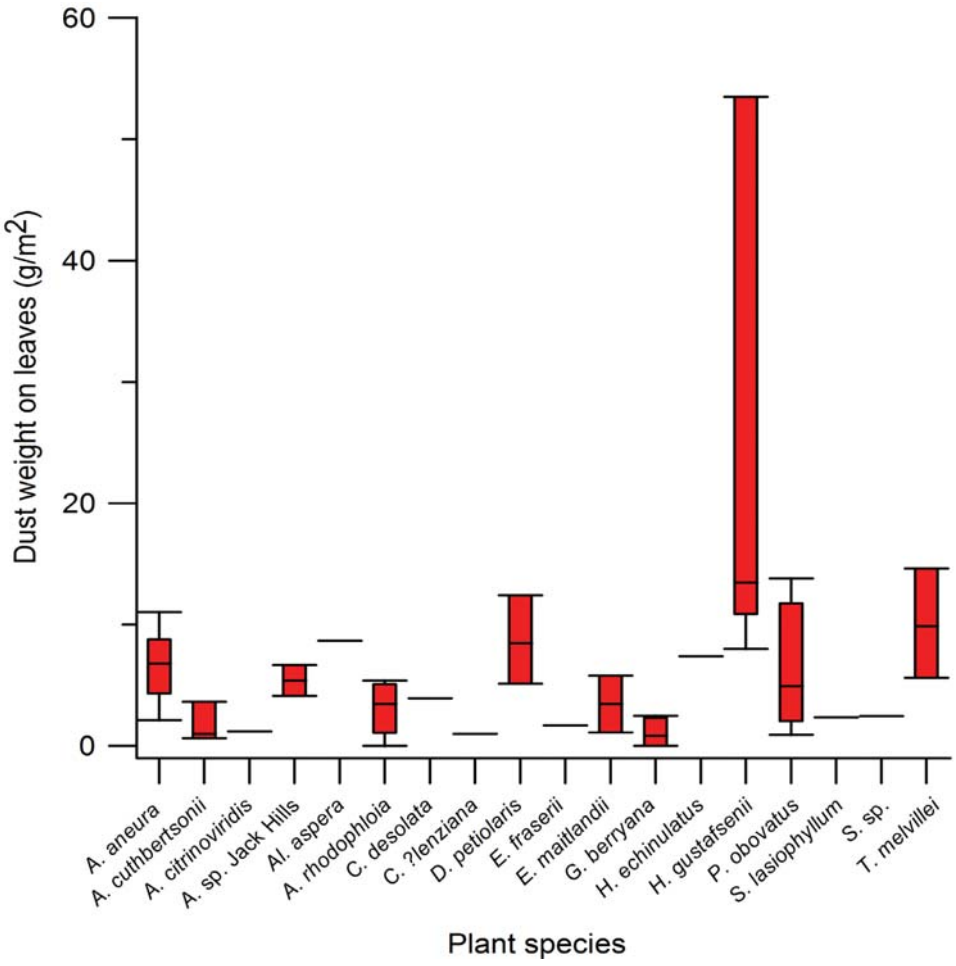

Figure 12: Box-plot of the dust weight (g/m^2) quantified on the leaves of the eighteen dominant plant species identified at the Jack Hills. The single flat lines represent only one data point.

3.6 Interaction between plant traits and leaf dust

The identified plant traits and the distance to dust source were analysed in the LMEM as predictor variables against the response variable of 'leaf dust weight'. The plant traits 'leaf surface configuration', '3D leaf shape' and 'trichome cover and type' and the 'distance to dust' were the strongest factors explaining accumulated dust weight, identified using a likelihood ratio test on the full linear mixed effects model (Table 5).

These four factors were then used in the simplified LMEM (Table 6), and all factors significantly influenced dust weight on leaves (ANOVA $P < 0.004$). The full model, diagnostic plots and the likelihood ratio tests for the models are provided in Appendix 3.D.

Table 5: Results of the LR test for each of the predictor variables for dust deposition.

Response variable	Predictor variables	LR test ([1]df as subscript), P value
leaf dust weight	plant height	$LR_{16} = 0.86$, $P < 0.35$
	leaf area	$LR_{16} = 1.48$, $P < 0.22$
	2D leaf shape	$LR_{16} = 0.60$, $P < 0.44$
	3D leaf shape	**$LR_{14} = 6.76$, $P < 0.08$**
	petiole length	$LR_{16} = 1.22$, $P < 0.30$
	leaf orientation	$LR_{15} = 3.82$, $P < 0.15$
	trichome cover and type	**$LR_{15} = 11.75$, $P < 0.003$**
	resin	$LR_{17} = 0.77$, $P < 0.40$
	leaf surface configuration	**$LR_{15} = 14.10$, $P < 0.0009$**
	distance to dust source	**$LR_{16} = 12.60$, $P < 0.0004$**

[1]df represents degrees of freedom. Bold values are predictor variables retained in the final model; other variables were removed based on the likelihood ratio test (LR).

Table 6: ANOVA (analysis of variance) results of the predictor variables used in the simplified LMEM.

Response variable	Predictor variables	F values ([1]df num and df dom as subscript), P value
leaf dust weight	3D leaf shape/posture	$F_{3,30} = 10.00$, $P < 0.0001$
	trichome cover and type	$F_{2,30} = 6.73$, $P < 0.004$
	leaf surface configuration	$F_{2,30} = 9.5$, $P < 0.0006$
	distance to dust source	$F_{1,10} = 15.04$, $P < 0.003$

[1]df num and df dom represents the numerator and denominator degrees of freedom respectively.

The minimum distance to the closest dust source significantly influenced dust loading on the leaf surfaces ($F_{1,10} = 15.04$, $P \leq 0.003$). Plants closer to the dust source collected more dust than plants at a greater distance from the dust source. The SE of the average dust weight of plants closest to the dust source however is highly variable, with some values

immediately adjacent to the pit comparable to those at control sites (Figure 13A). However, the SE of mean dust load on plant leaves decreased with increasing distance from the dust source, indicating a potential interaction between plant traits and dust loading.

'3D leaf shape' was a strong predictor of dust accumulation ($F_{3,30}$ = 10.0, $P \leq 0.0001$). Leaves that were 'revolute' (or curled downwards) of the species *G. berryana*, accumulated the lowest concentrations of dust (1.09 g/m^2 ± SE 0.45). In contrast, species with 'involute' leaves (curled upwards) of species including *H. gustafsenii*, *P. obovatus*, *D. petiolaris*, and *T. melvillei*, collected seven times that of 'revolute' leaves (7.99 g/m^2 ± SE 0.99 SE). The 'flat' leaves of the *Acacia* spp. and *C. ?lenziana* accumulated an average dust load of 4.06 g/m^2 (± 0.62 SE) (Figure 13B).

In terms of hair type, plants with 'tomentose' leaves collected 6.96 g/m^2 (± 1.27 SE) of dust, while species with 'glabrous' leaves collected only a gram of dust less, with 5.91 g/m^2 (± 1.27 SE). Species with 'strigose' trichomes (coarse, bent hair type) collected the least amount of dust (3.65 g/m^2 ± 0.74 SE). 'Leaf surface configuration' also significantly ($F_{2,30}$ = 9.5, $P \leq 0.0006$) influenced average dust loading. Plants with 'unevenly textured' leaves, for example bumpy leaves, those with raised reticulate lines, grooves, dimples and pits, experienced average dust loads of approximately twice the amount of that of smooth leaves (8.87 g/m^2 ± 1.17 versus 3.39 g/m^2 ± 0.81). Leaves with a 'striate' 'leaf surface configuration' accumulated more dust than 'smooth' leaves, but less than 'unevenly textured' ones, with an average of 6.04 g/m2 ± 0.85 (Figure 13D).

'Plant height' (m), 'leaf area' (mm^2), '2D leaf shape', 'leaf orientation', 'petiole length' and the presence or absence of 'resin' were not good predictors of the amount of dust accumulated on leaves ($P > 0.05$, Table 5).

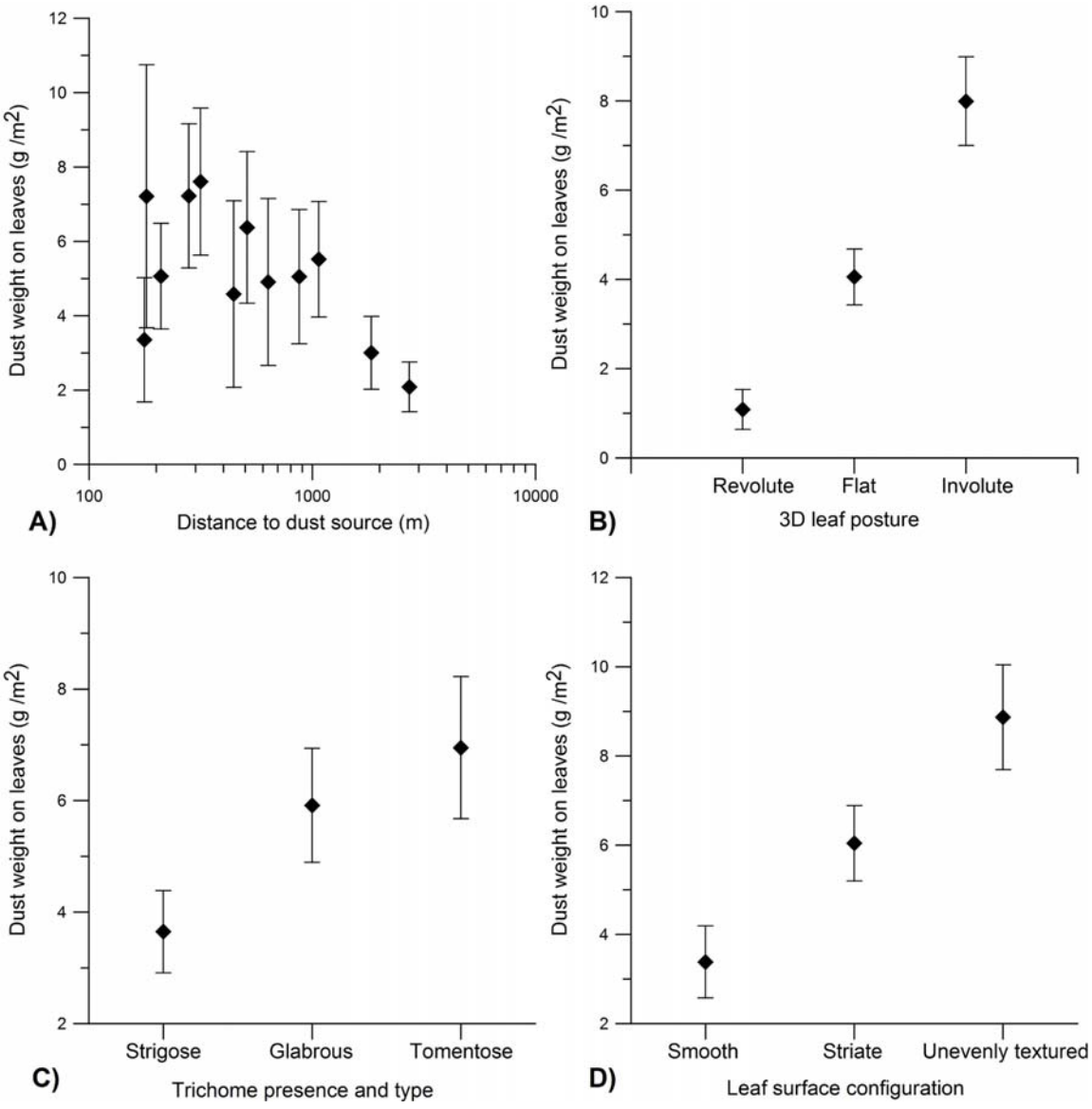

Figure 13: Average dust loading on plant foliar surfaces (± SE) for the predictor variables. A) Minimum distance to dust, B) 3D leaf shape/posture, C) trichome presence and type and D) leaf surface configuration.

3.7 Plant trait group classification and interaction with leaf dust

The final dataset for the plant trait groups consisted of 53 species and the associated traits (See Appendix 3.E for final dataset). The hierarchical cluster analysis resulted in seven

plant groups based on similar traits (Figure 14). The Analysis of Similarities (ANOSIM) showed that the seven groupings were significantly different from each other (global R = 0.84, $P < 0.1\%$) (Analysis outputs and pair-wise tests are provided as Appendix 3.F. Results of the SIMPER analysis, which provide the average contribution of plant traits to average similarity between groups, are listed in Table 7, as 'contribution %'. Plant structural traits which contributed most consistently to the plant group classifications were 'plant height' and 'petiole length'. The leaf morphological trait which contributed most consistently to the classification was 'leaf surface configuration', although the contributing traits varied across groups.

Group 1 contained eight species of shrub characterised by a 'smooth' leaf surface configuration and a short 'petiole' (0.1 – 10 mm). Group 2 contains nine species of shrub (< 1 m), characterised by a 'smooth' leaf surface configuration and 'involute' leaf posture. Group 3 contains three shrub species (< 1 m), characterised by an 'unevenly textured' leaf surface configuration, 'involute' leaf posture and an 'inclined' leaf orientation. Group 4 contains 13 shrub species (< 1 – 2 m) characterised by an 'unevenly textured' leaf surface configuration, 'glabrous' trichome type and an 'inclined' leaf orientation. Group 5 contains four grass species characterised by a 'linear' leaf shape, no petiole, 'striate' surface configuration and 'glabrous' trichome type. Group 6 contains nine tree species (> 2 m) including most of the acacias (*A. aneura*, *A. rhodophloia*, *A.* sp. Jack Hills, *A. cuthbertsonii*, *A. citrinoviridis*) and *G. berryana*, characterised by a 'linear' leaf shape, 'flat' leaf posture, an 'appressed' leaf orientation and mostly 'strigose' trichome type. Lastly, Group 7 contains six tree species (> 2 m) including *C. ?lenziana*, characterised by a 'linear' leaf shape, 'smooth' surface configuration, short petiole (0.1 – 10 mm) and 'glabrous' trichome type.

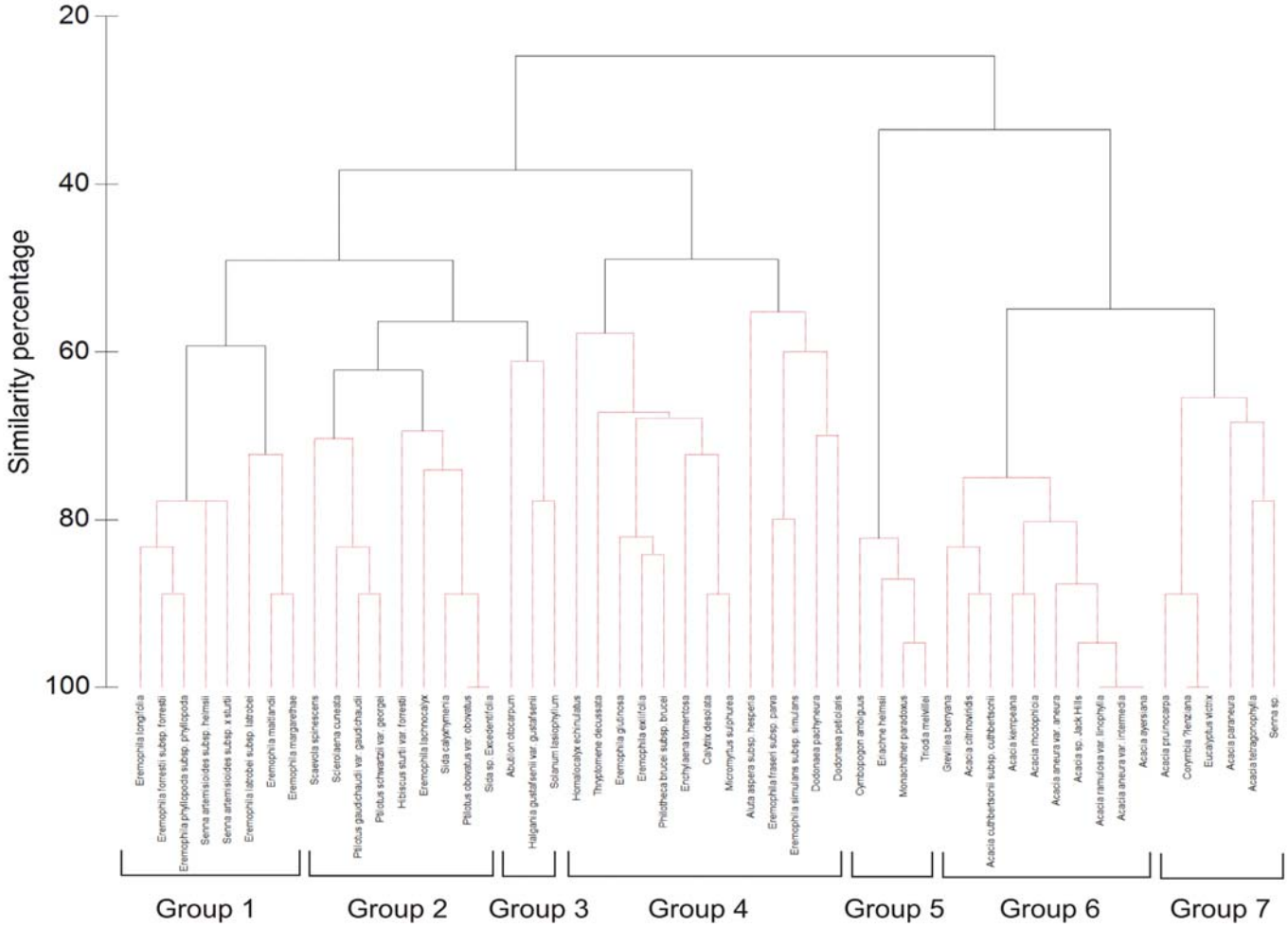

Figure 14: Hierarchical cluster analysis of plant species based on plant traits. Seven groups were determined. Significance at $P < 0.05$ (SIMPROF) is obtained above the red lines.

Table 7: Average similarity of each group and the plant traits providing highest contribution (i.e., > 10%) to the groupings (according to SIMPER analysis).

Group (average similarity)	Plant trait	Description	Contribution %
group 1 (8 species) (68.65%)	life form	shrub	16.18
	surface configuration	smooth	16.18
	petiole length	0.1-10 mm	16.18
	3D leaf shape	flat	12.14
	trichome type	tomentose	12.14
group 2 (9 species) (69.14%)	life form	shrub	16.07
	surface configuration	smooth	16.07
	mature height	< 1 m	16.07
	3D leaf shape	involute	16.07
group 3 (3 species) (66.67%)	life form	shrub	16.67
	mature height	< 1 m	16.67
	3D Leaf shape	involute	16.67
	surface configuration	unevenly textured	16.67
group 4 (13 species) (57.32%)	life form	shrub	18.46
	surface configuration	unevenly textured	18.46
	trichome type	glabrous	12.9
group 5 (4 species) (85.96%)	life form	grass	12.26
	mature height	< 1m	12.26
	surface configuration	striate	12.26
	trichome cover	glabrous	12.26
group 6 (10 species) (81.29%)	life form	tree	13.53
	mature height	> 2 m	13.53
	petiole length	0.1-10 mm	13.53
	leaf orientation	appressed	13.53
group 7 (6 species) (72.09%)	mature height	> 2 m	15.14
	2D leaf shape	linear	15.14
	trichome type	glabrous	15.14
	petiole length	0.1-10 mm	15.14

To determine if the plant trait groups could predict dust accumulation, the groups were analysed in a LMEM. Only plant species that were quantified for leaf dust could be used in the analysis. Plant groups, which had a sample size of $n \leq 2$, were removed from the analysis, as were those which did not have replication at varying distances from disturbance. This left a total of 14 out of 53 species. Groups 1 and 7 were removed. Groups 2 to 6 were analysed in the LMEM, and were shown to influence dust loading significantly (Table 8, Figure 15).

Table 8: ANOVA results of the predictor variable 'plant group' in the LMEM.

Response variable	Predictor variables	F values ([1]df num and df dom as subscript), P value
leaf dust loading	plant group	$F_{1,36} = 7.15$, $P < 0.01$

[1]df num and df dom represents the numerator and denominator degrees of freedom respectively.

The average dust weights for the analysed plant groups are shown on Figure 15, with group 3 (two species, *H. gustafsenii* and *S. lasiophyllum*) accumulating the most dust (19.90 g/m^2 ± 7.80), and group 6 (*A. aneura, A. rhodophloia, A. citrinoviridis, A cuthbertsonii* and *A.* sp. Jack Hills, and *G. berryana*) collecting the least (3.51 g/m^2 ± 0.59). Group 5, represented by the single species *T. melvillei*, collected the second highest dust load (10.00 g/m^2 ± 2.00) followed by group 4 (7.66 g/m^2 ± 1.22) and group 2 (6.38 g/m^2 ± 1.67). Group 4 is represented by four species, *D. petiolaris, Al. aspera, H. echinulatus* and *C. desolata*. Group 2 is represented by the single species *P. obovatus*.

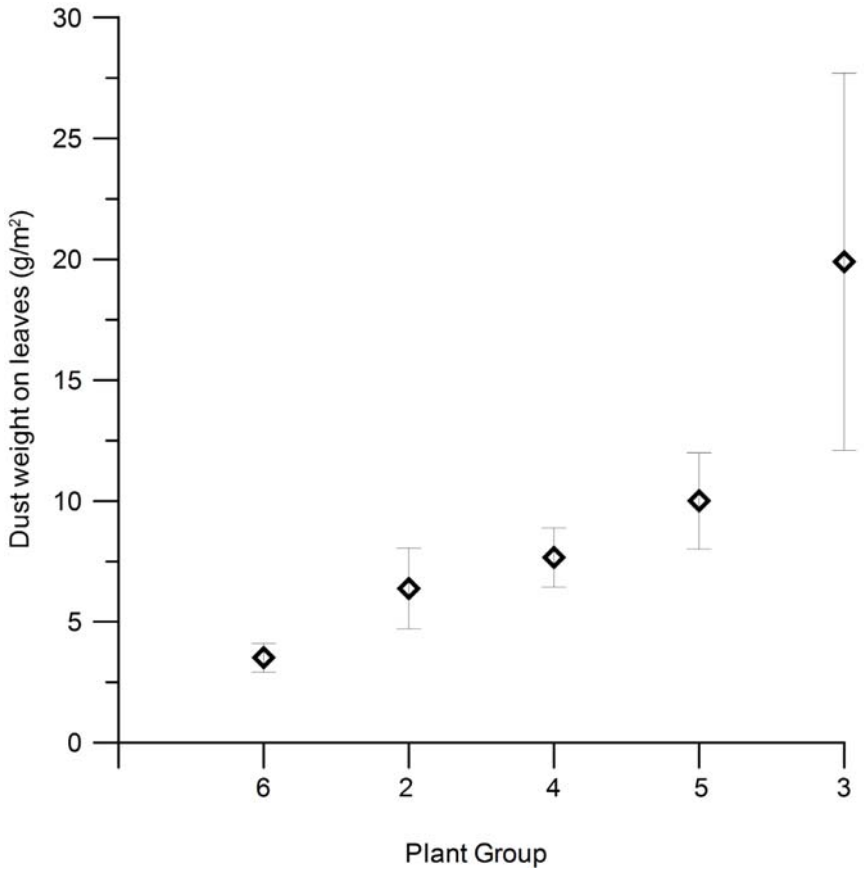

Figure 15: Average dust weight the five plant groups (± SE), in order of lowest to highest dust accumulators.

4 Discussion

4.1 Patterns of dust deposition, grain-size distribution and mineralogy

The concentration of dust was greatly elevated (>5 g/m^2) proximate to the mining operations (ca. 350 m in April and ca. 600 m in October), with dust negligible above background levels at a distance of ca. 2000 m away. This distance of influence has been reported in a number of studies specifically looking at iron ore operations, which report dust deposition on vegetation up to 1 – 2 km from emission sources (Ong et al., 2003, Kuki et al., 2008). Dust concentrations at the Jack Hills mine were consistent with background or

"reference" concentrations beyond ca. 1000 m in April and ca. 2000 m in October. However, unlike my original hypothesis that dust particle size would decrease with increasing distance, this study found that mean dust particle size increased with increasing distance from the mine. Dust collected closest to the mine had the greatest proportion of particles < 30 μm in size. I expected larger dust particles would drop out of suspension closer to the source while smaller dust particles were transported further downwind (Bullard and Livingstone, 2009, Prospero, 1999). My counterintuitive results may be explained by artefacts of the spatial scale of the sampling design. Medium to large dust particles tend to move relatively short distances and drop out of suspension quickly due to gravitational forces (Pye, 1987, Bullard and Livingstone, 2009), with smaller particles (< 20 μm) becoming suspended in the atmosphere (Gillette, 1981, Pye, 1987, Prospero, 1999, Shao, 2008). For example, road dust particles > 30 μm dropped out of suspension between 5 - 35 m from an unsealed road surface in the Pilbara (Butler, 2009). In my study, the dust monitoring sites closest to the emission sources were at least 100 m away, primarily for safety reasons, and thus the coarser dust fraction was probably not sampled. Much of the small dust fractions < 30 μm collected close to the mining operations represent the mid- to small-scale range of the particle size distribution, which can enter long-term suspension given dust particle size ranges from 0 – 100 μm. As the dust plume with the smaller dust particles moves away from the mining operations, it thus spreads out and the concentration of dust particles in the atmosphere decreases (Raupach and Leys, 1999). Therefore as we move away from the mine the percentage of this suspended dust fraction in the atmosphere decreases, and thus the amount of dust collected in the traps. The larger dust fractions observed at the control sites may be from sand and dust particles suspended locally due to natural saltation processes, rather than dust generated from the mining operations.

Topography is also likely to influence the dust deposition patterns, as there are significant topographic gradients around the mine (e.g., the Jack Hills ridgeline, the pits, etc.). Topography perturbs wind patterns and leads to local turbulence (Armbrust et al., 1964), and this can be shown at the Jack Hills by the marked asymmetry of the dust deposition pattern, which is inconsistent with the dominant wind direction (Figure 8 and Figure 9). This deposition pattern is therefore most likely induced by topographic effects.

The mineralogy of the dust reflects the source material from which it is derived. This study demonstrates that increased dust levels around the mine are directly attributable to mining activities. The dust from control sites contained mostly quartz (> 50%), which is the most common material in natural dust (Bullard and Livingstone, 2009), suggesting that the dust collected at these points is from local sources and not derived from the mine. In contrast, dust collected close to the crushing facility and stockpile area is dominated by magnetite (between 20 to > 50%), which is the main mineral mined at the Jack Hills. Dust associated with the mining pit and haul roads was composed mostly of the minerals quartz (20 – 50%), talc (5 – 20%), chlorite (< 5 – 20%) and magnetite (< 5 – 20%), also typical of the materials that are being mined or disturbed in the mining process.

4.2 Plant traits that influence leaf dust

My results show that leaf morphological traits significantly influence dust accumulation on leaf surfaces. The three morphological traits identified as increasing a plant's ability to collect and retain dust were, thick dense hairs ('tomentose'), an 'unevenly textured' surface configuration, and an 'involute' (curled upwards) leaf posture. Plants with thick dense hairs (e.g., *H. gustafsenii* and *P. obovatus*) doubled dust accumulation compared to plants with a 'strigose' hair type (coarse bent hairs). Densely hairy leaves have been shown to increase dust weights significantly (Little, 1977, Naidoo and Naidoo, 2005, Butler, 2009), consistent

with this study. However, a lack of hairs ('glabrous') did not correlate with the lowest dust weights in this study. This data may reflect the importance of considering the interaction of other traits (multiple trait interaction) when assessing a leaves ability to accumulate dust.

Species with 'unevenly textured' leaf surface more than doubled dust weights compared to species with 'smooth' leaves. The trait 'involute' (curled upwards) leaf posture collected eight times the amount of dust than 'revolute' (curled downwards) leaves, and twice the amount of 'flat' leaves. The 'involute' posture is likely to increase the ability of the leaf to retain dust once it is deposited, as the leaf creates a bowl shape. 'Revolute' leaves on the other hand do not allow dust to collect on the leaf surface, and thus reduce dust accumulation. In summary, the above data confirm that dust deposition is influenced by two leaf-scale properties: surface roughness and leaf posture.

I found that structural traits including 'plant height', 'leaf area', 'petiole length', 'leaf orientation' and '2D leaf shape' did not significantly influence dust loading (Table 5). Structural traits increase a plant's overall ability to capture dust from the atmosphere at the plant scale (Raupach and Leys, 1999, Chamberlain, 1975, Beckett et al., 2000). However, this study focused on the leaf scale. For the purpose of accumulating dust on the leaf surface, structural traits may not be so important (Litschke and Kuttler, 2008). There are a number of other explanations for not identifying any significant structural traits. Previous studies that identified structural traits as important for plant dust capture ability (Raupach and Leys, 1999, Chamberlain, 1975, Beckett et al., 2000) found that a combination of structural traits increased dust capture, for example, tall and wide trees with a high packing density of leaves and branches. So, unless a wide and densely packed canopy accompanies the structural trait 'plant height', this trait alone may not increase dust capture significantly. Another reason could be that some structural traits investigated here, such as 'petiole

length', did not show a large variation in their dimensions. Therefore, they unlikely show a difference in dust trapping potential.

4.3 Plant trait groups

Seven plant trait groups were defined by hierarchical cluster analysis based on similar structural and morphological traits, with percentage similarity within groups ranging from 57 – 86 %. Five of these groups could be analysed for levels of dust accumulation, and these groups significantly influenced dust loading ($F_{1,32} = 7.5$, $P < 0.001$). The five groups and their component species, are (in descending order of dust load): group 3 (*H. gustafsenii* and *S. lasiophyllum*), group 5 (*T. melvillei*), group 4 (*H. echinulatus*, *C. desolata, Al. aspera, E. fraseri* and *D. petiolaris*), group 2 (*P. obovatus*) and group 6 (*A. aneura, A. cuthbertsonii, A. citrinoviridis, A. rhodophloia, A. sp. Jack Hills* and *G. berryana*).

The contributing traits, which defined groups attracting the highest dust load (groups 3, 5, 4 and 2), contained a trait or a combination of traits identified in the univariate analysis as increasing dust deposition. Group 3, which had the highest dust loading, was represented by two species, which had 'unevenly textured', 'tomentose' and 'involute' leaves. Thus, the combination of individual leaf morphological traits relevant in the univariate analysis not surprisingly also influenced dust loading at the plant group level. However, dust weights at the plant group level were greater than the average weights collected by the individual traits, indicating multiple traits working in combination. While structural traits did not exhibit a statistically significant correlation to dust load in the univariate analysis on their own, these structural traits may provide additional influence to the overall dust capture ability of plant groups. For example, group 3 had an 'inclined' (15 – 75°) leaf orientation, which could help to retain dust. In contrast, group 6 had the lowest dust levels and an 'appressed' (1 – 15°) leaf orientation, which could reduce dust retention. In other words,

particular structural traits might amplify dust retention if they occur in combination with specific morphological traits.

The above findings, however, highlight two key limitations of my study. First, the dust footprint of the mine extends across three broad plant communities, which feature a relevant degree in species variability. Indeed, not all identified groups could be analysed because they contained species which did not occur across the study area (i.e., group 1 and 7). Groups 2 and 5 contained only one species. Therefore, they cannot be considered a "group". In other words, the spatial distribution of plant species in the research area does not permit a statistically thorough analysis of the plant groups and their influence on dust capture and retention.

Second, the hierarchical cluster analysis groups species based on the most similar combination of traits at a particular locality, irrespective of their potential relation to dust capture and retention. The overall degree of similarity used for grouping varies between 57 – 86%. Hence, within groups, species might exhibit different traits (accounting for the dissimilarity of 14 – 43%), which may be very important for dust loading. An example is presented by group 6. It mainly consists of *Acacia* spp. but also features *Grevillea berryana*. These species are similar in terms of 'height' and 'leaf shape'. But they differ in the traits '3D leaf shape' and 'surface configuration'. The *Acacia* ssp. have 'flat, striate leaves' while *Grevillea berryana* has 'revolute, smooth leaves'. These traits show a large yet differing influence on dust load (Figure 13). Therefore, a meaningful grouping of plants requires that traits and groups of traits relevant to the dependent variable of interest (here, dust load) are determined first and then used in the grouping process. This identification of relevant traits can be achieved by individual trait analysis combined with, for example, linear mixed modelling considering the various permutations of trait interactions. This

procedure was not attempted in the study at hand because of the sampling restrictions imposed by the study area, as explained in the previous paragraph. In addition, physiological measurements could only be obtained for 11 species out of the 53 used in the grouping analysis (presented in Chapter 4). It is highly doubtful that ~ 20% of the entire species volume used for defining the morphological groups are representative of their plant function with regards to increased dust loading, especially keeping the aforementioned sampling and methodological restrictions in mind. Therefore, I restrict the following correlational analysis of plant physiological response and dust load (chapter 4) to individual species and traits, which I found to be predictive of dust load in my research area. While this precludes the applicability of my results to predicting ecosystem-scale dust responses elsewhere, I identified important leaf-scale traits, which are predictive of dust load. They may be helpful for establishing plant functional types in regards to morphology, dust load, and its related physiological function in future studies.

5 Final summary of findings from this Chapter

The following conclusions are drawn:

1. The Jack Hills mine generates dust greater than natural background levels, which thus imposes elevated dust loads on the surrounding vegetation.

2. Dust decreases rapidly and non-linearly with increasing distance from dust emission sources, and was negligibly above background levels beyond 2000 m.

3. Dust concentration was greatly elevated (>5 g/m^2) proximate to the mining operations (ca. 350 m in April and ca. 600 m in October), exhibiting levels 5 fold that of background levels.

4. Dust loading is affected by seasonal variations, wind direction, and local topography.

5. Most dust in the main zone of influence of the mine displays grain sizes < 30 μm, with the most frequent grain size of 2.55 μm. Such fine grains have the potential to block stomata.

6. Leaf morphological traits, which relate to surface roughness and 3D shape of leaves, exhibit a significant correlation to dust load on leaves. These include 'tomentose' trichome type, 'unevenly textured' surface configuration and 'involute' leaf posture. Structural traits did not significantly influence dust accumulation.

7. Spatial distribution of plant species in the research area precludes a statistically meaningful analysis of plant trait groups and their relation to dust loading.

8. Trait-based grouping criteria should be selected once a correlational relationship between the respective traits and/or groups of traits and the parameter of interest (here, dust load) has been established.

6 References

ARMBRUST, D. V., CHEPIL, W. S. & SIDDOWAY, F. H. 1964. Effects of Ridges on Erosion of Soil by Wind. *Soil Science Society of America Proceedings,* 28**,** 557-560.

BECKETT, K. P., FREER-SMITH, P. H. & TAYLOR, G. 2000. Particulate pollution capture by urban trees: Effects of species and windspeed. *Global Change Biology,* 6**,** 995-1103.

BRINDLEY, G. W. & BROWN, G. 1980. *Crystal Structures of Clay Minerals and their X-Ray Identification,* London, Mineralogical Society.

BULLARD, J. E. & LIVINGSTONE, I. 2009. *Geomorphology of Desert Environments*, Springer Science.

BURNHAM, K. P. & ANDERSON, D. R. 2002. *Model Selection and Multimodel Inference: A Practical Information-Theoretic Approach,* New York, Springer Science+Business Media Inc.

BUTLER, R. 2009. *Vulnerability of plant functional types to dust deposition in the Pilbara, NW Australia.* Bachelor of Science (Environmental Science) (Honours), The University of Western Australia.

CHAMBERLAIN, A. C. 1975. *The movement of particles in plant communities* New York, Academic Press.

CLARKE, K. R. & GORLEY, R. N. 2006. PRIMER v6: User Manual/Tutorial. Plymouth: PRIMER-E.

CLARKE, K. R. & WARWICK, R. M. 2001. *Change in Marine Communities: An approach to statistical analysis and interpretation,* Plymouth, PRIMER-E Ltd.

EVELING, D. W. & BATAILLÉ, A. 1984. The effect of deposits of small particles on the resistance of leaves and petals to water loss. *Environmental Pollution Series A, Ecological and Biological,* 36**,** 229-238.

EVERETT, K. R. 1980. Distribution and properties of road dust along the northern portion of the haul road. *In:* BROWN, J. & BERG, R. (eds.) *Environmental Engineering and Ecological Baseline Investigations along the Yukon River - Purdhoe Bay Haul Road.* CRREL: US Army Cold Regions Research and Engineering Laboratory.

FARMER, A. M. 1993. The effects of dust on vegetation--a review. *Environmental Pollution,* 79**,** 63-75.

GILLETTE, D. A. 1981. Production of dust that mat be carried great distances. *Geological Society of America,* 186**,** 11-26.

GRANTZ, D. A., GARNER, J. H. B. & JOHNSON, D. W. 2003. Ecological effects of particulate matter. *Environment International,* 29**,** 213-239.

HIRANO, T., KIYOTA, M. & AIGA, I. 1995. Physical effects of dust on leaf physiology of cucumber and kidney bean plants. *Environmental Pollution,* 89**,** 255-261.

KUKI, K., OLIVA, M. & PEREIRA, E. 2008. Iron Ore Industry Emissions as a Potential Ecological Risk Factor for Tropical Coastal Vegetation. *Environmental Management,* 42**,** 111-121.

LITSCHKE, T. & KUTTLER, W. 2008. On the reduction of urban particle concentration by vegetation - a review. *Meteorologische Zeitschrift,* 17**,** 229-240.

LITTLE, P. 1977. Deposition of 2.75, 5.0 and 8.5 μm particles to plant and soil surfaces. *Environmental Pollution,* 12**,** 293-305.

MATHWORKS INC. 2000. MATLAB v. 6.1. 6.1 ed. Natick, MA.

MATTISKE CONSULTING PTY LTD 2005. Flora and Vegetation on the Jack Hills project area. Mattiske Consulting Pty Ltd.

NAIDOO, G. & NAIDOO, Y. 2005. Coal Dust Pollution Effects on Wetland Tree Species in Richards Bay, South Africa. *Wetlands Ecology and Management,* 13**,** 509-515.

ONG, C. C. H., CUDAHY, T. J., CACCETTA, M. S. & PIGGOTT, M. S. 2003. Deriving quantitative dust measurements related to iron ore handling from airborne hyperspectral data. *Mining Technology,* 112**,** 158-163.

PALING, E. I., HUMPHRIES, G., MCCARDLE, I. & THOMSON, G. 2001. The effects of iron ore dust on mangroves in Western Australia: Lack of evidence for stomatal damage *Wetlands Ecology and Management,* 9**,** 363-370.

PETROFF, A., MAILLIAT, A., AMIELH, M. & ANSELMET, F. 2008. Aerosol dry deposition on vegetation canopies. Part I: Review of present knowledge. *Atmospheric Environment* 42**,** 3625-3653.

PINHEIRO, J. C. & BATES, D. M. 2000. *Mixed-Effect Models in S and S-Plus,* New York, Springer Verlag.

PROSPERO, J. M. 1999. Long-range transport of mineral dust in the global atmosphere: Impact of African dust on the environment of the southeastern United States. *Proceedings of the National Academy of Sciences of the United States of America,* 96**,** 3396-3403.

PYE, K. 1987. *Aeolian Dust and Dust Deposition,* London, Academic Press.

R DEVELOPMENT CORE TEAM 2012. R: A language and environment for statistical computing. Vienna, Austria: R Foundation for Statistical Computing.

RASBAND, W. S. 1997-2012. ImageJ. Maryland, USA: U.S. National Institutes of Health.

RAUPACH, M. R. & LEYS, J. F. 1999. The efficacy of vegetation in limiting spry drift and dust movement. Canberra: CSIRO.

SHAO, Y. 2008. *Physics and Modelling of Wind Erosion*, Springer Science.

SIMPSON, M. G. 2006. *Plant Systematics,* London, UK, Elsevier Academic Press.

SINGH, B. & GILKES, R. J. 1992. XPAS: An Interactive Computer Program for X-ray Powder Diffraction Patterns. *Powder Diffraction 7.*

Chapter 4 –Physiological Responses of Plants to Dust Deposition at the Jack Hills

1 Introduction

The physical impacts of high dust deposition on vegetation in semi-arid and arid environments can reduce physiological function and thus photosynthesis and growth (Sharifi et al., 1997, Gleason et al., 2007). For example, three Mojave Desert shrubs (*Larrea tridentata* Coville, *Hymenoclea salsola* Torr. & A.Gray and *Atriplex canescens* (Pursh) Nutt.) showed reductions in net photosynthesis (of up to a 58%) as well as reductions in stomatal conductance and transpiration under heavy dust loads. Dusted leaves were also 2 – 3°C higher than control plants due to an increase in absorbance of light energy (Sharifi et al., 1997). Limited information, however, is available on the effects high dust levels have on Australian plants (see, for example Paling et al., 2001, Chaston and Doley, 2006), and even fewer studies have been conducted under field conditions in semi-arid and arid environments in Australia, where natural dust levels are generally high (see, for example Butler, 2009). As closely related plant species can respond differently to dust based on their mechanisms or strategies to deal with dust exposure (Kuki et al., 2008), it is difficult to extrapolate results from these studies to predict species response to dust on Australian species.

The purpose of this chapter is to measure the physiological response of plant species at the Jack Hills to dust levels that are above natural background levels (Chapter 3), and to identify the potential mechanisms through which increased dust loading may damage plant health. I thus identify species that act as reliable environmental indicators for monitoring effects of anthropogenic dust on vegetation. I also test if the plant traits correlated to dust

load predict the physiological response. To this end, I examined the physiological response of perennial plants surrounding the mine using the measures stomatal conductance (g_s), chlorophyll fluorescence (maximum efficiency of PSII photochemistry (Φ_{PSII})) and stable carbon isotope composition ($\delta^{13}C$) of plants. g_s is a measure of the rate of carbon dioxide (CO_2) or water vapour (H_2O) movement through the stomata of a leaf. The control of g_s and stomatal movements (e.g., aperture) are affected by light, water availability/water stress, humidity and CO_2 concentration (Lambers et al., 2008). Thus, if a plant is water stressed, it may close its stomata and downgrade photosynthesis. Alternatively, the stomata may become blocked by dust particles (Hirano et al., 1995). Chlorophyll fluorescence can be used to measure the photosynthetic performance of plants (Baker, 2008). Fluorescence is a measure of the efficiency of electron transport through Photosystem II (PSII). When plants are stressed, photosynthesis is often down-regulated. Carbon discrimination values ($\Delta^{13}C$), calculated from the stable isotopic carbon composition of plant material (ratio of $^{13}C/^{12}C$, $\delta^{13}C$, relative to source CO_2), can provide a measure of water and/or other physiological stress due to a reduced supply of CO_2, resulting in depletion of ^{13}C. Environmental parameters also affect plant health and function. Hence, I recorded soil parameters including soil moisture and soil pH to investigate if they correlate with plant function.

I predict that the physiological stress of plants will increase with increasing dust loads and with decreasing dust particle size. I also predict that plants that possess traits that increase dust loading will experience a greater physiological stress.

2 Materials and Methods

2.1 Sampling design

Physiological measurements of plants and soil samples were taken at 16 of the 28 sample sites established in October 2010 (Figure 1). These sites represent stations from all three axes at increasing distance from the disturbance areas. Eleven of the eighteen species identified at the sample sites (see Chapter 3) were measured for physiological performance in October 2011 (Section 2.2). These species were selected as they occurred at a range of sites and distances across the study area. Three individuals of each species were selected, recorded and tagged with numbered aluminium tags for reference. Qualitative observations of plant health were also recorded at each site in April and October 2011. Soil samples for soil analysis (Section 0) were collected at these sites in April and October 2011.

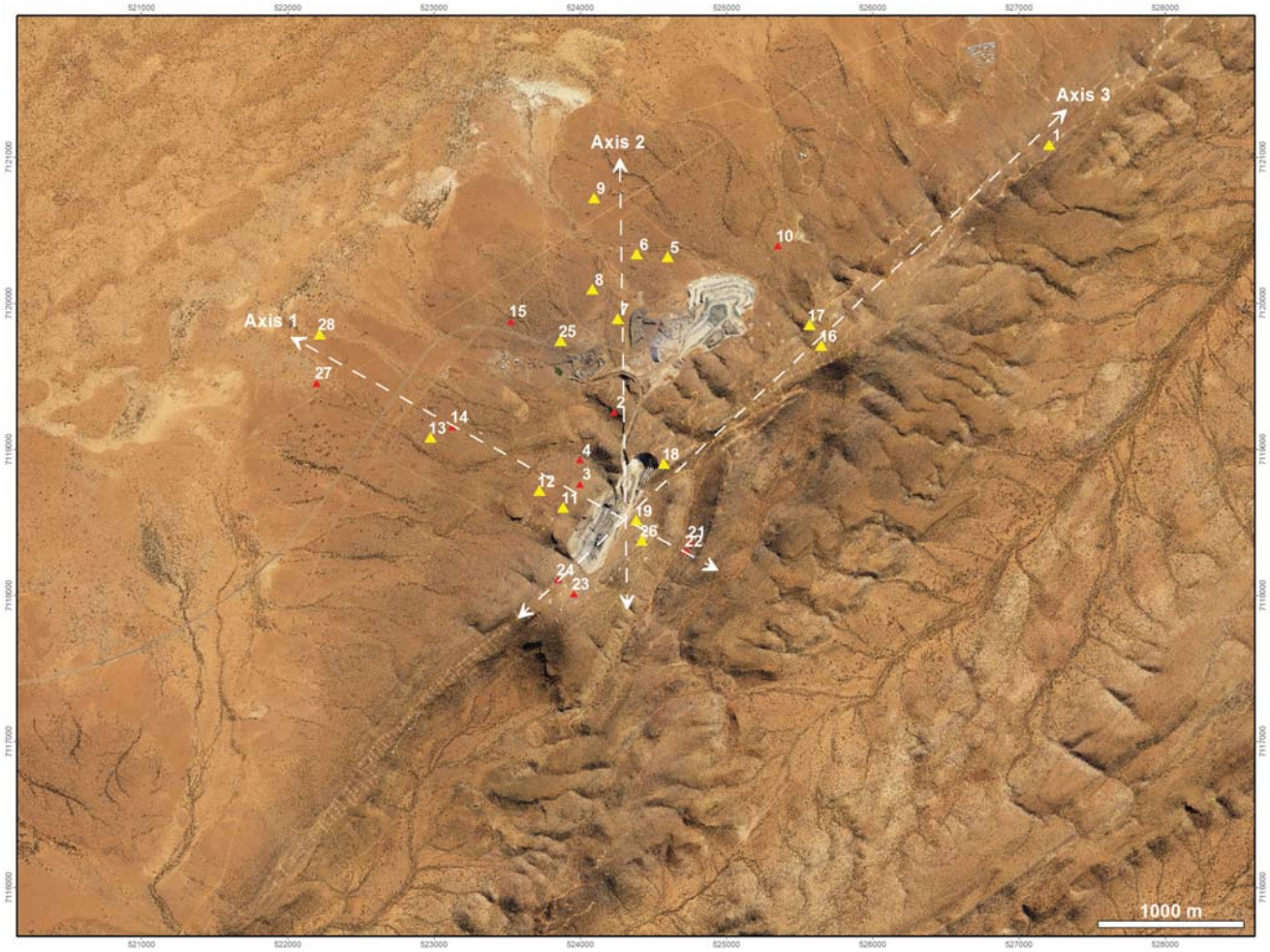

Figure 1: Location of sites used for measurement of plant physiological response and soil parameters (yellow triangles). Red triangles are remaining dust collector stations established for dust measurements (see Chapter 3), but not used for measurements of plant physiological function.

2.2 Plant physiological parameters

2.2.1 Stomatal conductance

Stomatal conductance (g_s) of leaves of the selected and tagged individuals was measured using a SC-1 "Leaf Porometer" (Decagon Devices, 2005-2012). Three to five measurements were recorded for each individual plant because g_s values can be highly variable. g_s was measured for the abaxial (upper surface) of the leaves in [mmol/(m^2s)]. This is the gas mass flux per unit area. g_s measurements were taken between approximately 6:00 am (sunrise) to 11:00 am each day, to coincide with the plants most active period (Ullmann, 1989).

2.2.2 Chlorophyll fluorescence

Chlorophyll fluorescence was measured using a Pulse-Amplitude-Modulation (PAM) fluorometer using the Saturation Pulse Method (Schreiber, 2004). One measurement was recorded for each individual tagged plant. First, a leaf of each plant was 'dark adapted' by putting small clips on each plant to block light for 10 minutes. In this state, all electron receptors are empty and thus a reference value, the zero fluorescence level (F_0), can be determined (Maxwell and Johnson, 2000). The F_0 value is determined at very low light energy, which ensures that all the PSII reaction centres are in the 'open' state and therefore capable of photochemistry.

The leaves were then exposed to a short pulse of light of high energy. This short light pulse saturates all electron receptors instantaneously, and thus the maximum fluorescence yield (F_m) can be determined. This short light pulse transiently drives a very high proportion of PSII reaction centres into the 'closed' state, thereby decreasing the capacity for PSII photochemistry almost to zero. From these two values, the maximum efficiency of PSII photochemistry (Φ_{PSII}), is calculated by the following equation:

Equation 1:

$$\frac{F_m - F_0}{F_m} = \frac{F_v}{F_m} = \Phi_{PSII}$$

where F_v is the difference of F_m and F_0, also termed "variable fluorescence". In other words, the maximum efficiency of PSII photochemistry, or maximum quantum yield, Φ_{PSII}, measures the maximum photochemical efficiency that could be achieved if all electron receptors were open. For a detailed review of the method, the reader is referred to Maxwell and Johnson (2000). Chlorophyll fluorescence measurements were recorded between approximately 6:00 to 11:00 am each day.

2.2.3 Stable isotope analysis of foliage ($\delta^{13}C$)

At each site, a bulk sample of approximately 20 leaves was collected from each individual tagged species. Leaves were collected in seed envelopes, labelled and transported back to the laboratory. The stable isotopic composition of carbon (ratio of $^{13}C/^{12}C$, $\delta^{13}C$) was measured for the plant foliar using a continuous-flow isotope ratio mass spectrometer (IRMS) at the West Australian Biogeochemistry Centre, The University of Western Australia.

To prepare the samples, the material was ground to a fine powder, and 0.5 g was weighed into a small tin cup. The weighed samples were then analysed using the IRMS system consisting of a SerCon 20-22 mass spectrometer connected with an Automated Nitrogen Carbon Analyzer (Sercon Group, UK). The raw-$\delta^{13}C$ data of samples were measured relative to the isotopic composition of a laboratory working gas, then converted and reported on an international isotope reference scale. $\delta^{13}C$ values were converted using the Vienna PeeDee Belemnite (VPDB) scale, established by the International Atomic Energy Authority (IAEA).

The conversion of the raw $\delta^{13}C$ ratios to the international scale was done with a multi-point linear regression method, also known as multi-point normalization (Paul et al., 2007). For the $\delta^{13}C$ normalization, the international certified reference standards used were NBS 22 (Oil), USGS 24 (Graphite), L-SVEC (Lithium carbonate), USGS 40 (L-glutamic acid) and USGS 41 (L-glutamic acid), provided by the International Atomic Energy Agency (IAEA) and based on the updated scale in (Coplen et al., 2006). The external precision of the isotope ratio analysis was one standard (σ) deviation < 0.1‰ for $\delta^{13}C$.

The converted $\delta^{13}C_{VPDB}$ is then reported as the relative difference, in parts per thousand (‰), between the foliar $\delta^{13}C_{VPDB}$ and the laboratory working gas. This is known as Carbon discrimination or $\Delta^{13}C$.

2.2.4 Soil parameters

Three soil cores were collected randomly within each site (i.e., a 15 m radius around the dust collectors) and bulk-sampled. Soil cores were dug to a depth of approximately 20 cm, extracting approximately 100 to 200 g of soil. Samples were double-bagged in airtight plastic bags and stored in a cool, dark place prior to processing in the laboratory.

Soil moisture content of the soil samples collected in April and October 2011 was determined gravimetrically using the method of Black (1965). A 5 g sample was sieved to < 2 mm fraction, placed in a pre-weighed tin cup and weighed on a balance (accuracy of ±0.001 g). The soil was then dried in an oven at 100 °C for five days. Over the 5 days, several samples were weighed to ensure weights became constant, indicating the soil was dry. Samples were then re-weighed, and the final weight of the soil is the difference of the dry weight and the weight of the tin cup. Soil moisture content was then calculated as a

percentage by dividing the weight of the dry soil by the weight of the wet soil and multiplying by 100.

Soil pH, EC and nutrients were measured from soils collected in April only. For soil pH and soil EC, a 10 g sample of air-dried soil (sieved to < 2 mm fraction) was mixed in a beaker with 20 ml of double de-ionised water (1:2 ratio). The aqueous solution was then stirred intermittently for 30 minutes and allowed to rest for one hour. Soil pH was measured using a soil pH meter (Orion 520A, Thermo Electron Corporation) and soil EC with a soil EC meter (Orion 105, Thermo Electron Corporation) at room temperature (25°C).

Nitrate (NO_3^--N) and ammonium (NH_4^+-N) were measured using the methods of Rayment and Higginson (1992) and Bundy and Meisinger (1994). A 5 g sample of air-dried soil (sieved to < 2 mm fraction) was weighed out into a 100 ml extraction bottle. 50 ml of 1 M Potassium Chloride (KCl) was then added and the bottle shaken for 60 minutes on a shaker. The sample was then filtered into a 30 ml vial and stored at 4°C until analysis. Analysis was undertaken using an automated colorimetric method with an Auto-analyser (AA) Technicon AAII Manifold and Bran & Luebbe AA3 Digital Colorimeter.

2.3 Data analysis

2.3.1 Univariate analysis to determine plant physiological response to dust deposition

To analyse whether dust weight influences plant physiological response, a Linear Mixed Effect Model (LMEM) was developed using R Studio (R. 0.95.265) and the nlme package (R Development Core Team, 2012). The physiological performance of the plants measured by the parameters of stomatal conductance (g_s), chlorophyll fluorescence (Φ_{PSII}) and carbon discrimination ($\Delta^{13}C$) (response variable) was modelled as a function of the 'plant species',

'dust weight', 'distance to mine' and soil parameters (e.g. soil pH, soil EC, soil moisture) (predictor variables). The dust weight value used was that of the October dust weight collected in the dust traps. Dust weight on the individual plant leaves could not be used as there was not enough replication across species and distances to run the model. The non-linearly distributed response variables were transformed via the natural logarithm (LN), thus yielding a normal distribution, which is needed for the LMEM.

I included a nested random-effect structure: repeated measures of individual species were nested in repeated species, which in turn were nested within sample location, thus establishing a scale-dependent nesting of random effects. This is reasonable because it can be expected that random effects at the scale of an individual plant are smaller than, for example, random effects concerning this species found at multiple locations separated by hundreds of meters in spatial distance. In addition, I used maximum likelihood (ML) to investigate the contribution of the fixed effects. The model assumptions (data is normally distributed and independence of errors) were confirmed using diagnostic plots, including quantile-quantile plots and residual plots, in R. The equation that represents the LMEM is:

Equation 2:

$PP_{ij} = \beta_0 + \beta PS_{1ij} + \beta DW_{2ij} + \beta PH_{3ij} + \beta EC_{4ij} + \beta SM_{5ij} + \beta SA_{6ij} + \beta SN_{7ij}$ (**fixed**) + $u_j + e_{ij}$ (**random**),

where PP = Physiological parameters (g_s, Φ_{PSII} and $\Delta^{13}C$), the indices i and j represent the value of the response variable at plot i nested within site j; β_n represent the fixed intercept (n = 0) and the fixed effects of variables (n = 1, 2,…7); PS = 'Plant species', DW = 'Dust weight', PH= 'Soil pH', EC = 'Soil EC', SM = 'Soil moisture', SA = 'Soil ammonium', SN

= ‘Soil Nitrate’; u_j is the random effect associated with the intercept for site j, and e_{ij} represents the residual associated with the observation on an individual plot i at site j.

I used Likelihood Ratio (LR) tests to simplify the fixed effects and Akaike’s Information Criterion for small samples (AICc) (Burnham and Anderson, 2002), and found similar results to the LR tests. Finally, I used F-tests (ANOVA) to determine the significance of the fixed effects within the simplified models (Pinheiro and Bates, 2000).

2.3.2 Univariate analysis to determine plant trait responses to dust deposition

To analyse if the plant traits (which influenced dust loading in Chapter 3) correlate to plant physiological response, the traits were added to the LMEM and analysed against the physiological measures. The significant plant traits (‘trichome type and cover’, ‘leaf surface configuration’ and ‘3D leaf shape’) identified in Chapter 3 replace the variables ‘plant species’, ‘dust weight’, ‘distance to mine’ and environmental parameters as fixed effects in the model (Equation 2).

3 Results

3.1 Qualitative observation of plant health

Qualitative observations of plant health were recorded at the sub-set of dust stations in April and October 2011 (Figure 1). These observations are provided in Table 1, while photographs of the dust stations for both the April and October 2011 visits are provided as Appendix 4.A. A number of sites close to the mine site, e.g., site 25, site 7 and site 8, displayed obvious signs of stress such as: dead *Acacia* spp., low diversity of understory species and high dust loads on leaves that were easily noticeable with the naked eye. The most stressed and dusty sites were site 25, located adjacent to the crushing facility, and site 7, which is adjacent to the main waste rock dump. At these sites, there was noticeable

Acacia spp. death (*A. aneura*, *A. rhodophloia*) and a lack of annual and understory species, compared to similar communities at greater distances from the mine.

Physiological measurements could only be taken from species that were still alive at the time of sampling (October 2011). Therefore, the physiological results (Section 3.2) do not consider the three *A. aneura* species at sites 25, 7 and 8 which died between the April and October sampling periods.

Table 1: Qualitative observations of plant health at the sub-set of dust stations at which physiological plant measurements were taken. The sites are ordered first by axis (see Figure 1), then distance to the mine.

Axis	Site	Distance to mine (m)	Species observations		[1]Number of plants dead	
			April 2011	Oct 2011	April 2011	Oct 2011
1	26	280	Plant species appear healthy.	Plant species appear healthy. Some browning *Triodia melvillei*.	0	0
1	11	309	*T. melvillei* healthy.	*T. melvillei* appears stressed, patches of browning/dead *Triodia*.	0	0
1	12	502	*Acacia* spp. look slightly stressed. Low abundance of annual species.	*Acacia* spp. slightly stressed. No annual species remaining.	0	0
1	13	1218	Overstorey healthy. Understorey species recovering after long period of low rainfall.	Overstorey healthy. Some understory species recovering.	0	0
1	28	1838	Plant species healthy. Abundant annual grasses and herbs.	Healthy. Abundant annual grasses.	0	0
2	25	210	Understorey species dead. *Acacia* spp. stressed, losing leaves. No annual grasses or herbs. High dust loads	Understorey species dead. *Acacia* spp. stressed, many dead and losing/dropping leaves. One tagged *A. aneura* species had died between April and October. No annual grasses or herbs. High dust loads.	0	1
2	7	316	Many under and overstorey species dead. Spares annual species. Leaves	Many under and overstorey species dead or very stressed. One tagged *A. aneura* species had died	0	1

Axis	Site	Distance to mine (m)	Species observations		[1]Number of plants dead	
			April 2011	Oct 2011	April 2011	Oct 2011
			visibly dusty.	between April and October. High levels of dust present.		
2	8	445	Many understorey species dead. Some *A.* spp. stressed. Annual species sparse.	Regrowth of understorey species. Some *A.* spp. dead or very stressed. One tagged Acacia aneura species had died between April and October.	0	1
2	5	510	Species appear Healthy. Annual species present. Limited dust on vegetation observed.	Some death of understorey species. Some stressed Acacia species.	0	0
2	6	635	Healthy	Healthy	0	0
2	9	1069	All species healthy. Some annual species present.	*Ptilotus obovatus* and *Halgania gustafsenii* very dry/almost dead.	0	0
3	18	177	Species appear healthy. Some flowering of *T. melvillei.*	Over- and understorey species appear healthy.	0	0
3	19	181	Species appear healthy. Some dust present.	*T. melvillei* and *Senna* sp. appear stressed. High levels of dust present.	0	0
3	17	784	All species healthy. *T. melvillei* green and flowering.	Healthy. Limited visible dust.	0	0
3	16	873	All species healthy, *T. melvillei* green and flowering.	Healthy. Limited visible dust.	0	0

Axis	Site	Distance to mine (m)	Species observations		[1]Number of plants dead	
			April 2011	Oct 2011	April 2011	Oct 2011
3	1	2723	Old dead *Acacia* trees, otherwise Healthy.	Healthy	0	0

[1]Number of plants dead refers only to plants that were tagged for physiological measurements, not all plants within the site location.

3.2 Plant Physiological Response

3.2.1 Stomatal conductance

Stomatal conductance (g_s) values of the eleven plant species ranged from 14.1 to 477 mmol/m^2/s^{-1} recorded in the October 2011 sampling period (Figure 2). The highest g_s values belonged to the species *Dodonaea petiolaris* and *Halgania gustafsenii*, with median values of 261 and 127 mmol/m^2/s^{-1}, respectively. The species *Aluta aspera* and *Grevillea berryana* both exhibited relatively low g_s values, with median values of and 61.2 and 38.9 mmol/m^2/s^{-1} and maxima of 103 and 123 mmol/m^2/s, respectively. The species *Acacia aneura, A.* sp. Jack Hills, *A. rhodophloia, Calytrix desolata, Eremophila maitlandii, Ptilotus obovatus* and *Triodia melvillei* had consistent median values ranging from approximately 55-100 mmol/m^2/s. The species *A. aneura, A.* sp. Jack Hills, *Al. aspera, A. rhodophloia* and *T. melvillei* recorded a number of higher outliers (Figure 2).

3.2.1 Chlorophyll fluorescence

The maximum efficiency of PSII photochemistry (Φ_{PSII}) values ranged from 0.43 to 0.88. The median values for the measured species ranged from 0.66 to 0.83 (Figure 3). The theoretical maximum of Φ_{PSII} is 0.8 or 80%. Therefore, most species operated at or close to maximum photosynthetic efficiency. *Al. aspera* and *T. melvillei* had a slightly reduced Φ_{PSII}, with a median value of 0.66 and 0.68, respectively (Figure 3).

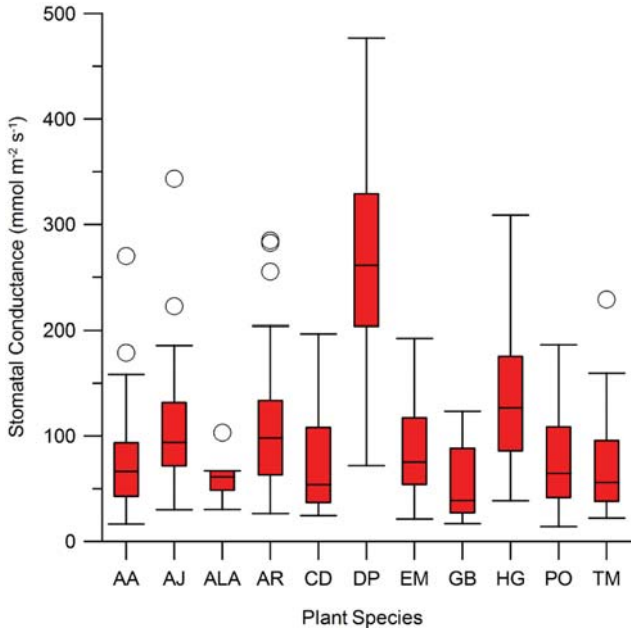

Figure 2: Stomatal conductance (g_s) measurements for the plant species AA (*A. aneura*), AJ (*A.* sp. Jack Hills), ALA (*Al. aspera*), AR (*A. rhodophloia*), CD (*C. desolata*), DP (*D. petiolaris*), EM (*E. maitlandii*), GB (*G. berryana*), HG (*H. gustafsenii*), PO (*P. obovatus*) and TM (*T. melvillei*) in October 2011 using Box-and-whisker plots. Solid circles denote outliers.

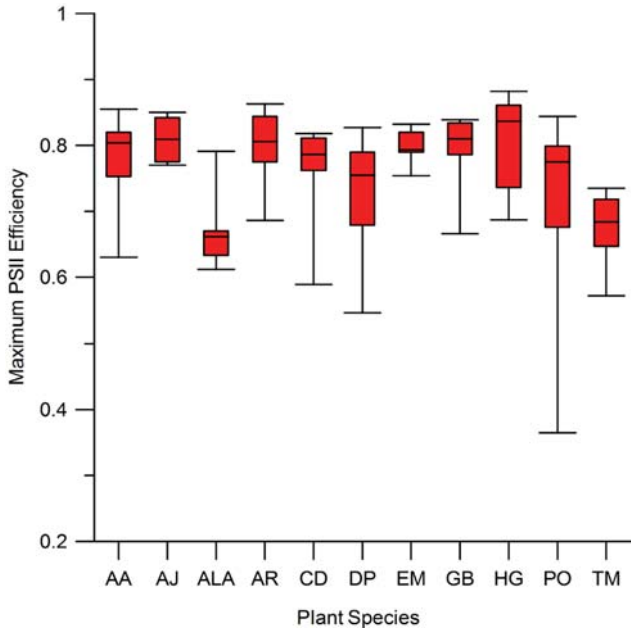

Figure 3: Φ_{PSII} for the species AA (*A. aneura*), AJ (*A.* sp. Jack Hills), ALA (*Al. aspera*) AR (*A. rhodophloia*), CD (*C. desolata*) DP (*D. petiolaris*), EM (*E. maitlandii*) GB (*G. berryana*), HG (*H. gustafsenii*), PO (*P. obovatus*) and TM (*T. melvillei*) for the October 2011 sampling period using box-and-whisker plots.

3.2.2 Carbon isotope discrimination

Carbon discrimination ($\Delta^{13}C$) values ranged from 37.7 $\%_{VBDP}$ in *P. obovatus* up to 53.0 $\%_{VBDP}$ in *A.* sp. Jack Hills (Figure 4). Median species values ranged from 40.85 $\%_{VBDP}$ (*H. gustafsenii*) to 50.1 $\%_{VBDP}$ (*A.* sp. Jack Hills). High variability is observed between species.

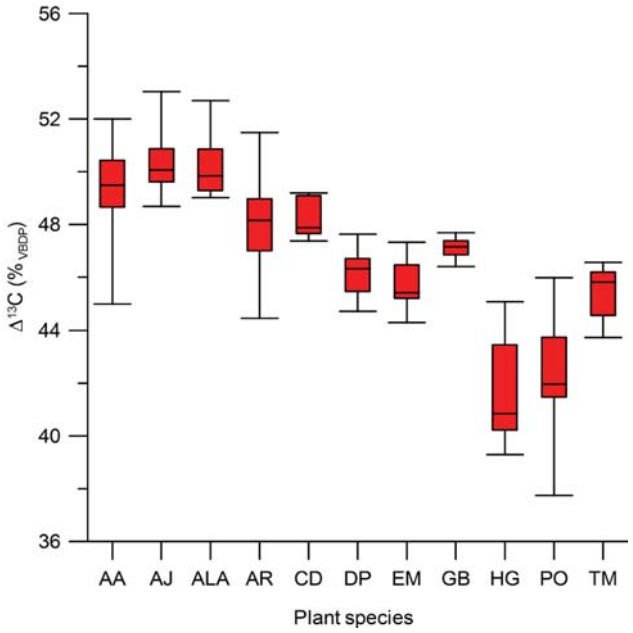

Figure 4: $\Delta^{13}C$ measured as the difference between foliar $\delta^{13}C_{VPDB}$ compared to a laboratory working $C0_2$ gas for AA (*A. aneura*), AJ (*A.* sp. Jack Hills), ALA (*Al. aspera*), AR (*A. rhodophloia*), CD (*C. desolata*), DP (*D. petiolaris*), EM (*E. maitlandii*), GB (*G. berryana*), PO (*P. obovatus*) and TM (*T. melvillei*) for the October 2011 sampling period using a box-and-whisker plot.

3.1 Variation in soil attributes

Soil moisture ranged from 0.287 to 4.78% in April and from 0.3 to 0.78% in October, showing a decrease from the autumn to summer sampling periods. Soil pH values ranged from 4.08 to 5.81 and were correlated to topography (Figure 5A), with pH values increasing from the upper slopes (average of 4.7) to the foot slopes and surrounding plains (average of 5.5). Soil EC values ranged from 24.8 to 116 µs/cm, soil nitrate from 0.188 to 1.118 µg/g and soil ammonium from 0.059 to 1.401 µg/g. Soil EC, nitrate and ammonium

concentrations showed no distinct topographic influence. However, soil EC was positively correlated with dust deposition levels (Figure 5B). The soil parameters recorded at each site are provided as Appendix 4.B.

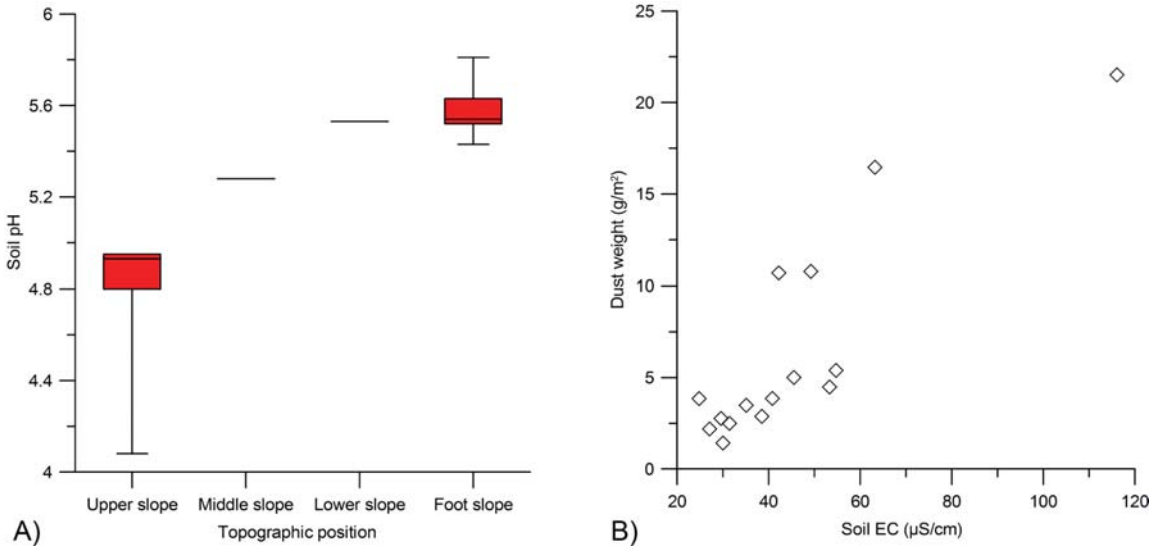

Figure 5 A) Soil pH plotted against topographic position reveled a positive correlation between these two variables, with soil pH increasing from the upper slopes down to the foot slopes and plains (using box-and-whisker plot) B) Dust weight recorded in the October sampling period is roughly linearly correlated with soil EC (scatter plot).

3.2 Analysis of dust impact on plant physiological response

3.2.1 Stomatal conductance

The LMEM analysis indicated that 'plant species', 'dust weight' and the interaction between 'plant species' and 'dust weight' correlate significantly with g_s (Table 2). Soil EC was removed from the model because it was highly linearly correlated with October dust weight (Figure 5B), thus giving similar results.

The model was simplified to include only 'plant species' and 'dust weight' and the interaction. Application of an analysis of variance (ANOVA) to the model suggested that

'plant species' and 'dust weight' as main effects were correlated significantly to g_s ($F_{10,15}$ = 11.60, $P < 0.0002$ and $F_{1,11}$ = 14.03, $P < 0.0011$, respectively). The interaction between species and dust weight was not significantly correlated: $F_{10,15} = 1.04$, $P < 0.4$ (Table 3).

Table 2: Predictor variables and their significance in the best-fit models of stomatal conductance with a random effect structure of: site location/species/species at site/replication of species at site.

Response variable	Predictor variable	LR test ([1]df subscript), P value
stomatal conductance	plant species: dust weight	**$LR_9 = 65.00$, $P < 0.0001$**
	soil pH	$LR_{29} = 0.11$, $P < 0.74$
	soil nitrate	$LR_{29} = 0.43$, $P < 0.50$
	soil ammonium	$LR_{29} = 0.06$, $P < 0.80$

[1]df represents degrees of freedom. Bold values are predictor variables retained in the final model; other variables were removed based on the likelihood ratio test (LR).

Table 3: ANOVA results of the predictor variables used in the simplified LMEM.

Response variable	Predictor variable	F values ([1]df num, df dom as subscript), P value
stomatal conductance	plant species	**$F_{10,15} = 11.60$, $P < 0.0002$**
	dust weight	**$F_{1,11} = 14.03$, $P < 0.0011$**
	plant species: dust weight	$F_{10,15} = 1.04$, $P < 0.4$

[1]df num and df dom represents numerator and denominator degrees of freedom respectively. Bold values are those that returned a significant ANOVA result.

The LN-transformed g_s values for each species are provided in Figure 6A. Figure 6B shows dust weight plotted against LN-transformed g_s for each species. The graph reveals that g_s of some species (e.g., *A. aneura* and *A. rhodophloia*) is negatively correlated to dust loading, while others exhibit no correlation (e.g., *D. petiolaris* and *G. berryana*).

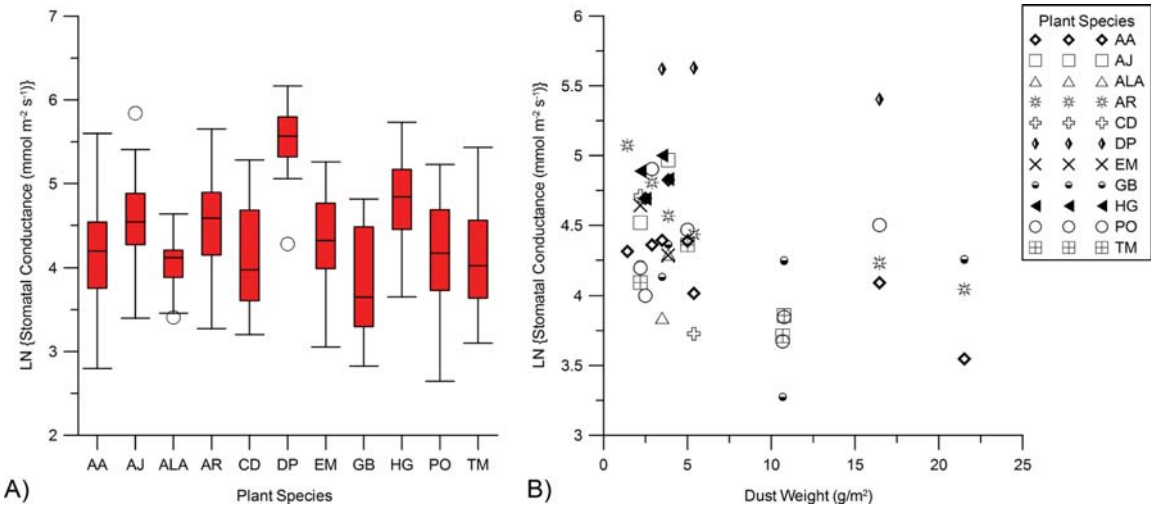

Figure 6: A) Box-and-whisker plot of LN- transformed g_s for all plant species. Solid circles denote outliers, B) LN-transformed stomatal conductance of all plant species as a function of dust load. Plant species for both plots are AA (*A. aneura*), AJ (*A.* sp. Jack Hills, ALA (*A. aspera*), AR (*A. rhodophloia*), CD (*C. desolata*), DP (*D. petiolaris*), EM (*E. maitlandii*), GB (*G. berryana*), HG (*H. gustafsenii*), PO (*P. obovatus*) and TM (*T. melvillei*).

The interaction between 'plant species' and 'dust weight', however, did not show a significant correlation ($F_{10,15}$=1.04, P<0.4). This indicates that g_s is not significantly influenced by dust loading in all species, which is consistent with the scatter plot in Figure 6B. However, individual species appear to be significantly influenced by dust deposition. Therefore, separate models were run for each species to determine which species, if any, were significantly influenced by dust loading. Only species that were present at three or more sites were used in the separate analysis. Hence, *A.* sp. Jack Hills, *Al. aspera, C. desolata* and *E. maitlandii* could not be analysed further.

The results of the species-specific analysis are shown in Table 4. Only *A. aneura* ($F_{1,7}$ = 8.27, P < 0.02) and *A. rhodophloia* ($F_{1,4}$ = 18.10, P < 0.01) exhibited a significant stomatal response to dust loading. Figure 7 shows scatter plots of normalised g_s (division by maximum value) over dust loading for individually analysed species.

Table 4: ANOVA results of individual species in the simplified LMEM. Each species g_s values was analysed in separate models with the predictor value of dust level.

Plant species	F values ([1]df num and df dom as subscript), P value
Acacia aneura	**$F_{1,7} = 8.27$, $P < 0.02$**
Acacia rhodophloia	**$F_{1,4} = 18.10$, $P < 0.01$**
Dodonaea petiolaris	$F_{1,1} = 1.13$, $P < 0.50$
Grevillea berryana	$F_{1,3} = 0.04$, $P < 0.90$
Halgania gustafsenii	$F_{1,2} = 0.04$, $P < 0.90$
Ptilotus obovatus	$F_{1,6} = 2.34$, $P < 0.20$
Triodia melvillei	$F_{1,3} = 3.05$, $P < 0.20$

[1]Df num and df dom represent numerator and denominator degrees of freedom, respectively. Bold values are those that returned a significant ANOVA result.

This plot reveals that g_s of *A. aneura* and *A. rhodophloia* was reduced by 50% at dust loads of ~ 5 g/m^2 (Figure 7). At the highest dust loads both *Acacia* spp. exhibited a reduction of g_s to levels below 40% of the maximum (down to ca. 25% for *A. aneura*). *G. berryana* and *D. petiolaris* were clearly not affected by dust loading. *P. obovatus* and *T. melvillei*, did not yield a significant correlation ($F_{1,6} = 2.34$, $P < 0.02$ and $F_{1,3} = 3.05$, $P < 0.20$, respectively). However, in the scatter plot, *T. melvillei* and *P. obovatus* appears to have a negative correlation with dust loading. More data are needed to decide if the g_s of these species are sensitive to dust loading.

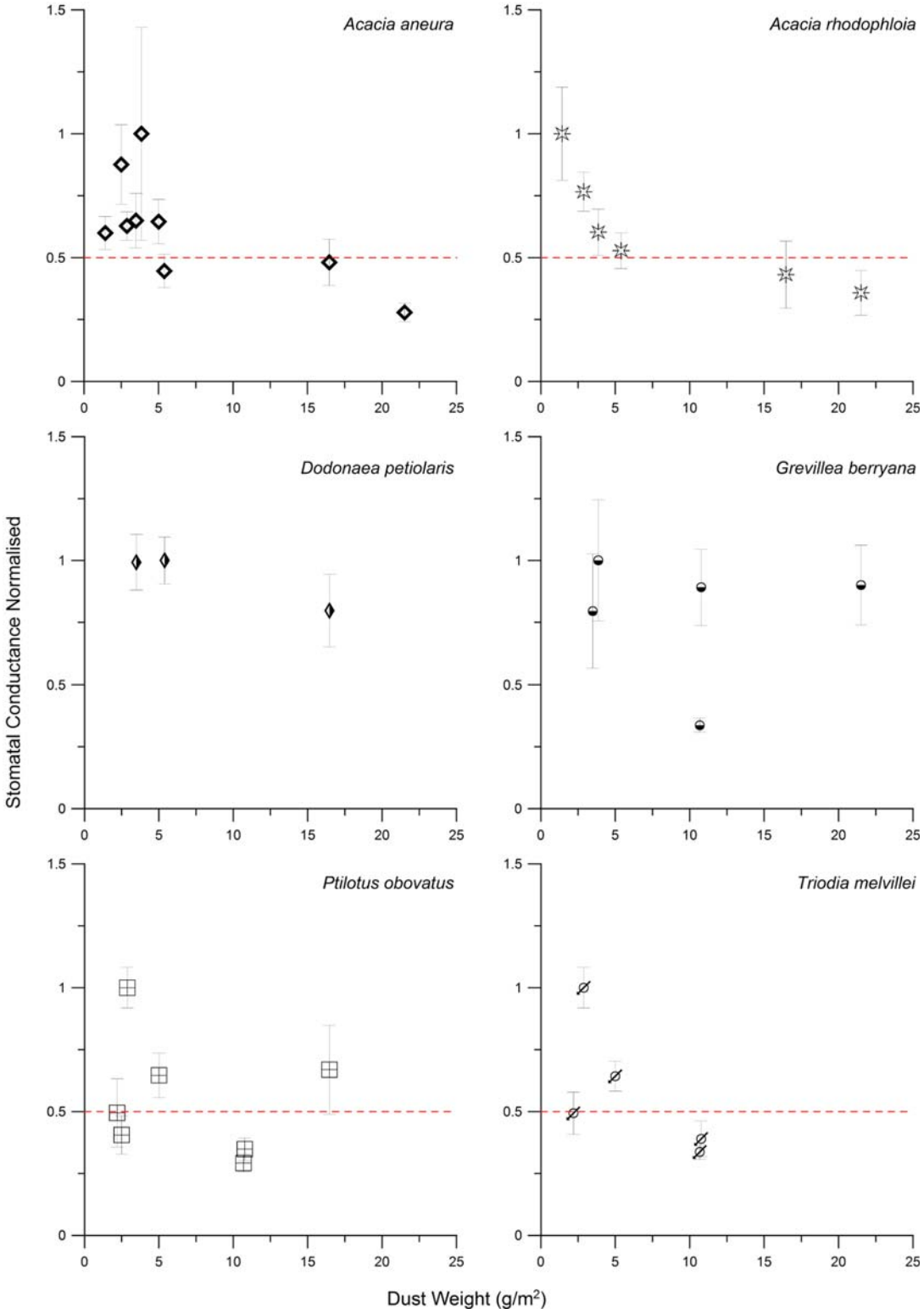

Figure 7: Normalised g_s (vertical bars denote normalized standard error; normalisation was conducted relative to maximum g_s) as a function of dust weight shown separately for the species *A. aneura, A. rhodophloia, D. petiolaris, G. berryana, P. obovatus and T. melvillei*. The red dashed line highlights the 50% level compared to the maximum g_s.

3.2.2 Chlorophyll fluorescence

The response variable, maximum efficiency of PSII photochemistry (Φ_{PSII}), was analysed against the predictor variables 'plant species', 'dust weight' and soil properties in a LMEM. Φ_{PSII} values were LN-transformed. To simplify the model, the Likelihood Ratio test was employed and singled out 'plant species', 'dust weight' and the interaction between 'plant species' and 'dust weight' as significantly influencing Φ_{PSII} (Table 5).

These factors were used in the simplified LMEM (Table 6), which resulted in plant species as a main effect with a significant correlation to Φ_{PSII} (Figure 8A). Dust weight was not correlated ($F_{1,10} = 0.06$, $P < 0.80$), nor was the interaction between species and dust (Figure 8B).

Table 5: Predictor variables and their significance in the best-fit models of Φ_{PSII} with a nested random effect structure of: site location/species/species at site/replication of species at site.

Response variable	Predictor variable	LR test ([1]df as subscript), P value
Maximum PSII efficiency	plant species: dust weight	**$LR_9 = 38.47$, $P < 0.0004$**
	soil pH	$LR_{21} = 2.48$, $P < 0.12$
	soil nitrate	$LR_{21} = 0.07$, $P < 0.80$
	soil ammonium	$LR_{21} = 0.02$, $P < 0.89$
	soil moisture	$LR_{21} = 0.17$, $P < 0.70$

[1]df represents degrees of freedom. Bold values are predictor variables retained in the final model.

Table 6: ANOVA results of the predictor variables used in the simplified LMEM.

Response variable	Predictor variable	F values ([1]df num and df dom as subscript), P value
Maximum PSII Efficiency	plant species	**$F_{6,13} = 9.23$, $P < 0.0005$**
	dust weight	$F_{1,10} = 0.06$, $P < 0.80$
	plant species: dust weight	$F_{6,13} = 2.096$, $P < 0.13$

[1]df num and df dom represents the numerator and denominator degrees of freedom respectively. Bold values are those that returned a significant ANOVA result.

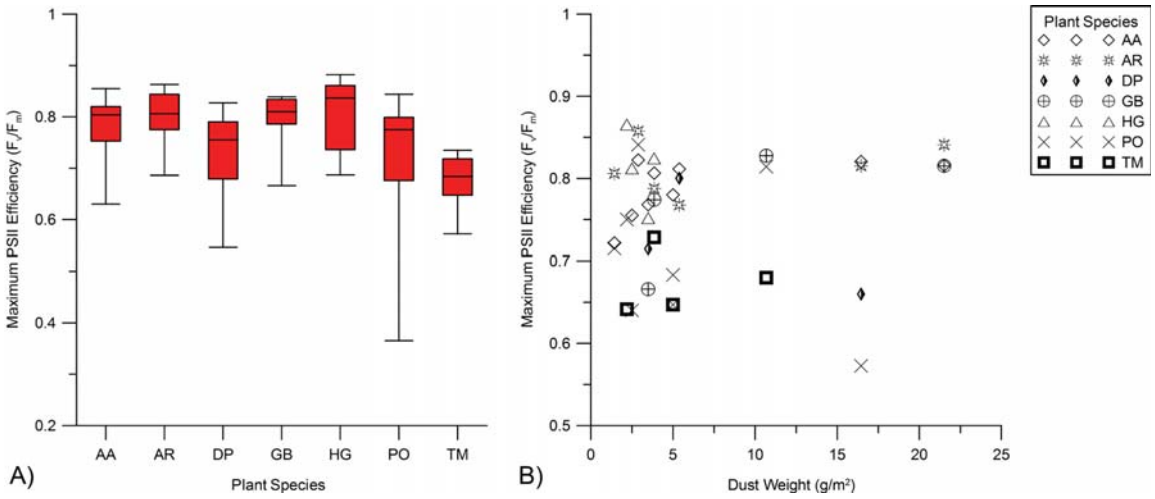

Figure 8: A) Box-and-whisker plot of Φ_{PSII} of different plant species, B) Scatter plot of maximum photosynthetic efficiency of plants over October dust loadings.

3.2.3 Carbon isotope discrimination

$\Delta^{13}C$ was measured against the predictor variables 'plant species', 'dust weight' and soil properties in a LMEM. $\Delta^{13}C$ values were LN-transformed. To simplify the model, the Likelihood Ratio test was employed. It only identified 'plant species' as significant predictor (Table 7). Therefore, 'dust weight' and the soil properties are not significantly correlated to $\Delta^{13}C$. 'Plant species' was used in the simplified LMEM and determined to be a significant factor ($F_{11,29} = 46.7$, $P < 0.0001$).

Table 7: Predictor variables and their significance in the best-fit models of carbon discrimination with a random effect structure of: site location/species/species at site/replication of species at site.

Response variable	Predictor variable	LR test (df as subscript), P value
carbon discrimination	species	**LR_{11} = 122.57, *P* < 0.0001**
	dust weight	LR_{21} = 0.61, *P* < 0.5
	soil pH	LR_{21} = 0.35, *P* < 0.6
	soil nitrate	LR_{21} = 1.23, *P* < 0.3
	soil ammonium	LR_{21} = 0.08, *P* < 0.8
	soil moisture	LR_{21} = 0.025, *P* < 0.9

Bold values are predictor variables retained in the final model; other variables were removed based on the likelihood ration test (LR). df represents degrees of freedom.

3.3 Relationship between stomatal response and plant traits

As 'dust weight' was correlated negatively with g_s ($F_{1,11}$ = 14.03, *P* < 0.0011) (Section 3.2.1), the plant traits that influenced dust loading on leaves (results in Chapter 3) were analysed for their correlation to stomatal conductance. Because 'dust weight' was not significantly correlated to Φ_{PSII} or $\Delta^{13}C$, plant traits were not analysed in relation to these parameters.

The traits identified in Chapter 3 as influencing dust levels on leaves are: 'Trichome type and cover', 'leaf surface configuration' and '3D leaf posture' and were analysed using a LMEM (Table 8). The normalised g_s values were LN-transformed. The results of the analysis (Table 8) identified '3D leaf posture' and 'leaf surface configuration' as significantly correlated to g_s values ($F_{3,28}$ = 4.95, *P* < 0.007 and $F_{2,28}$ = 3.75, *P* < 0.04, respectively). The plant trait 'Trichome type and cover' can be considered slightly significant ($F_{2,28}$=3.11, *P*<0.06).

Table 8: Predictor variables and their significance in the best-fit models of stomatal conductance with a random effect structure of: site location/species/species at site/replication of species at site.

Response variable	Predictor variable	F values ([1]df num, df dom as subscript), P value
Stomatal Conductance	3D Leaf posture	**$F_{3,28}$=4.95, *P*<0.007**
	Leaf surface configuration	**$F_{2,28}$=3.75, *P*<0.04**
	Trichome type and cover	$F_{2,28}$=3.11, *P*<0.06

[1]df num and df dom represents the numerator and denominator degrees of freedom respectively. Bold values are ANOVA results that returned a significant value.

For '3D leaf posture', plants with 'flat' leaves (e.g. *A. aneura* and *A. rhodophloia*) had the lowest mean normalised g_s values (0.33 ±0.02). Species with 'Involute' leaves (curled upwards) had the second lowest mean normalised g_s at 0.40 (± 0.02) (e.g. *P. obovatus* and *T. melvillei*). Only one species had 'revolute' leaves (curled downwards), and this was *G. berryana* with the highest mean normalised g_s of 0.47 ± 0.05 (Figure 9A).

For the trait 'leaf surface configuration', plants with 'unevenly textured' leaves (e.g., *H. gustafsenii* and *D. petiolaris*) had the highest mean normalised g_s (0.48 ± 0.02), closely followed by 'smooth' leaved species (0.43 ± 0.02). Finally, species with 'striate' leaves (*A. aneura, A. rhodophloia* and *T. melvillei* (Figure 9B)) had the lowest normalised mean g_s value (0.31 ± 0.01).

'Trichome type and cover' can be considered slightly significant ($F_{2,28}$=3.11, *P*<0.06). 'Tomentose' leaves had the highest g_s (6.948 ± 1.27), followed by 'glabrous' (5.91 ± 1.02), and 'strigose' leaves exhibited the lowest g_s (3.65 ±0.74). Plants with 'strigose' hairs include *A. aneura* and *A. rhodophloia.*

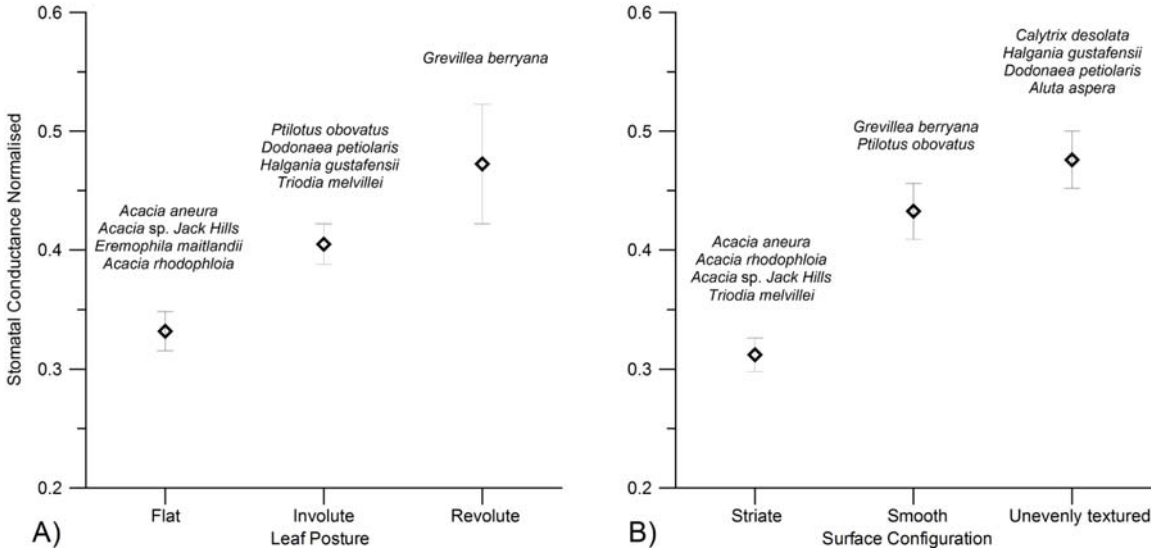

Figure 9: Combined normalised mean g_s (±SE) of plants and their associated plant traits: A) Leaf Posture, and B) surface configuration. Plant species associated with each trait are identified in the figure.

4 Discussion

4.1 Does dust loading increase physiological stress?

The main question of this thesis is if dust generated by mining operations at the Jack Hills has a negative impact on the surrounding vegetation. I found that g_s of the species *A. aneura* and *A. rhodophloia* was decreased to 25 % of the maximum value under high, mining-induced dust loads (Figure 7). This change in g_s was not correlated to any of the soil parameters. *T. melvillei* and *P. obovatus* may also show a sensitivity to dust loading. However, the data are sparse (i.e., these species do not have the same amount of replication over distance) the thus not conclusive. *G. berryana, D. petiolaris* and *H. gustafsenii* were unaffected. There was no evidence for a correlation between dust loading and the other two physiological parameters recorded, except that *T. melvillei* had an overall reduced Φ_{PSII} (median value of 0.68).

The question arises: if g_s is inhibited by dust loading in *A. aneura* and *A. rhodophloia* while the other two physiological performance indicators appear to be normal, is the overall impact of dust damaging to these species? Qualitative observations of plant health at sites with high dust loading suggest that dust indeed damages these plants. Consider Site 25 (Figure 10A) and Site 7 (Figure 10B). Site 25 is adjacent to the crushing facility and Site 7 is adjacent to the waste stockpile, both recorded high dust loadings, and both *A. aneura* and *A. rhodophloia* were extremely stressed at these localities. Many specimens dropped leaves or had died. Leaf shedding can indicate water stress in plants (Kozlowski, 1976). In contrast, *G. berryana*, which displayed no inhibition of physiological performance due to dust, looked healthy with only minor to negligible growth stunting and no observable tree death (Figure 10A). The understorey shrubs were just woody stems at Site 25. There were limited dried remnants of annual grasses and herbs. Both Site 25 and 7 appear to have been heavily damaged by dust loading, although the physiological parameters did not reflect the full extent of this effect. Site 12 and Site 9 (Figure 10C and Figure 10D, respectively), however, which occur at a greater distance from the mining operations, but on the same land zone, topography and within the same broad plant community, have much healthier looking *Acacia* spp., with *A. aneura* present at both sites, and site 12 featuring *A. rhodophloia*.

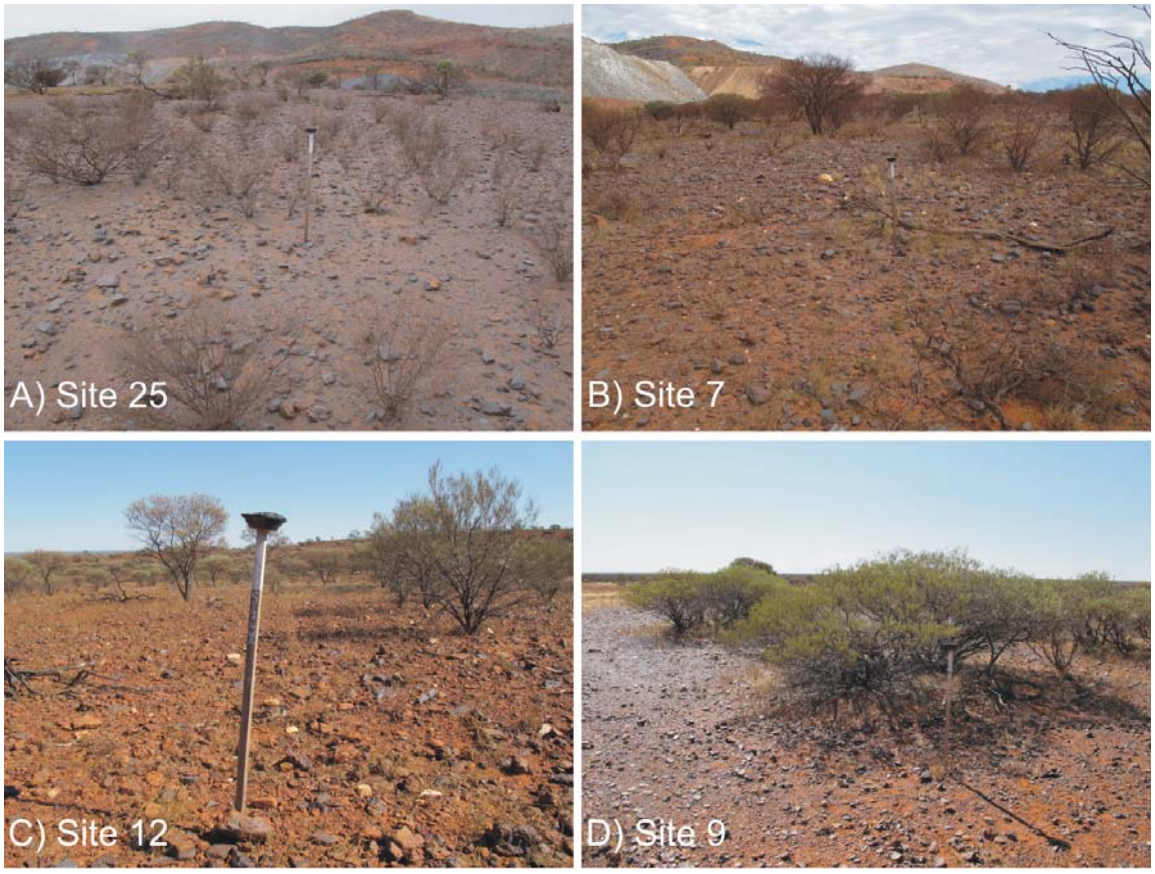

Figure 10: Comparison of dust collector sites, showing: A) Site 25, adjacent to the crushing facility with heavy noticeable dark dust high in magnetite observable. Small woody shrubs are dead, and many *A. aneura* and *A. rhodophloia* are also dead or with significant leaf shedding. *G. berryana* is the light green tree in the background, which looks comparatively healthy. B) Site 7, adjacent to the waste stockpile, does not have such a heavy magnetite load, but many *A. aneura* and *A. rhodophloia* in the background are dead or shedding leaves. C) Site 12 (509 m from the mining pit) did not have noticeable acacia death or significantly visible dust loads. D) Site 9 (control site and 1069 m from disturbance) also displays healthy acacia species.

There could be a number of explanations for this counterintuitive observation of no reduction in the other two physiological measurements. The first possible explanation is self-selective sampling. The specimens that survived at the highly stressed sites must be more resilient than their highly damaged or dead fellows. This might indicate a stronger individual and result in sampling that favours specimens performing above the average. In addition, I obviously could not sample specimens, which had already died. Hence, they do

not appear in my statistics as zero values. The second reason may be sampling bias. All physiological parameters exhibited significant spread, even at the scale of a single plant. To my knowledge, it is unknown to which degree sparse sampling of physiological performance is representative for a whole plant. It is clearly unfeasible to sample thousands of leaves per specimen. However, there might be a significant sampling bias inherent to the method employed here. Third, soil EC is linearly correlated to dust load (Figure 5B), and thus removed from the models due to confounding variables. An increase in electrical conductivity of soil can be obtained for a number of reasons, for example, due to salinity increase, the presence of clay (mostly fine-grained phyllosilicates), higher porosity and thus more pore fluid, etc. (Grisso et al., 2009). The dust produced by the mine is rich in chlorite (the phyllosilicate mineral, not the anion) and talc, which probably explains the observed increase in soil EC (Hersir and Arnason, 2010) correlated to dust load. To my knowledge, both minerals do not have a toxic effect on plants. Therefore, I deem it unlikely that the increased soil EC is related to the observed damage and decrease in stomatal conductance of the acacias. Fourth, the mining-derived dust is rich in magnetite, especially near the crushing facility (Site 25). Although the solubility of magnetite is low and inorganic iron is generally not available to plants, iron can accumulate to levels toxic to plants (heavy metal toxicity), and, if accompanied by low pH, can be mobilise in soils, resulting in interactions with plants (Lambers et al., 2008). Iron excess can be damaging to plant growth and seedling germination (Kuki et al., 2009). Considering that soil pH is generally low across the whole study area (~ 4 – 6), I cannot rule out that the dust loading at the Jack Hills imposes chemical damage on the *Acacia* ssp. However, iron toxicity would also present an inhibition of photosynthetic ability. This question requires further study.

4.2 Do plant traits influence dust accumulation and thus increase stress?

Of the three leaf traits influencing dust loading (‘leaf posture’, ‘leaf surface configuration’ and ‘trichome type and cover’), the traits ‘leaf posture’ and ‘leaf surface configuration’, also significantly influenced stomatal conductance values ($F_{3,28} = 4.95$, $P < 0.007$ and $F_{2,28} = 3.75$, $P < 0.04$, respectively). ‘Trichome type and cover’ was slightly significant ($F_{2,28} = 3.11$, $P < 0.06$). These results confirm a relationship between dust accumulation, plant traits and physiological response. My original hypothesis, however, must be rejected: plant traits collecting the most amount of dust *do not* correlate to increased physiological stress. In contrast, the traits, which collected the highest, dust loads, also correlated to the highest stomatal conductance. For example, the leaf trait ‘leaf posture’, collected dust in the following way ‘involute’ > ’flat’ > ’revolute’, whereas the stomatal conductance response to this trait was ‘revolute’ > ‘involute’ > ‘flat’. So, while ‘flat’ leaves only collected a medium amount of dust, these species recorded the lowest stomatal conductance values. Similarly, the plant trait ‘leaf surface configuration’ collected dust in the following order: ‘unevenly textured’ > ‘striate’ > ‘smooth’. In contrast, the stomatal conductance response was ‘unevenly textured’ > ‘smooth’ > ‘striate’. This shows that it is not the heaviest dust loading that predicts stomatal response, but the way the dust physically interacts with the leaf surface.

To test this idea, eSEM photographs of *A. rhodophloia* and *A. aneura* (Figure 11A and C, respectively) were obtained, which confirm that there are noticeable ‘deposits’ of dust, which coat the leaf surface and are concentrated within the ‘striate’ grooves of the leaves. The dust also appears to be more densely packed on the leaf surface, when compared to the other leaf types (Figure 11). The deposition pattern observed for *A. aneura* was also observed in a study by Butler (2009) in the Pilbara, who writes that dust accumulated in the

troughs of the ridges of *A. aneura*. Dust deposited on leaves can accumulate to form stable 'crusts', for example, in the axil of leaf blades (Brabec et al., 1981), or within the 'striate' grooves of *Acacia* spp. (Butler, 2009), the stability of which is known to increase through weather factors such as humidity and rainfall (Brabec et al., 1981, Grantz et al., 2003). Dust crusts may persist even after rainfall events (Hirano et al., 1990, Ong et al., 2003), indicating a more stable form of deposit. Therefore, the physical mechanism for reduction in stomatal conductance of the *Acacia* spp. could be explained by the accumulated dust deposits coating or occluding stomata, especially within the 'striate' grooves of the leaves.

This type of deposition pattern was not observed on other leaf types in my study. For example, *P. obovatus* (Figure 11B) has thick, dense dendritic hairs holding the dust above the leaf surface. This could explain why tomentose leaves collected the most dust whilst exhibiting the highest stomatal conductance. In addition, as the dust does not form a stable deposit, it can perhaps be more easily removed by wind or rain. Hairy leaves can protect plant species from dust effects (Naidoo and Naidoo, 2005, Paling et al., 2001). *D. petiolaris* (Figure 11D) has an 'involute, unevenly textured, resinous' leaf with a large amount of dust on the surface. However, the stomata appear to be protected underneath the outer resinous layer, which act as a sticky dust trap. Moreover, there are no "dust sinks" such as the deep striae on *Acacia* leaves. This resinous coat may also dry and flake off, thus removing dust particles (Figure 11D).

In addition, careful inspection of the heavily dusted *Acacia* leaves reveals jagged edges parallel to the striae and dust particles, which seem to be embedded in the leaf surface (Figure 11A and C). These features may represent mechanical leaf damage, i.e., abrasion. Surface abrasion on leaf surfaces may increase transpiration and thus induce water stress

(Eveling and Bataillé, 1984). Therefore, mechanical abrasion may be another important factor affecting susceptibility to dust damage.

In summary, plant traits, which accumulate the greatest amount of dust, do not necessarily predict vulnerability to dust damage. Increased dust levels only result in a decreased gas exchange (stomatal conductance) and thus probably physical stress where dust can easily interact with those parts of the leaf surface that contain stomata. Moreover, mechanical damage due to dust may increase negative effects in the *Acacia* spp. An important outcome of my results is that the *Acacia* spp., especially *A. aneura*, might be ideal indicator species for measuring the anthropogenic dust impacts in semi-arid Australia. *A. aneura* exhibits the strongest negative physiological correlation to dust load and is one of the most ubiquitous species across semi-arid Australia. Therefore, It could be selected as potential indicator species in mining operations across Australia.

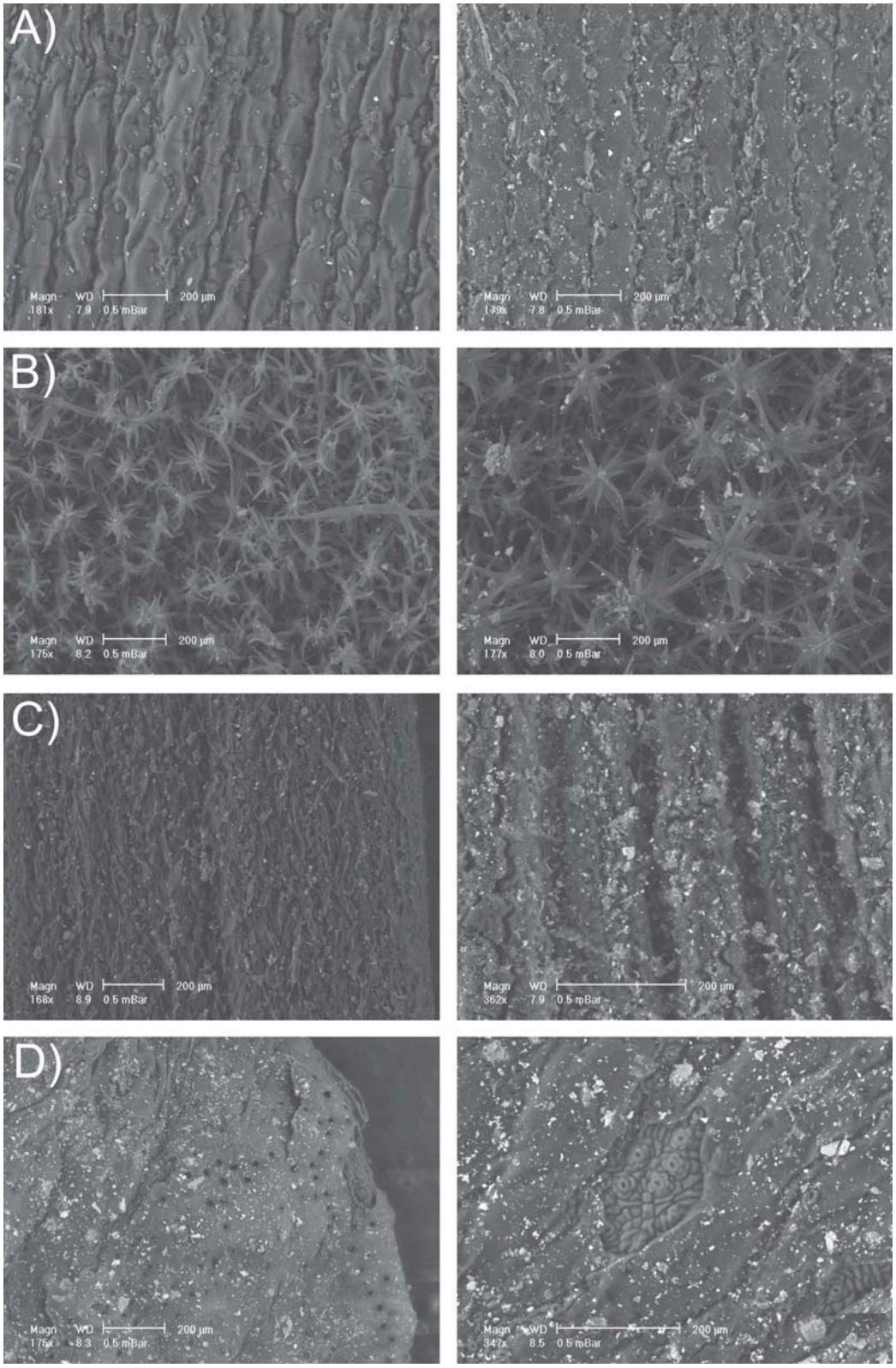

Figure 11: eSEM images of 'control' leaves on left and dusty leaves on the right for the species A) *A. rhodophloia*, B) P. *obovatus*, C) *A. aneura* and D) *D. petiolaris*.

5 Final Summary and Findings from this Chapter

The following conclusions can be drawn from this chapter:

1. The stomatal conductance (g_s) of *Acacia aneura* and *Acacia rhodophloia* was reduced to 50 % of its maximum at dust levels of 5 g/m^2 and up to 25% of its maximum under heavy mining-induced dust (> 20g/m^2), while the other physiological performance measures did not indicate a significant reduction in health.

2. Qualitative observations confirm the above results: *Acacia* spp. at sites with the highest dust load are either dead or heavily stressed and exhibit high leave shedding, while *G. berryana* appeared healthy.

3. Iron toxicity effects due to deposition of dust onto the soil surface could explain the negative effects for *Acacia* health at heavily dust-loaded sites. This requires further investigation.

4. Two of the significant plant traits identified in Chapter 3 ('leaf posture' and 'leaf surface configuration') were significantly correlated to physiological response. The traits, which resulted in greatest dust loading, surprisingly did not predict lowest stomatal conductance values.

5. Blocking or occlusion of the stomata is likely to be the physical mechanism for the reduction in stomatal conductance, supported by the dust accumulation on the leaf surface and the significant correlation to the 'leaf surface configuration' trait. Therefore, leaf surface morphology, and perhaps leaf toughness (i.e., resistance to abrasion), is critical for plant susceptibility to dust damage.

6 References

BAKER, N. R. 2008. Chlorophyll Flourescence: A Probe of Photosynthesis In Vivo. *Annual Review of Plant Biology,* 59**,** 89-113.

BLACK, C. A. 1965. *Methods of Soil Analysis: Part 1Physical and Mineraloginal Properties,* Madison, Wisconsin, USA, American Society of Agronomy.

BRABEC, E., KOVÁR, P. & DRÁBKOVÁ, A. 1981. Particle deposition in three vegetation stands: A seasonal change. *Atmospheric Environment (1967),* 15**,** 583-587.

BUNDY, L. G. & MEISINGER, J. J. 1994. Nitrogen Availability Indices. *In:* MICKELSON, S. H. (ed.) *Methods of Soil Analysis, Part 2: Microbiological and Biochemical Properties.* Madison, Wisconsin: Soil Society of America and American Society of Agronomy.

BURNHAM, K. P. & ANDERSON, D. R. 2002. *Model Selection and Multimodel Inference: A Practical Information-Theoretic Approach,* New York, Springer Science+Business Media Inc.

BUTLER, R. 2009. *Vulnerability of plant functional types to dust deposition in the Pilbara, NW Australia.* Bachelor of Science (Environmental Science) (Honours), The University of Western Australia.

CHASTON, K. & DOLEY, D. 2006. Mineral particulates and vegetation: Effects of coal dust, overburden and flyash on light interception and temperature *Clean air and environmental quality,* 40**,** 40-44.

COPLEN, T. B., BRAND, W. A., GEHRE, M., GRÖNING, M., MEIJER, H. A. J., TOMAN, B. & VERKOUTEREN, R. M. 2006. New Guidelines for $\delta^{13}C$ Measurements. *Analytical Chemistry,* 78.

DECAGON DEVICES 2005-2012. Leaf Porometer: Operators Manual. *In:* INC., D. D. (ed.). Pullma, WA.

EVELING, D. W. & BATAILLÉ, A. 1984. The effect of deposits of small particles on the resistance of leaves and petals to water loss. *Environmental Pollution Series A, Ecological and Biological,* 36**,** 229-238.

GLEASON, S., FAUCETTE, D., TOYOFUKU, M., TORRES, C. & BAGLEY, C. 2007. Assessing and Mitigating the Effects of Windblown Soil on Rare and Common Vegetation. *Environmental Management,* 40**,** 1016-1024.

GRANTZ, D. A., GARNER, J. H. B. & JOHNSON, D. W. 2003. Ecological effects of particulate matter. *Environment International,* 29**,** 213-239.

GRISSO, R., ALLEY, W., HOULSHOUSER, D. & THOASON, W. 2009. Precision Farming Tools: Soil Electrical Conductivity. *Virginia Cooperation Extension.* Virgnia Polytechnic Institution and State University.

HERSIR, G. P. & ARNASON, K. 2010. Resistivity of Rocks. Geothermal Development Company, United Nations University and Kenya Electricity Generating Co. Ltd.

HIRANO, T., KIYOTA, M. & AIGA, I. 1990. The physical effects of dust on photosynthetic rate of plant leaves. . *Agricultural and Forest Meteorology,* 46**,** 1-7 (in Japanese with English summary).

HIRANO, T., KIYOTA, M. & AIGA, I. 1995. Physical effects of dust on leaf physiology of cucumber and kidney bean plants. *Environmental Pollution,* 89**,** 255-261.

KOZLOWSKI, T. T. 1976. Water Deficits and Plant Growth. *In:* KOZLOWSKI, T. T. (ed.) *Soil Water Measurements, Plant Responses, and Breeding for Drought Resistance.* London, England: Academic Press.

KUKI, K., OLIVA, M. & COSTA, A. 2009. The Simulated Effects of Iron Dust and Acidity During the Early Stages of Establishment of Two Coastal Plant Species. *Water, Air, & Soil Pollution,* 196**,** 287-295.

KUKI, K. N., OLIVA, M. A., PEREIRA, E. G., COSTA, A. C. & CAMBRAIA, J. 2008. Effects of simulated deposition of acid mist and iron ore particulate matter on photosynthesis and the generation of oxidative stress in Schinus terebinthifolius Radii and Sophora tomentosa L. *Science of The Total Environment,* 403**,** 207-214.

LAMBERS, H., CHAPIN, F. S. & PONS, T. L. 2008. *Plant Physiological Ecology,* New York, NY, USA, Springer New York.

MAXWELL, K. & JOHNSON, N. 2000. Chlorophyll flourescence - a practical approach. *Journal of Experimental Botany,* 51**,** 659-668.

NAIDOO, G. & NAIDOO, Y. 2005. Coal Dust Pollution Effects on Wetland Tree Species in Richards Bay, South Africa. *Wetlands Ecology and Management,* 13**,** 509-515.

ONG, C. C. H., CUDAHY, T. J., CACCETTA, M. S. & PIGGOTT, M. S. 2003. Deriving quantitative dust measurements related to iron ore handling from airborne hyperspectral data. *Mining Technology,* 112**,** 158-163.

PALING, E. I., HUMPHRIES, G., MCCARDLE, I. & THOMSON, G. 2001. The effects of iron ore dust on mangroves in Western Australia: Lack of evidence for stomatal damage *Wetlands Ecology and Management,* 9**,** 363-370.

PAUL, D., SKRZYPEK, G. & FORIZS, I. 2007. Normalization of Measured Stable Isotopic Compositions to Isotope Reference Scales - A Review. *Rapid Communications in Mass Spectrometry,* 21**,** 3006-3014.

PINHEIRO, J. C. & BATES, D. M. 2000. *Mixed-Effect Models in S and S-Plus,* New York, Springer Verlag.

R DEVELOPMENT CORE TEAM 2012. R: A language and environment for statistical computing. Vienna, Austria: R Foundation for Statistical Computing.

RAYMENT, G. E. & HIGGINSON, F. R. 1992. *Australian Laboratory Handbook of Soil and Water Chemical Analysis Methods*, Inkata Press.

SCHREIBER, U. 2004. Pulse-Amplitude-Modulation (PAM) flourescence and saturation pulse method: An overview. *In:* PAPAGEORGIOU, G. C. & GOVINDJEE (eds.) *Chlorophyll flouresence: a signature of photosynthesis.* Springer.

SHARIFI, M. R., GIBSON, A. C. & RUNDEL, P. W. 1997. Surface Dust Impacts on Gas Exchange in Mojave Desert Shrubs. *Journal of Applied Ecology*, 34**,** 837-846.

ULLMANN, I. 1989. Stomatal conductance and transpiration of *Acacia* under field conditions: similarities and differences between leaves and phyllodes. *Structure and Function of Trees*, 3**,** 45-56.

Chapter 5. Summary and Implications

1 Summary and implications

My study shows that the Jack Hills mine generates dust above natural background levels up to ca. 2000 m away from the mining operations. It thus imposes elevated dust loads on the surrounding vegetation. Dust levels were significantly increased (> 5 g/m^2) within ca. 350 m of the mine in April and within ca. 600 m of the mine in October. Average dust levels increased 5 fold against background levels within these radii. The size of dust particles produced by the mine is generally < 30 μm with a modal grain size of 2.55 μm. Mine dust composition reflects the harvested rocks: magnetite (up to > 50% close to the mine), talc, chlorite, and quartz.

I found that morphological leaf traits of plants at the Jack Hills influence the accumulation of dust on leaves. Three traits were correlated significantly to dust loading: 1) 'trichome type and coverage' (presence and type of hair), 2) 'leaf surface configuration' (smooth, striate or unevenly surfaced) and, 3) '3D leaf shape' (revolute, involute, or flat). Plants with thick dense hairs (e.g., *Halgania gustafsenii*) doubled dust accumulation compared to plants with a 'strigose' hair type (coarse bent hairs), such as *Acacia aneura*. Species with 'unevenly textured' leaf surface (e.g. *Dodonaea petiolaris*) more than doubled dust weights compared to species with 'smooth' leaves. Finally an 'involute' (curled upwards) leaf posture collected eight times the amount of dust than 'revolute' (curled downwards) leaves (e.g. *Grevillea berryana*), and twice the amount of 'flat' leaves (e.g. *A. aneura*). They affect dust load because traits 1 and 2 control the surface roughness and specific surface area of the leaf, and thus dust capture, while trait 3 contributes to dust retention.

Structural traits, including plant height and leaf orientation, did not significantly contribute to dust accumulation of plants in this study. Structural traits increase the dust capture ability of plants at the plant scale (Raupach and Leys, 1999, Beckett et al., 2000). My study, however, focused on leaf-scale dust accumulation because the interaction between plant leaves and dust is most important for physiological function. At the leaf scale, structural traits may not be so important (Litschke and Kuttler, 2008). Nevertheless, they may amplify the overall dust capture ability of a plant in combination with other traits. To test this idea, I attempted a plant trait group approach. Unfortunately, the identified plant trait groups could not be analysed meaningfully, mainly owing to the spatial distribution of plant species in the research area, and the limitations of the statistical analysis employed. Therefore, my results cannot be applied to predicting ecosystem-scale dust responses elsewhere. However, I identified leaf-scale traits predictive of dust load, which may be helpful for establishing plant functional types in regards to morphology, dust load, and related physiological functions in future work.

My data on physiological performance revealed that the species *Acacia aneura* and *Acacia rhodophloia* both exhibited stress associated with heavy dust loads. Stomatal conductance of *A. aneura* and *A. rhodophloia* was reduced by 50% of its maximum under dust loads of 5 g/m^2 and reduced down to 25% of its maximum under heavy dust loads (> $20g/m^2$). Other physiological performance measures (chlorophyll fluorescence and carbon isotope discrimination) did not indicate a significant reduction as a function of dust load.

Importantly, qualitative observations confirm negative effects of elevated dust loads: the *Acacia* spp. at the sites with highest dust loading were either dead or heavily stressed and exhibited high levels of leaf shedding. Leaf shedding can indicate water stress in plants (Kozlowski, 1976), potentially resulting from blocked or occluded stomata (Hirano et al.,

1995). Understorey shrubs were also highly stressed or dead at these sites. *Triodia melvillei* and *Ptilotus obovatus* may also show a sensitivity to dust loading. However, the data are sparse and thus not conclusive in a statistical sense. *Grevillea berryana, Dodonaea petiolaris* and *Halgania gustafsenii* were unaffected.

The leaf traits identified as influencing dust accumulation were also correlated to stomatal conductance, confirming a relationship between dust accumulation, plant traits and physiological response. Surprisingly, traits attracting the highest dust load did not correlate to the lowest stomatal conductance. Therefore, it is not the total dust load that controls if a plant experiences physiological damage but the physical interaction of the dust with the leaf surface. Leaf micro-morphological observations of the *A. aneura* and *A. rhodophloia* leaves showed that the dust accumulated in the 'striate' grooves of the plants, in accordance with a previous study on *A. aneura* in the Pilbara (Butler, 2009). This is because the striae increase the surface roughness, surface area and create dust "sinks" so that dust can be trapped on the leaf. The increased dust load in these species likely led to blocked or occluded stomata, which may explain the observed decrease in stomatal conductance (Hirano et al., 1995). In addition, both plants appeared to exhibit signs of mechanical surface damage due to dust, which can also affect plant health (Eveling and Bataillé, 1984, Eveling, 1986, Gleason et al., 2007). Finally, it is conceivable that the mining-induced dust increased magnetite and hematite concentration in soil close to the mine, which, in the presence of low pH as found in the study area, may lead to iron mobilisation and metal toxicity (Kuki et al., 2008b, Lambers et al., 2008). This requires further study.

My study has a number of important outcomes for monitoring dust impacts around mining installations and associated regulatory measures. First, the physiologically relevant dust footprint around the Jack Hills mine extends over a radius of at least 600 m. At this

distance, the dust level is ≥ 5 g/m^2. This dust level is on average 5 times higher than the natural background dust level and relates to a reduction in stomatal conductance of about 50% in *A. aneura* and *rhodophloia*. This is consistent with Farmer (1993), who noted that dust imposes negative impacts on plants at levels of ca. 7g/m^2. Therefore, I identified a critical dust load, which may be seen as a threshold for negative health effects in arid and semi-arid Australian plant species. Second, I identified a critical distance over which dust effects may be felt. The dust footprint of the mine extends up to ca. 2000 m with dust levels exceeding 5 g/m^2 at ca. 600 m. This distance is comparable with the radii of impact determined at other locations (Ong et al., 2003, Kuki et al., 2008a).

Third, *A. aneura* and *A. rhodophloia* proved most sensitive to dust loading. *A. aneura* in particular is one of the most ubiquitous species across semi-arid Australia. Therefore, it might be an ideal indicator species for measuring the environmental dust footprint around mining operations at the Jack Hills and elsewhere in Australia. Therefore, I propose that it should be considered as potential indicator species.

Fourth, species with similar traits as the *Acacia spp.*, i.e., 'striate, flat' leaves, may also be susceptible to dust damage. This hypothesis could be examined in the future to identify other indicator species in different regions.

2 References

BECKETT, K. P., FREER-SMITH, P. H. & TAYLOR, G. 2000. Particulate pollution capture by urban trees: Effects of species and windspeed. *Global Change Biology,* 6**,** 995-1103.

BUTLER, R. 2009. *Vulnerability of plant functional types to dust deposition in the Pilbara, NW Australia.* Bachelor of Science (Environmental Science) (Honours), The University of Western Australia.

EVELING, D. W. 1986. Scanning Electron Microscopy of Damage by Dust Deposits to Leaves and Petals. *Botanical Gazette,* 147**,** 159-165.

EVELING, D. W. & BATAILLÉ, A. 1984. The effect of deposits of small particles on the resistance of leaves and petals to water loss. *Environmental Pollution Series A, Ecological and Biological,* 36**,** 229-238.

FARMER, A. M. 1993. The effects of dust on vegetation--a review. *Environmental Pollution,* 79**,** 63-75.

GLEASON, S., FAUCETTE, D., TOYOFUKU, M., TORRES, C. & BAGLEY, C. 2007. Assessing and Mitigating the Effects of Windblown Soil on Rare and Common Vegetation. *Environmental Management,* 40**,** 1016-1024.

HIRANO, T., KIYOTA, M. & AIGA, I. 1995. Physical effects of dust on leaf physiology of cucumber and kidney bean plants. *Environmental Pollution,* 89**,** 255-261.

KOZLOWSKI, T. T. 1976. Water Deficits and Plant Growth. *In:* KOZLOWSKI, T. T. (ed.) *Soil Water Measurements, Plant Responses, and Breeding for Drought Resistance.* London, England: Academic Press.

KUKI, K., OLIVA, M. & PEREIRA, E. 2008a. Iron Ore Industry Emissions as a Potential Ecological Risk Factor for Tropical Coastal Vegetation. *Environmental Management,* 42**,** 111-121.

KUKI, K. N., OLIVA, M. A., PEREIRA, E. G., COSTA, A. C. & CAMBRAIA, J. 2008b. Effects of simulated deposition of acid mist and iron ore particulate matter on photosynthesis and the generation of oxidative stress in Schinus terebinthifolius Radii and Sophora tomentosa L. *Science of The Total Environment,* 403**,** 207-214.

LAMBERS, H., CHAPIN, F. S. & PONS, T. L. 2008. *Plant Physiological Ecology,* New York, NY, USA, Springer New York.

LITSCHKE, T. & KUTTLER, W. 2008. On the reduction of urban particle concentration by vegetation - a review. *Meteorologische Zeitschrift,* 17**,** 229-240.

ONG, C. C. H., CUDAHY, T. J., CACCETTA, M. S. & PIGGOTT, M. S. 2003. Deriving quantitative dust measurements related to iron ore handling from airborne hyperspectral data. *Mining Technology,* 112**,** 158-163.

RAUPACH, M. R. & LEYS, J. F. 1999. The efficacy of vegetation in limiting spry drift and dust movement. Canberra: CSIRO.

Appendix 3.A

Image Analysis Routine for Dust Grain Size Frequency Distribution

In the first step, an image is loaded as a grey-scale image. Mathematically, each image is a matrix (or table) with 1944 rows and 2592 columns, where each entry corresponds to a square image pixel with a grey value between 0 and 255. In the second step, grains are segmented from the image background via binary thresholding (Figure 3.A1). This was possible because of the high contrast difference between grains and background. I determined the threshold empirically (Figure 3.A1). The segmented image contains black (value 0) pixels, representing grains, and white pixels (value 1) denoting the background.

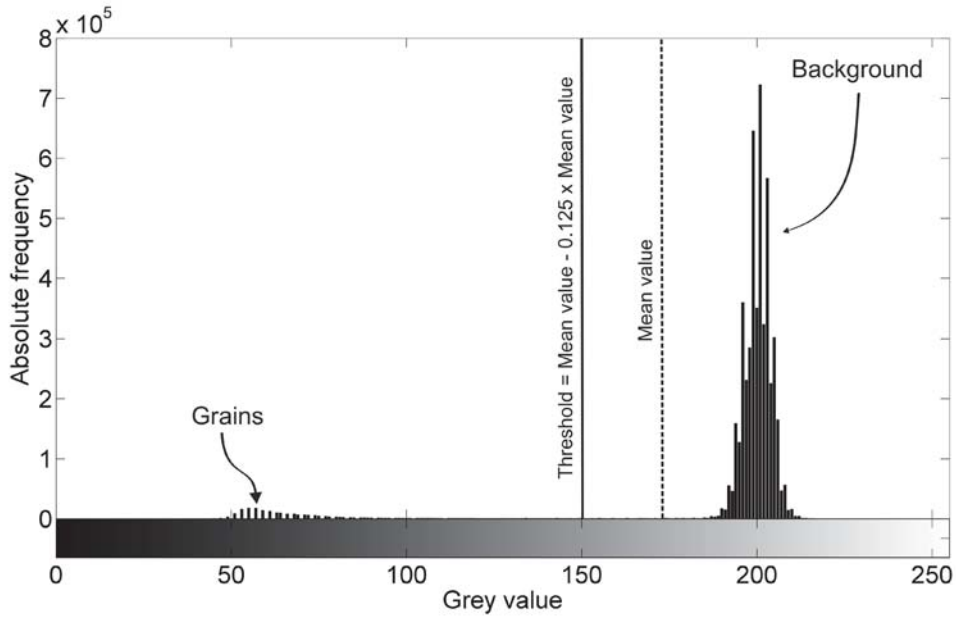

Figure 3.A1: Typical histogram of a grey-scale image used for grain-size analysis. The grains form a well-separated cluster at the lower end of the histogram, while the background pixels cluster at the upper end. The threshold value was defined empirically. It is calculated as the mean grey value (172.6) minus an eighth of the mean value.

In the third step, the grains in the binary image are analysed with Matlab's "regionprops" function. This function determines the best-fit ellipsoid for each cluster of connected black pixels (i.e., each grain in the binary image) and its related major and minor principal axis. I here define the major axis of the ellipsoid as the grain size. The grain aspect ratio (AR) is defined as the ratio of major-axis length over minor-axis length. Hence, round grains have an AR of 1; for elliptical grains, this value increases >

1. In the fourth step, the results of the grain-size analysis are filtered by removing all grains that are smaller than 6 pixels and that have an AR > 6. Grains < 6 pixels are too close to the resolution limit of the method. Visual inspection confirmed that objects with AR > 6 are usually detached hairs of leaf surfaces or other plant fragments. In the fifth step, the resulting grain-size data are written into a table. Steps 1 to 4 are then repeated for each image related to a particular dust sample. In the last step, the results for all images of a dust sample are compiled in a single table, from which statistical information such as histograms, cumulative frequency distributions, and mean grain size are derived for the dust sample of interest.

Appendix 3.B

Dust Mineralogy Results and a Selection of XRD patterns from individual Dust Collector Sites

Table 3.B: Mineral composition of dust collected at the dust stations in October 2011.

Dust Collector	Mineral					
	Quartz	Talc	Chlorite	Magnetite	Hematite	Halite
Site 1	✓✓✓✓	✓✓	✓✓			
Site 5	✓✓✓✓	✓✓✓	✓✓✓	✓✓✓	✓	
Site 6	✓✓✓	✓✓✓	✓✓✓	✓✓✓	✓	
Site 7	✓✓✓	✓✓✓	✓✓	✓✓✓✓	✓✓	
Site 8	✓✓	✓✓✓✓	✓✓	✓✓✓	✓	
Site 9	✓✓✓✓	✓✓		✓		
Site 11	✓✓✓✓	✓✓✓	✓✓✓	✓		
Site 12	✓✓✓✓	✓✓✓	✓✓✓	✓		
Site 13	✓✓✓✓	✓✓✓	✓✓		✓	
Site 16	✓✓✓✓	✓✓	✓✓			
Site 17	✓✓✓✓	✓✓	✓✓			
Site 18	✓✓✓✓	✓✓✓	✓✓	✓		
Site 19	✓✓✓	✓✓✓	✓✓✓	✓✓		✓
Site 25	✓✓✓	✓✓	✓✓	✓✓✓✓	✓✓	
Site 26	✓✓✓	✓✓✓	✓✓	✓	✓	✓
Site 28	✓✓✓✓	✓✓	✓✓	✓	✓	

✓	trace (< 5%)
✓✓	little (5-20 %)
✓✓✓	moderate (20-50%)
✓✓✓✓	much (>50%)

For the following figures: T = Talc, C = Chlorite, Q = Quartz, H = Hematite and M = Magnetite.

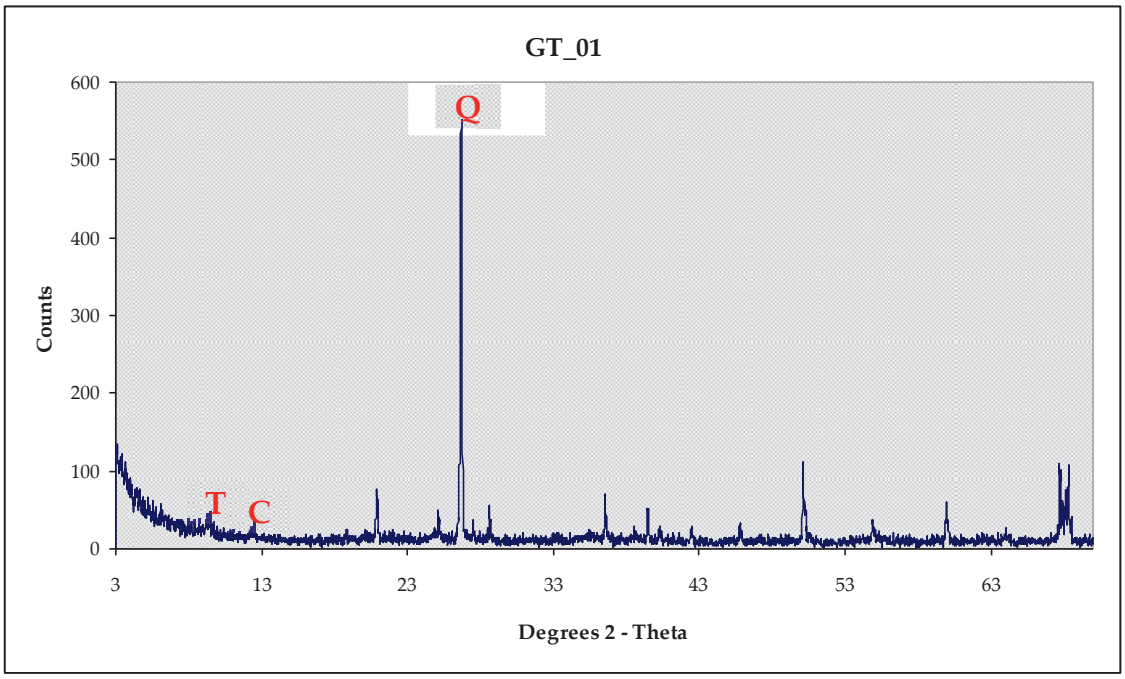

Figure 3.B1: Dust Collector Site 1, a 'control' site located at a distance of 2,723 m from the mining operations along the main range of the Jack Hills.

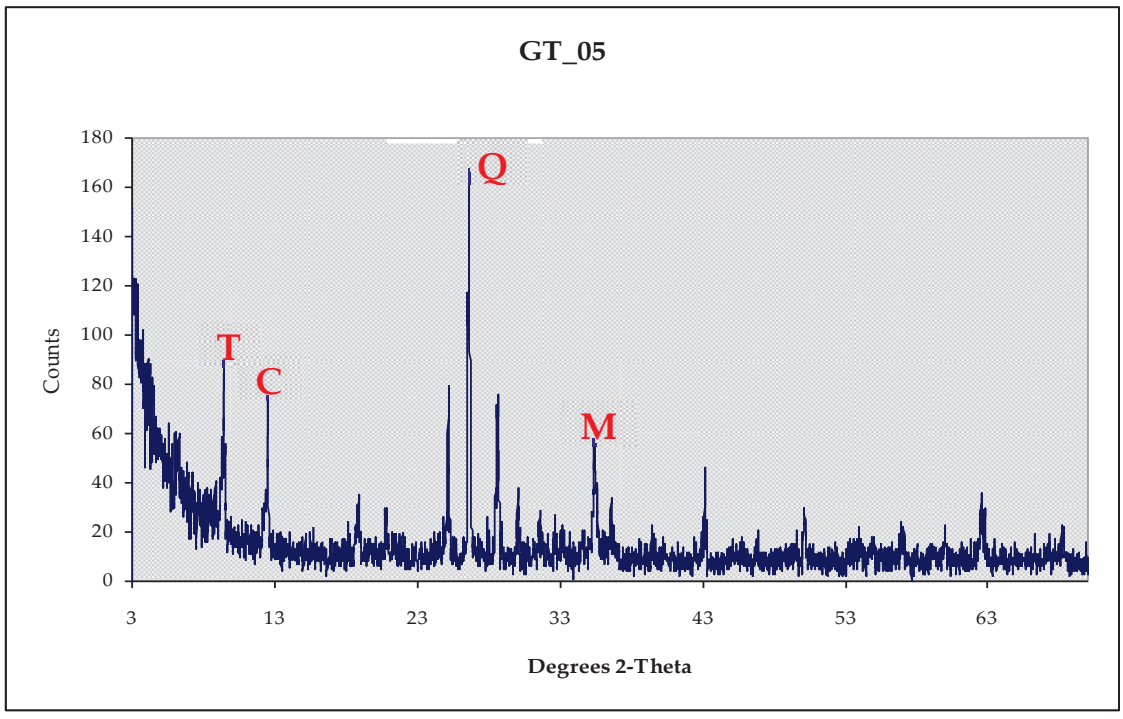

Figure 3.B2: Dust Collector Site 5, located on the foothills surrounding the Jack Hills, at a distance of 510 m from the waste rock stockpile.

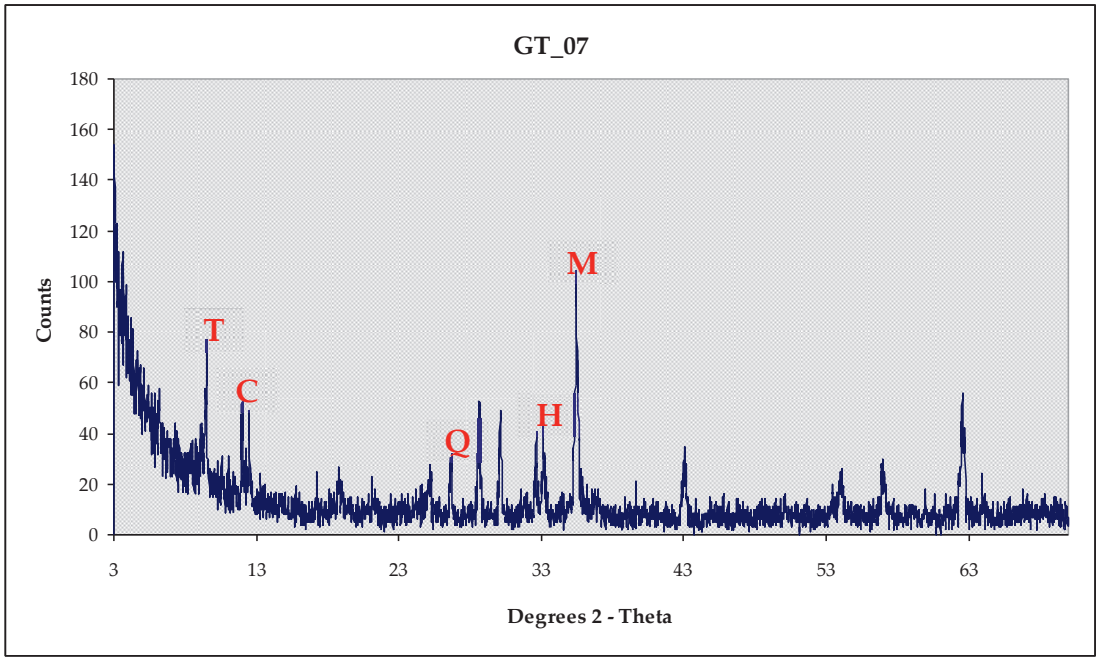

Figure 3.B3: Dust Collector Site 7, located on the foothills surrounding the Jack Hills, at a distance of 316 m from the waste rock stockpile.

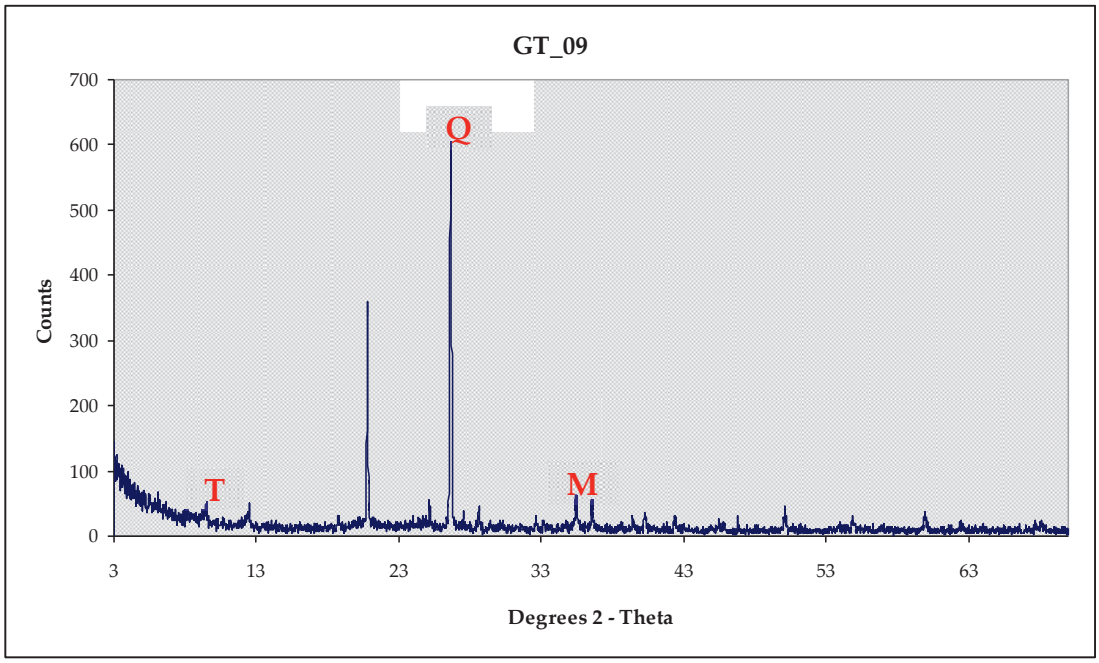

Figure 3.B4: Dust Collector Site 9, located at a distance of 1,069 m from the mining operations on the surrounding plain of the Jack Hills.

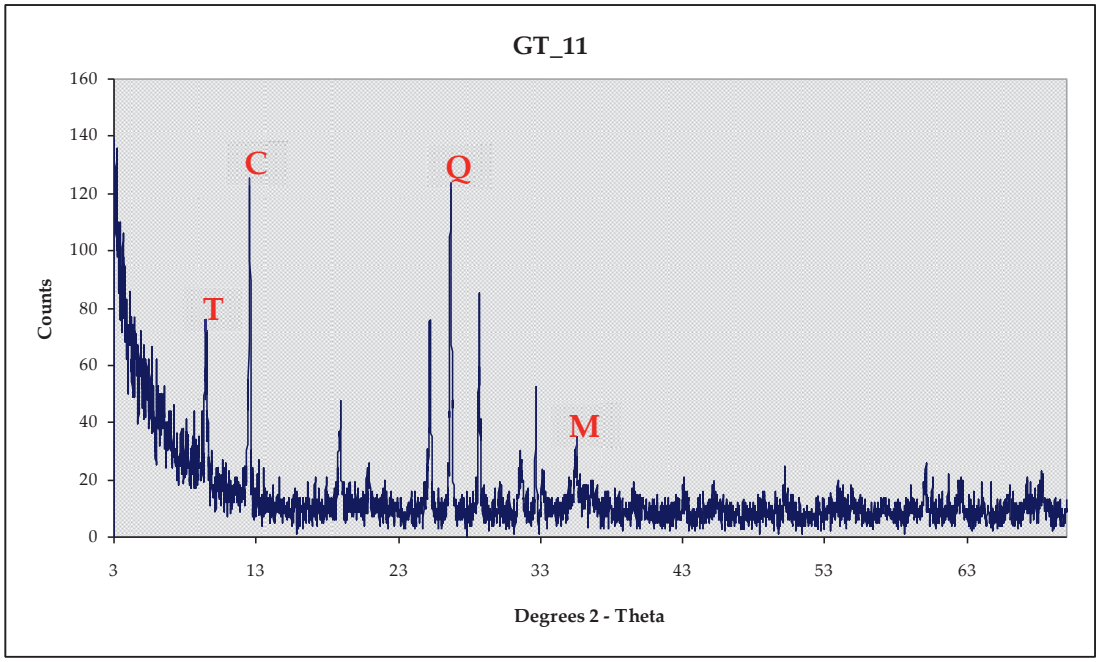

Figure 3.B5: Dust Collector Site 11 is located on the lower slopes of the Jack Hills, 309 m below the mining pit to the west.

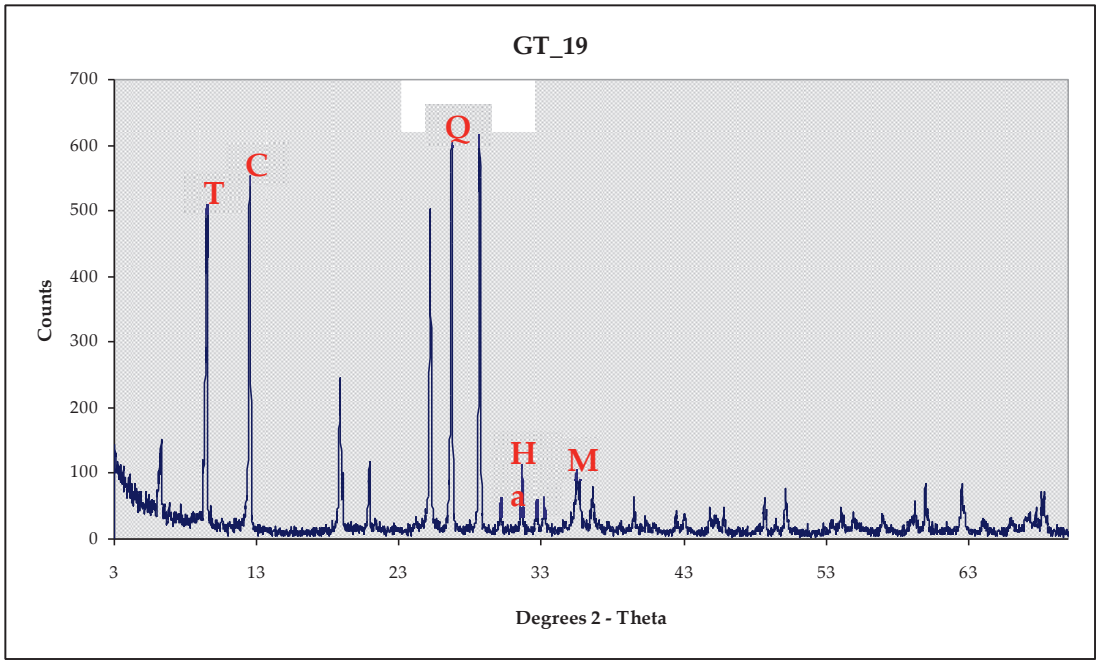

Figure 3.B6: Dust Collector Site 19 is located only 181 m from the mining pit, on the eastern side of the pit.

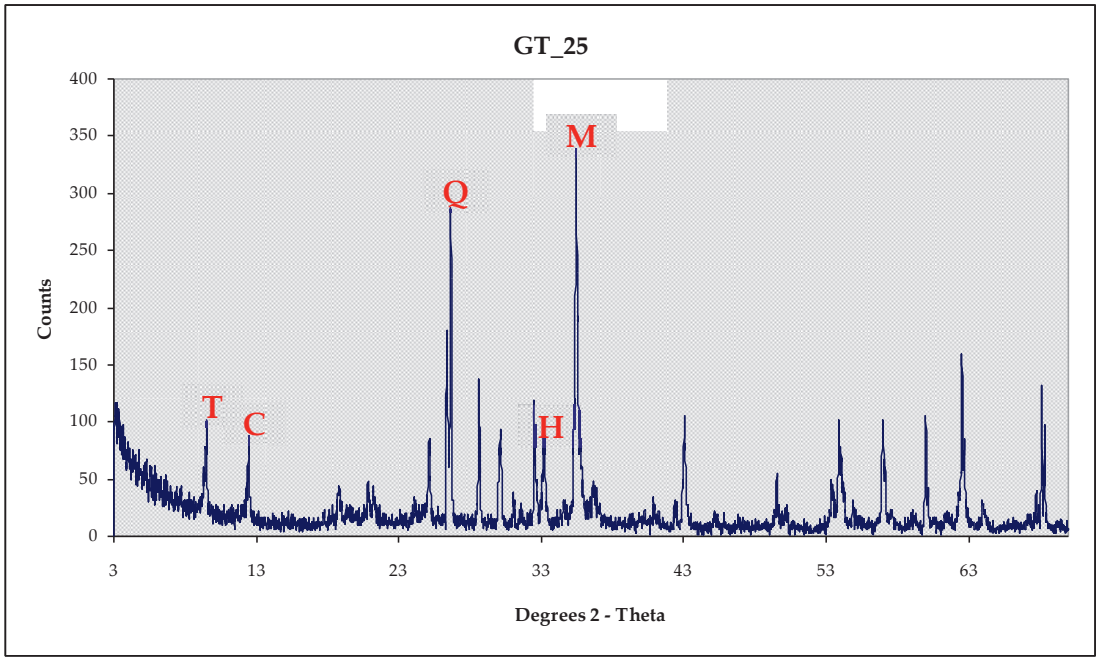

Figure 3.B7: Dust Collector Site 25 is 210 m from the ore crushing facility.

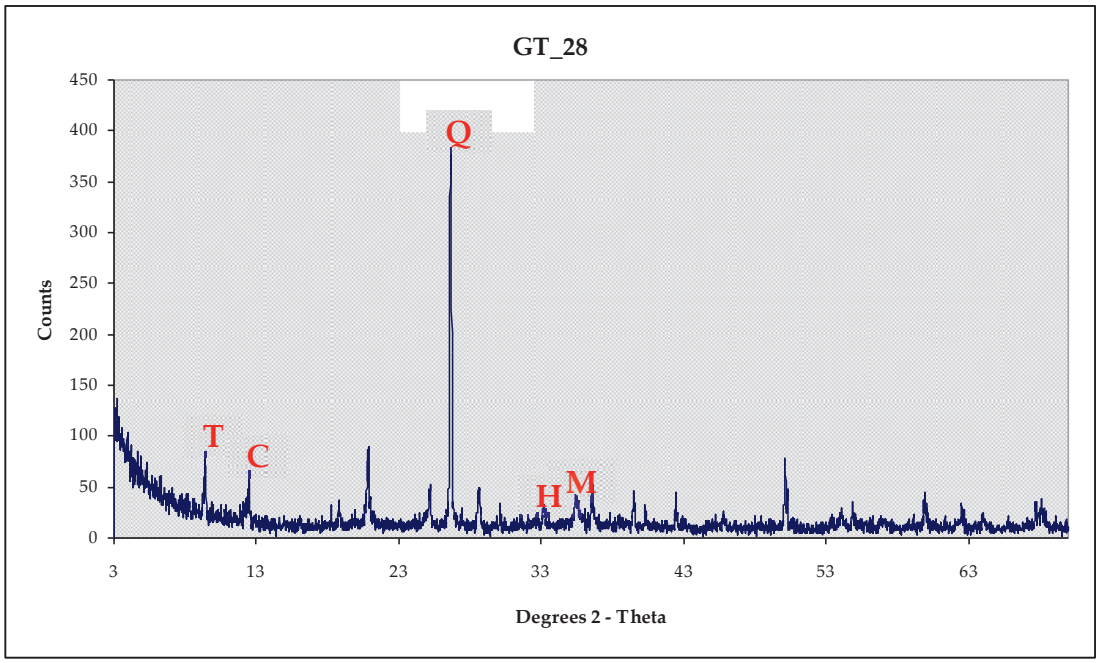

Figure 3.B8: Dust Collector Site 28, is a ‘control’ site, located 1,838 m on the surrounding plains of the Jack Hills to the west.

Appendix 3.C

Plant Traits of the Dominant Perennial Plant Species Recorded at the Jack Hills

Table 3.C: Dominant perennial plant species recorded at the Jack Hills sampling sites (i.e. within 15 m of the dust collectors) and their associated plant traits.

Species	Life form	Max. height (m)	Leaf area (mm^2)	Leaf area (SD)	[1]2D leaf shape	[2]3D leaf shape	Petiole length (mm)	[3]Leaf orientation	[4]Trichome	[5]Resin	[6]Surface configuration
Acacia aneura	T	5	52.0	1.89	L	F	1.5	A	St	N	St
Acacia citrinoviridis	T	5	518	86.8	L	F	0.1	A	St	N	S
Acacia cuthbertsonii	T	2.5	232	34.5	L	F	1.5	A	St	N	S
Acacia rhodophloia	T	4	131	9.89	NO	F	3.3	A	G	N	St
Acacia sp. Jack Hills	T	2.5	191	25.5	L	F	1.3	A	St	Y	St
Aluta aspera	S	1.5	3.96	0.33	O	C	0.5	A	G	N	U
Calytrix desolata	S	1	5.46	0.99	NO	C	0.0	A	G	N	U
Corymbia ?lenziana	T	6.5	608	142	L	F	5.8	D	G	N	U
Dodonaea petiolaris	S	1.5	167	1.32	NO	I	0.6	I	G	Y	U
Eremophila fraseri	S	1.5	64.3	17.9	O	I	10.5	I	G	Y	U
Eremophila maitlandii	S	1.1	23.3	3.69	NO	F	1.5	A	T	N	S
Grevillea berryana	T	7	187	32.6	L	R	4.0	A	St	N	S
Halgania gustafensii	S	0.7	572	46.5	L	I	1.7	I	S	N	U
Homalocalyx echinulatus	S	0.4	2.39	0.42	O	I	0.0	A	C	N	U
Ptilotus obovatus	S	1	66.6	22.7	O	I	0.3	I	T	N	S

Species	Life form	Max. height (m)	Leaf area (mm^2)	Leaf area (SD)	[1]2D leaf shape	[2]3D leaf shape	Petiole length (mm)	[3]Leaf orientation	[4]Trichome	[5]Resin	[6]Surface configuration
Senna sp.	S	2.5	59.6	6.71	L	I	0.5	I	G	N	S
Solanum lasiophyllum	S	1	710	408	O	I	8.5	I	T	N	U
Triodia melvillei	G	0.5	205	36.0	L	I	0.0	A	G	Y	St

[1]2D Leaf Shape: L = Linear, NO = Narrowly Oblong, O = Oblong

[2]3D Leaf Shape: F = Flat, C = Clavate, I = Involute, R = Revolute

[3]Leaf Orientation: A = Appressed, D = Depressed, I = Inclined

[4]Trichome: St = Strigose, G = Glabrous, T = Tomentose, S = Sericeous

[5]Resin: N = No, Y= Yes

[6]Surface configuration: St = Striate, U = Unevenly textured, S = Smooth.

Appendix 3.D

Plant Trait LMEM including Diagnostic Plots and Likelihood Ratio Test

Full Plant Trait Model 1:

Model1:<lme(leaf_dust~height_m+leaf_area_mm+X2d_leaf_shape+X3d_leaf_shape +petiole_length+leaf_orientation+trichome+surface_configuration+min_dist_dust, method="ML", random=~1|dust_station, data=trait1).

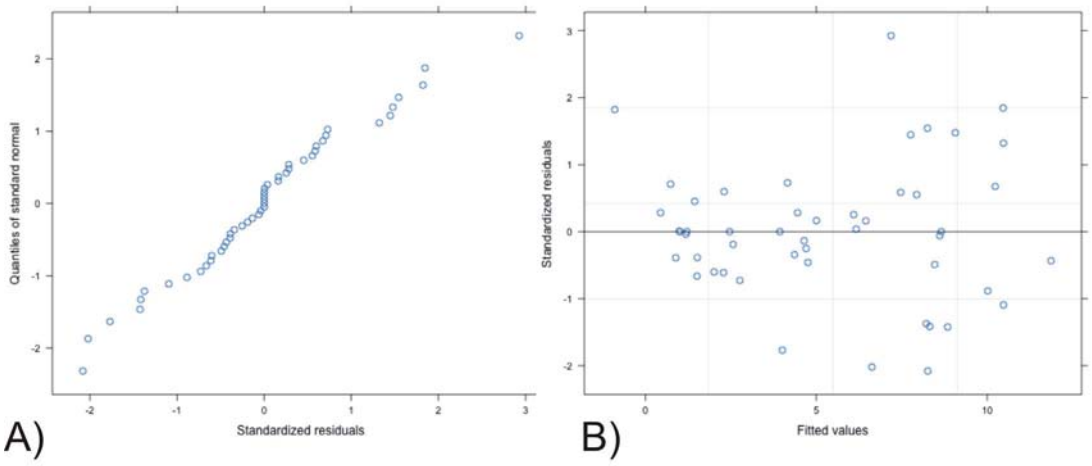

Figure 3.D1: Diagnostic plots for the full plant trait model, using A) Quantile-quantile (Q-Q) plot and B) Residual plot.

Likelihood Ratio Test for Model Simplification

Model 2 = Model 1 excluding ‘height_m’, anova (model 1, model 2)

Model	df	AIC	BIC	LogLik	Test	L.Ratio	p-value
1	17	253.8200	285.9809	-109.910			
2	16	252.6839	282.9531	-110.342	1 vs 2	0.8639498	0.3526

Model 3 = Model 1 excluding ‘leaf_area_mm’, anova (model 1, model 3)

Model	df	AIC	BIC	LogLik	Test	L.Ratio	p-value
1	17	253.8200	285.9809	-109.910			
3	16	253.3004	283.5695	-110.6502	1 vs 3	1.480423	0.2237

Model 4 – Model 1 excluding ‘2D_leaf_shape’, anova (model 1, model 4)

Model	df	AIC	BIC	LogLik	Test	L.Ratio	p-value
1	17	253.8200	285.9809	-109.910			
4	16	252.4172	252.4172	-110.2086	1 vs 4	0.5971748	0.4397

Model 5 = Model 1 excluding ‘3D_leaf_shape’, anova (model 1, model 5)

Model	df	AIC	BIC	LogLik	Test	L.Ratio	p-value
1	17	253.8200	285.9809	-109.910			
5	14	254.5788	281.0643	-113.2894	1 vs 5	6.758872	0.08

Model 6 = Model 1 excluding ‘petiole_length’, anova (model 1, model 6)

Model	df	AIC	BIC	LogLik	Test	L.Ratio	p-value
1	17	253.8200	285.9809	-109.910			
6	16	253.0436	283.3127	-110.5218	1 vs 6	1.223639	0.2686

Model 7 = Model 1 excluding ‘leaf_orientation’, anova (model 1, model 7)

Model	df	AIC	BIC	LogLik	Test	L.Ratio	p-value
1	17	253.8200	285.9809	-109.910			
7	15	253.6385	282.0158	-111.8192	1 vs 7	3.818504	0.1482

Model 8 = Model 1 excluding ‘trichome’, anova (model 1, model 8)

Model	df	AIC	BIC	LogLik	Test	L.Ratio	p-value
1	17	253.8200	285.9809	-109.910			
8	15	261.5941	289.9714	-115.7971	1 vs 8	11.77415	0.0028

Model 9 = Model 1 excluding ‘surface_configuration’, anova (model 1, model 9)

Model	df	AIC	BIC	LogLik	Test	L.Ratio	p-value
1	17	253.82	285.9809	-109.910			
9	15	263.91	292.2873	-116.955	1 vs 9	14.09003	9e-04

Model 10 = Model 1 excluding ‘min_dist_dust’, anova (model 1, model 10)

Model	df	AIC	BIC	LogLik	Test	L.Ratio	p-value
1	17	253.8200	285.9809	-109.910			
10	16	264.4273	294.6964	-116.2136	1 vs 10	12.6073	4e-04

Model 11 = Model 1 excluding ‘resin’, anova (model 1, model 11)

Model	df	AIC	BIC	LogLik	Test	L.Ratio	p-value
1	18	255.0518	289.1046	-109.5259			
11	17	253.8200	285.9809	-109.9100	1 vs 11	0.7681613	0.3808

Appendix 3.E

Plant Trait Dataset for the Plant Group Analysis

Species	Leaf Area (mm2)					Maximum Height (m)			Life Form		2D Leaf Shape			
	< 20	21-100	101-500	501-1000	>1000	< 1	1.1 - 2	> 2	Tree	Shrub	Grass	Linear	N_Oblong	Oblong
Abutilon otocarpum	0	0	1	0	0	1	0	0	0	1	0	0	0	0
Acacia aneura var. *aneura*	0	1	0	0	0	0	0	1	1	0	0	1	0	0
Acacia aneura var. *intermedia*	0	0	1	0	0	0	0	1	1	0	0	1	0	0
Acacia ayersiana	0	0	1	0	0	0	0	1	1	0	0	1	0	0
Acacia citrinoviridis	0	0	0	1	0	0	0	1	1	0	0	1	0	0
Acacia cuthbertsonii	0	0	1	0	0	0	0	1	1	0	0	1	0	0
Acacia kempeana	0	0	1	0	0	0	0	1	1	0	0	1	0	0
Acacia paraneura	0	1	0	0	0	0	0	1	1	0	0	1	0	0
Acacia pruinocarpa	0	0	0	1	0	0	0	1	1	0	0	1	0	0
Acacia ramulosa var. *linophylla*	0	0	1	0	0	0	0	1	1	0	0	1	0	0
Acacia rhodophloia	0	0	1	0	0	0	0	1	1	0	0	0	1	0
Acacia sp. Jack Hills	0	0	1	0	0	0	0	1	1	0	0	1	0	0
Acacia tetragonophylla	0	1	0	0	0	0	0	1	1	0	0	1	0	0
Aluta aspera subsp. *hesperia*	1	0	0	0	0	0	1	0	0	1	0	0	0	1
Calytrix desolata	1	0	0	0	0	1	0	0	0	1	0	0	1	0
Corymbia ?lenziana	0	0	0	1	0	0	0	1	1	0	0	1	0	0
Cymbopogon ambiguus	0	0	1	0	0	1	0	0	0	0	1	1	0	0
Dodonaea pachyneura	0	0	1	0	0	0	1	0	0	1	0	1	0	0
Dodonaea petiolaris	0	0	1	0	0	0	1	0	0	1	0	0	1	0
Enchylaena tomentosa	1	0	0	0	0	1	0	0	0	1	0	0	1	0
Eremophila exilifolia	1	0	0	0	0	1	0	0	0	1	0	0	1	0
Eremophila forrestii	0	0	1	0	0	0	1	0	0	1	0	0	0	1
Eremophila fraseri	0	1	0	0	0	0	1	0	0	1	0	0	0	1
Eremophila glutinosa	1	0	0	0	0	0	1	0	0	1	0	1	0	0
Eremophila lachnocalyx	0	1	0	0	0	1	0	0	0	1	0	0	0	1
Eremophila latrobei	0	1	0	0	0	1	0	0	0	1	0	1	0	0
Eremophila longifolia	0	0	1	0	0	0	1	0	0	1	0	1	0	0
Eremophila maitlandii	0	1	0	0	0	0	1	0	0	1	0	0	1	0
Eremophila margarethae	0	1	0	0	0	1	0	0	0	1	0	0	1	0
Eremophila phyllopoda	0	0	1	0	0	0	1	0	0	1	0	1	0	0
Eremophila simulans	0	1	0	0	0	1	0	0	0	1	0	0	0	1
Eriachne helmsii	0	1	0	0	0	1	0	0	0	0	1	1	0	0

Species	Leaf Area (mm2)					Maximum Height (m)			Life Form		2D Leaf Shape			
	< 20	21-100	101-500	501-1000	>1000	< 1	1.1 - 2	> 2	Tree	Shrub	Grass	Linear	N_Oblong	Oblong
Eucalyptus victrix	0	0	0	1	0	0	0	1	1	0	0	1	0	0
Grevillea berryana	0	0	1	0	0	0	0	1	1	0	0	1	0	0
Halgania gustafsenii	0	0	0	1	0	1	0	0	0	1	0	1	0	0
Hibiscus sturtii var. forrestii	0	0	1	0	0	1	0	0	0	1	0	0	0	0
Homalocalyx echinulatus	1	0	0	0	0	1	0	0	0	1	0	0	0	1
Micromyrtus sulphurea	1	0	0	0	0	1	0	0	0	1	0	0	1	0
Monachather paradoxus	0	0	1	0	0	1	0	0	0	0	1	1	0	0
Philotheca brucei	1	0	0	0	0	1	0	0	0	1	0	1	0	0
Ptilotus gaudichaudii	1	0	0	0	0	1	0	0	0	1	0	0	1	0
Ptilotus obovatus var. *obovatus*	0	1	0	0	0	1	0	0	0	1	0	0	0	1
Ptilotus schwartzii var. *georgei*	1	0	0	0	0	1	0	0	0	1	0	0	1	0
Scaevola spinescens	1	0	0	0	0	1	0	0	0	1	0	1	0	0
Sclerolaena cuneata	1	0	0	0	0	1	0	0	0	1	0	0	1	0
Senna artemisioides subsp. *helmsii*	0	1	0	0	0	0	1	0	0	1	0	0	0	1
Senna artemisioides subsp. x *sturtii*	0	0	1	0	0	0	1	0	0	1	0	0	0	1
Senna sp.	0	1	0	0	0	0	0	1	0	1	0	1	0	0
Sida calyxhymenia	0	0	1	0	0	1	0	0	0	1	0	0	0	1
Sida sp. *Excedentifolia*	0	1	0	0	0	1	0	0	0	1	0	0	0	1
Solanum lasiophyllum	0	0	0	1	0	1	0	0	0	1	0	0	0	1
Thryptomene decussata	1	0	0	0	0	0	1	0	0	1	0	0	0	0
Triodia melvillei	0	0	1	0	0	1	0	0	0	0	1	1	0	0

Species	3D Leaf Shape			3D Leaf Shape			Petiole length (mm)			Leaf orientation			
	Circular	Flat	Terete	Clavate	Involute	Revolute	No Petiole	0.1-10	> 10	Appressed	Inclined	Horizontal	Reclined
Abutilon otocarpum	1	0	0	0	1	0	0	0	1	0	1	0	0
Acacia aneura var. *aneura*	0	1	0	0	0	0	0	1	0	1	0	0	0
Acacia aneura var. *intermedia*	0	1	0	0	0	0	0	1	0	1	0	0	0
Acacia ayersiana	0	1	0	0	0	0	0	1	0	1	0	0	0
Acacia citrinoviridis	0	1	0	0	0	0	0	1	0	1	0	0	0
Acacia cuthbertsonii	0	1	0	0	0	0	0	1	0	1	0	0	0
Acacia kempeana	0	1	0	0	0	0	0	1	0	1	0	0	0
Acacia paraneura	0	1	0	0	0	0	0	1	0	0	1	0	0
Acacia pruinocarpa	0	1	0	0	0	0	0	1	0	0	1	0	0
Acacia ramulosa var. *linophylla*	0	1	0	0	0	0	0	1	0	1	0	0	0
Acacia rhodophloia	0	1	0	0	0	0	0	1	0	1	0	0	0
Acacia sp. Jack Hills	0	1	0	0	0	0	0	1	0	1	0	0	0
Acacia tetragonophylla	0	0	1	0	0	0	0	1	0	0	1	0	0
Aluta aspera subsp. *hesperia*	0	0	0	1	0	0	0	1	0	1	0	0	0
Calytrix desolata	0	0	0	1	0	0	1	0	0	1	0	0	0
Corymbia ?lenziana	0	1	0	0	0	0	0	1	0	0	0	0	0
Cymbopogon ambiguus	0	0	0	0	0	1	1	0	0	1	0	0	0
Dodonaea pachyneura	0	1	0	0	0	0	0	1	0	1	0	0	0
Dodonaea petiolaris	0	0	0	0	1	0	0	1	0	0	1	0	0
Enchylaena tomentosa	0	1	0	0	0	0	1	0	0	0	1	0	0
Eremophila exilifolia	0	0	0	0	1	0	1	0	0	0	1	0	0
Eremophila forrestii	0	1	0	0	0	0	0	1	0	0	1	0	0
Eremophila fraseri	0	0	0	0	1	0	0	0	1	0	1	0	0
Eremophila glutinosa	0	0	0	0	1	0	1	0	0	0	1	0	0
Eremophila lachnocalyx	0	0	0	0	1	0	1	0	0	0	0	1	0
Eremophila latrobei	0	0	0	0	1	0	0	1	0	1	0	0	0
Eremophila longifolia	0	1	0	0	0	0	0	1	0	1	0	0	0
Eremophila maitlandii	0	1	0	0	0	0	0	1	0	1	0	0	0
Eremophila margarethae	0	1	0	0	0	0	0	1	0	1	0	0	0
Eremophila phyllopoda	0	1	0	0	0	0	0	1	0	0	1	0	0
Eremophila simulans	0	0	0	0	1	0	0	1	0	0	1	0	0
Eriachne helmsii	0	0	0	0	1	0	1	0	0	1	0	0	0

Species	3D Leaf Shape			3D Leaf Shape			Petiole length (mm)			Leaf orientation			
	Circular	Flat	Terete	Clavate	Involute	Revolute	No Petiole	0.1-10	> 10	Appressed	Inclined	Horizontal	Reclined
Eucalyptus victrix	0	1	0	0	0	0	0	1	0	0	0	0	0
Grevillea berryana	0	0	0	0	0	1	0	1	0	1	0	0	0
Halgania gustafsenii	0	0	0	0	1	0	0	1	0	0	1	0	0
Hibiscus sturtii var. forrestii	1	0	0	0	1	0	0	1	0	0	0	1	0
Homalocalyx echinulatus	0	0	0	0	1	0	1	0	0	1	0	0	0
Micromyrtus sulphurea	0	0	0	1	0	0	1	0	0	0	1	0	0
Monachather paradoxus	0	0	0	0	1	0	1	0	0	1	0	0	0
Philotheca brucei	0	0	0	0	1	0	1	0	0	0	1	0	0
Ptilotus gaudichaudii	0	0	0	0	1	0	1	0	0	0	1	0	0
Ptilotus obovatus var. *obovatus*	0	0	0	0	1	0	0	1	0	0	1	0	0
Ptilotus schwartzii var. *georgei*	0	0	0	0	1	0	0	1	0	0	1	0	0
Scaevola spinescens	0	0	0	0	1	0	0	1	0	0	1	0	0
Sclerolaena cuneata	0	0	0	0	1	0	1	0	0	0	1	0	0
Senna artemisioides subsp. *helmsii*	0	1	0	0	0	0	0	1	0	0	1	0	0
Senna artemisioides subsp. x *sturtii*	0	1	0	0	0	0	0	1	0	0	1	0	0
Senna sp.	0	0	0	0	1	0	0	1	0	0	1	0	0
Sida calyxhymenia	0	0	0	0	1	0	0	1	0	0	1	0	0
Sida sp. *Excedentifolia*	0	0	0	0	1	0	0	1	0	0	1	0	0
Solanum lasiophyllum	0	0	0	0	1	0	0	1	0	0	1	0	0
Thryptomene decussata	1	0	0	1	0	0	1	0	0	0	1	0	0
Triodia melvillei	0	0	0	0	1	0	1	0	0	1	0	0	0

Species	Trichome cover and type						Resin	Leaf surface configuration		
	Depressed	Glabrous	Ciliate	Tomentose	Strigose	Sericeous	Resinous	Smooth	Striate	U_Texture
Abutilon otocarpum	0	0	0	1	0	0	0	0	0	1
Acacia aneura var. *aneura*	0	0	0	0	1	0	0	0	1	0
Acacia aneura var. *intermedia*	0	0	0	0	1	0	0	0	1	0
Acacia ayersiana	0	0	0	0	1	0	0	0	1	0
Acacia citrinoviridis	0	0	0	0	1	0	0	1	0	0
Acacia cuthbertsonii	0	0	0	0	1	0	0	1	0	0
Acacia kempeana	0	1	0	0	0	0	0	0	1	0
Acacia paraneura	0	1	0	0	0	0	1	0	1	0
Acacia pruinocarpa	0	1	0	0	0	0	0	1	0	0
Acacia ramulosa var. *linophylla*	0	0	0	0	1	0	0	0	1	0
Acacia rhodophloia	0	1	0	0	0	0	0	0	1	0
Acacia sp. Jack Hills	0	0	0	0	1	0	1	0	1	0
Acacia tetragonophylla	0	1	0	0	0	0	0	1	0	0
Aluta aspera subsp. *hesperia*	0	1	0	0	0	0	0	0	0	1
Calytrix desolata	0	1	0	0	0	0	0	0	0	1
Corymbia ?lenziana	1	1	0	0	0	0	0	1	0	0
Cymbopogon ambiguus	0	1	0	0	0	0	0	0	1	0
Dodonaea pachyneura	0	1	0	0	0	0	1	0	0	1
Dodonaea petiolaris	0	1	0	0	0	0	1	0	0	1
Enchylaena tomentosa	0	0	0	0	0	1	0	0	0	1
Eremophila exilifolia	0	1	0	0	0	0	1	0	0	1
Eremophila forrestii	0	0	0	1	0	0	0	1	0	0
Eremophila fraseri	0	1	0	0	0	0	1	0	0	1
Eremophila glutinosa	0	1	0	0	0	0	1	0	0	1
Eremophila lachnocalyx	0	0	0	1	0	0	0	1	0	0
Eremophila latrobei	0	0	0	1	0	0	0	1	0	0
Eremophila longifolia	0	0	0	1	0	0	0	1	0	0
Eremophila maitlandii	0	0	0	1	0	0	0	1	0	0
Eremophila margarethae	0	0	0	1	0	0	0	1	0	0
Eremophila phyllopoda	0	0	0	1	0	0	0	1	0	0
Eremophila simulans	0	1	0	0	0	0	1	0	0	1
Eriachne helmsii	0	1	0	0	0	0	1	0	1	0

Species	Trichome cover and type						Resin	Leaf surface configuration		
	Depressed	Glabrous	Ciliate	Tomentose	Strigose	Sericeous	Resinous	Smooth	Striate	U_Texture
Eucalyptus victrix	1	1	0	0	0	0	0	1	0	0
Grevillea berryana	0	0	0	0	1	0	0	1	0	0
Halgania gustafsenii	0	0	0	0	0	1	0	0	0	1
Hibiscus sturtii var. forrestii	0	0	0	1	0	0	0	1	0	0
Homalocalyx echinulatus	0	0	1	0	0	0	0	0	0	1
Micromyrtus sulphurea	0	1	0	0	0	0	0	0	0	1
Monachather paradoxus	0	1	0	0	0	0	0	0	1	0
Philotheca brucei	0	1	0	0	0	0	0	0	0	1
Ptilotus gaudichaudii	0	0	0	1	0	0	0	1	0	0
Ptilotus obovatus var. *obovatus*	0	0	0	1	0	0	0	1	0	0
Ptilotus schwartzii var. *georgei*	0	0	0	1	0	0	0	1	0	0
Scaevola spinescens	0	1	0	0	0	0	0	1	0	0
Sclerolaena cuneata	0	0	0	0	0	1	0	1	0	0
Senna artemisioides subsp. *helmsii*	0	0	0	1	0	0	0	1	0	0
Senna artemisioides subsp. x *sturtii*	0	0	0	0	0	1	0	1	0	0
Senna sp.	0	1	0	0	0	0	0	1	0	0
Sida calyxhymenia	0	0	0	1	0	0	0	1	0	0
Sida sp. *Excedentifolia*	0	0	0	1	0	0	0	1	0	0
Solanum lasiophyllum	0	0	0	1	0	0	0	0	0	1
Thryptomene decussata	0	1	0	0	0	0	0	0	0	1
Triodia melvillei	0	1	0	0	0	0	1	0	1	0

Appendix 3.F

Analysis of Similarities (ANOSIM) Results

Global Test: Sample statistic (Global R): 0.838, Significance level of sample statistic: 0.01%, Number of permutations: 9999 (Random sample from a large number), Number of permuted statistics greater or equal to Global R: 0

Table 3.F1: Pairwise tests for each plant trait group

Plant Group	R Statistic	Significance level %	Possible permutations	Actual permutations	Number >= observed
3, 6	1	0.3	286	286	1
3, 7	0.991	1.2	84	84	1
3, 4	0.422	0.2	560	560	1
3, 5	1	2.9	35	35	1
3, 1	0.879	0.6	165	165	1
3, 2	0.539	0.5	220	220	1
6, 7	0.851	0.01	8008	8008	1
6, 4	0.96	0.01	1144066	9999	0
6, 5	0.998	0.1	1001	1001	1
6, 1	0.957	0.01	43758	9999	0
6, 2	1	0.01	92378	9999	0
7, 4	0.894	0.01	27132	9999	0
7, 5	1	0.5	210	210	1
7, 1	0.921	0.03	3003	3003	1
7, 2	0.915	0.02	5005	5005	1
4, 5	0.777	0.04	2380	2380	1
4, 1	0.821	0.01	203490	9999	0
4, 2	0.612	0.01	497420	9999	0
5, 1	0.986	0.2	495	495	1
5, 2	0.999	0.1	715	715	1
1, 2	0.61	0.03	24310	9999	2

Appendix 4.A

Photographs of the Dust Collector Stations in April and October 2011

Dust collector stations at which plant physiological measurements and soil samples were taken in April (left) and October (Right) 2011

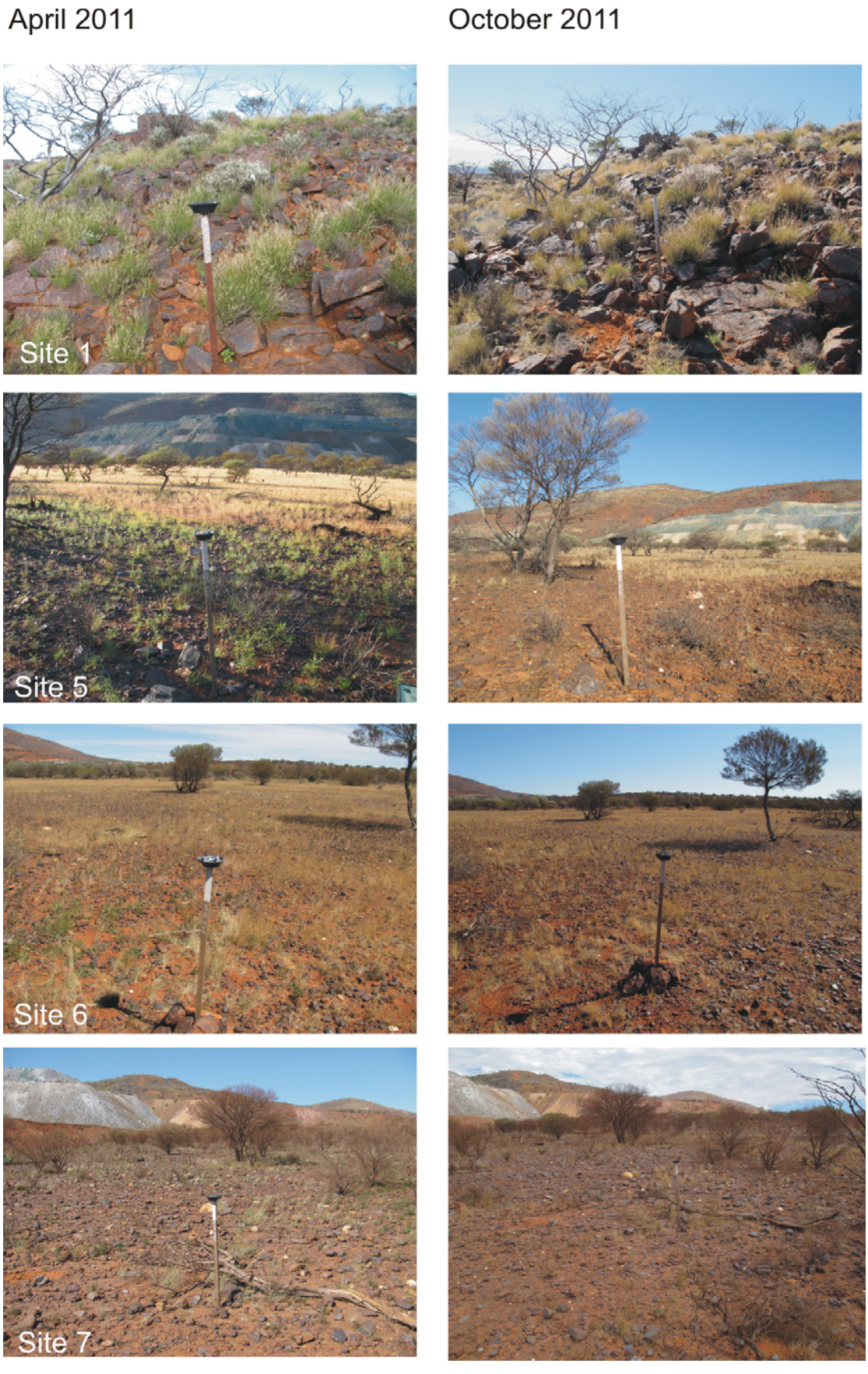

April 2011

October 2011

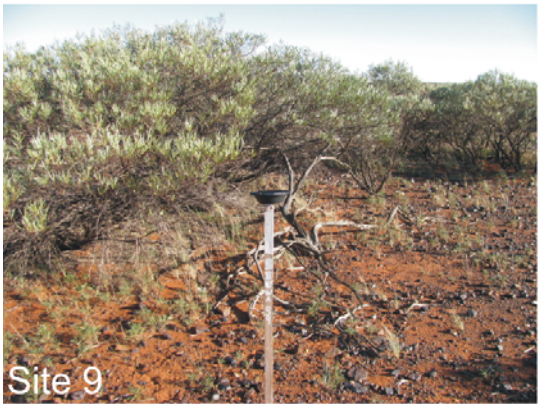

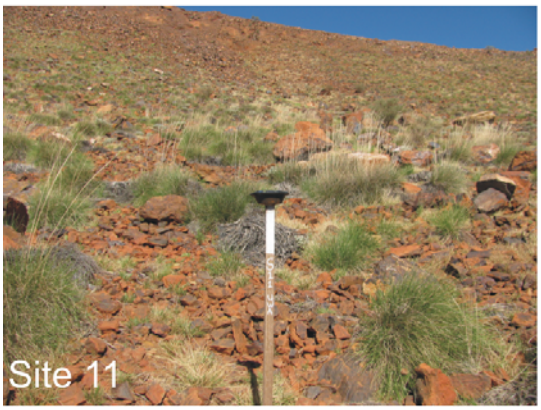

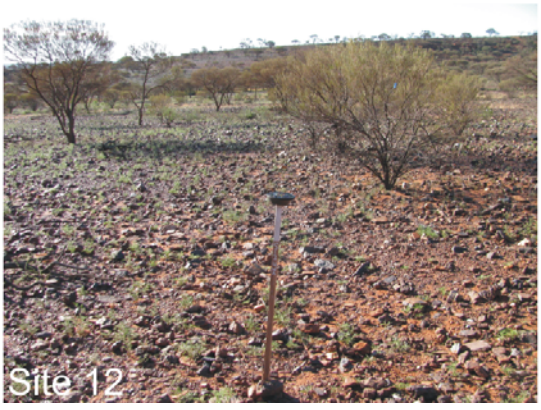

April 2011

October 2011

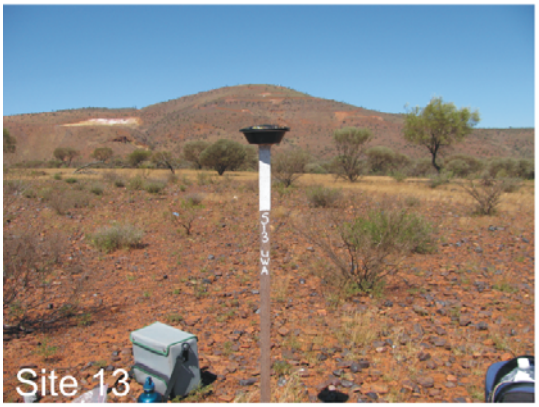

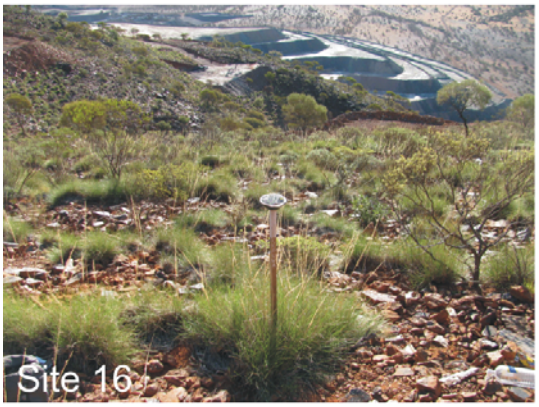

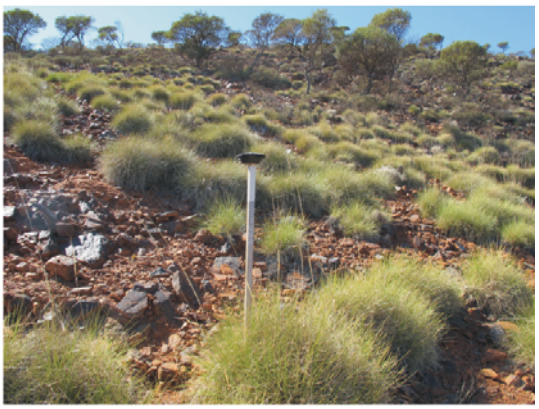

April 2011

October 2011

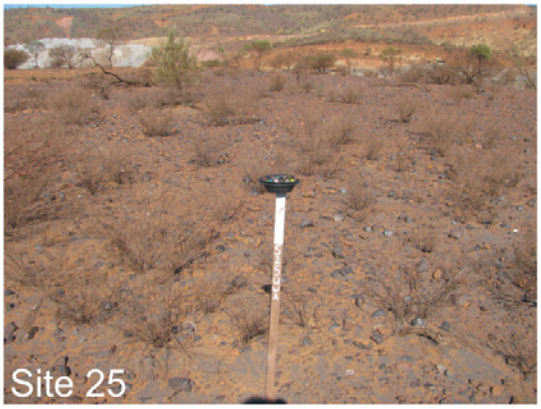

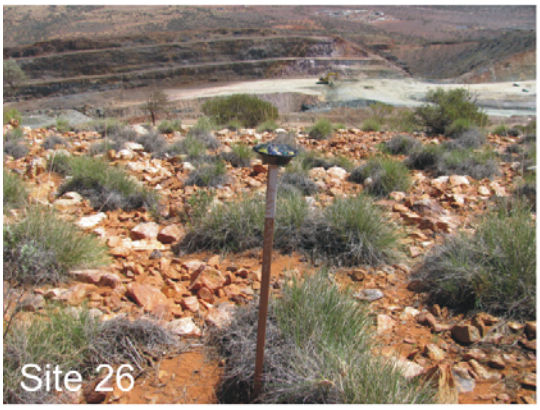

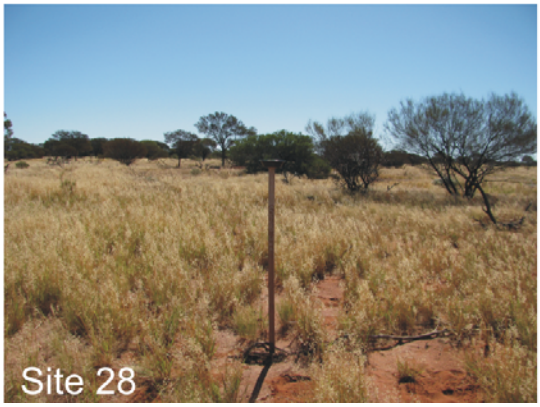

Appendix 4.B

Soil Parameters

Table 1: Soil parameters recorded at sampling sites at the Jack Hills, ordered by axis, then by distance from the mining operations (closest to farthest).

Axis	Dust collector	Topographic Position	Moisture (%) April	Moisture (%) October	Soil pH	Soil EC (µs/cm)	Nitrate (ppm)	Ammonium (ppm)	$\Delta^{13}C$	$\Delta^{15}N$
1	26	US	2.98	0.36	4.08	24.8	0.211	0.059	0.9	0.1
	11	LS	1.70	0.73	5.53	45.5	0.188	0.131	1.6	0.1
	12	FS	1.08	0.91	5.47	54.7	1.004	0.404	1.0	0.1
	13	FS	1.06	0.3	5.63	35.1	0.107	0.106	0.2	0.0
	28	FS	4.78	0.52	5.54	38.5	0.097	0.083	0.2	0.0
2	25	FS	0.28	0.48	5.52	116.1	0.611	0.43	0.3	0.0
	7	FS	0.82	0.6	5.81	63.2	0.754	0.061	0.2	0.0
	8	FS	1.18	0.66	5.43	40.8	0.218	0.146	0.2	0.0
	5	FS	1.36	0.46	5.52	29.6	0.486	0.047	0.7	0.1
	6	FS	1.74	0.78	5.6	53.3	1.118	0.184	0.5	0.0
	9	FS	1.4	0.52	5.58	31.4	0.157	0.038	0.2	0.0
3	18	US	2.2	0.68	4.95	49.2	0.970	0.49	0.8	0.1
	19	MS	2.56	0.7	5.28	42.2	0.456	0.133	0.7	0.0
	17	US	1.68	NA	4.80	67.9	0.714	1.401	1.2	0.1
	16	US	1.48	0.76	4.93	27.1	0.161	0.141	0.6	0.0
	1	US	2.82	0.6	4.95	30.0	0.175	0.058	0.4	0.0